

Copyright

by

Andrew Jackson Boydston

2007

**The Dissertation Committee for Andrew Jackson Boydston Certifies that this is the
Approved Version of the Following Dissertation:**

**Annulated Bis(imidazolium) Salts: Synthesis, Characterization, and
Applications**

Committee:

Christopher W. Bielawski, Supervisor

C. Grant Willson, Co-Supervisor

Eric V. Anslyn

Jennifer S. Brodbelt

Hung-wen Liu

**Annulated Bis(imidazolium) Salts: Synthesis, Characterization, and
Applications**

by

Andrew Jackson Boydston, B.S., M.S.

Dissertation

Presented to the Faculty of the Graduate School of

The University of Texas at Austin

in Partial Fulfillment

of the Requirements

for the Degree of

Doctor of Philosophy

The University of Texas at Austin

December, 2007

Dedication

*To my family, for their love and support. Also to Professor Michael M. Haley for
introducing me to my passion, and mentoring me since.*

Acknowledgements

First and foremost I am grateful to my research advisor, Dr. Christopher W. Bielawski, for his patience, commitment, and tireless pursuit of perfection, as well as his encouragement and guidance.

I am thankful to all of my labmates in the Bielawski group who have not only contributed greatly to my knowledge of chemistry, but also to my quality of life as a graduate student. Among these individuals, I want to give special thanks to Kyle A. Williams for his contributions on multiple research projects, insights on various aspects of life, and for being a model for composure, thoughtfulness, and selflessness. I also want to acknowledge countless hours and considerable intellectual contributions from the many undergraduate students whom I had the joy of mentoring.

I would like to thank Professor Eric Anslyn, Professor Jennifer Brodbelt, Penny Kile, and Kimberly Terry for helping and guiding me through a particularly difficult time in my graduate career.

I want to specifically thank Dr. Jeff Gorman for being a true best friend, and an exemplary mentor.

Annulated Bis(imidazolium) Salts: Synthesis, Characterization, and Applications

Publication No. _____

Andrew Jackson Boydston, Ph.D.

The University of Texas at Austin, 2007

Supervisors: Christopher W. Bielawski and C. Grant Willson

The design, synthesis, characterization, and applications of annulated bis(imidazolium) salts are described. New synthetic methodologies have been developed that allow access to a broad structural range of bis(imidazolium) salts. Initial studies focused on the use of bis(imidazolium) salts as comonomers in the formation of main-chain organometallic polymers. Two distinct polymer scaffolds were synthesized, one featuring metal(II)dihalides in the main-chain, and the other featuring a chelated metal center. Ultimately, polymerizations were conducted under ambient atmosphere, proceeded in excellent overall yield, and provided main-chain organometallic polymers comprising Ni(II), Pd(II), and Pt(II) with molecular weights up to 10^6 Da.

Departing polymer studies, focus was shifted toward the study of the physical and photophysical properties of the bis(imidazolium) salts. In few synthetic manipulations, a

series of highly photoluminescent bis(imidazolium) salts were prepared whose substituents enable emission in solution, in the solid-state, and, uniquely, as free-flowing liquids. Importantly, these materials display excellent physical properties, such as low glass-transition temperatures ($< 0\text{ }^{\circ}\text{C}$) and high thermal stabilities ($> 300\text{ }^{\circ}\text{C}$). In addition, the bis(imidazolium) platform enabled access to two new fluorescent ionic liquid crystals, demonstrating an ability to also control mesomorphic properties of these materials.

Further investigations were conducted regarding the photophysical properties of bis(imidazolium) salts. Focus was placed upon absorption and emission wavelength tunability, solvatochromism, red-edge excitation, and chemical stability. Through functional group modulation, the λ_{em} were varied from 329 – 561 nm with Φ_{fs} up to 0.91. Both the absorption and emission characteristics were found to display strong solvent-dependencies which were found to be strongly influenced by the nature of the bis(imidazolium) core. The red-edge effect was investigated for a series of bis(imidazolium) salts and was found to be similar between Br and BF_4 salts, but distinctly different when MeSO_4 anions were incorporated. The stability of an amphiphilic BBI was quantified in aqueous solutions of varying pH and $> 85\%$ of the emission intensity was retained after 2 h at pH levels of 3 – 9.

Table of Contents

Chapter 1:	A Modular Approach to Main-Chain Organometallic Polymers	1
1.1	Introduction	1
1.2	Synthesis of annulated bis(imidazolium) salts	1
1.3	Synthesis of main-chain organometallic polymers	3
1.4	Metal-center coordination and structural dynamicity	5
Chapter 2:	Synthesis and Study of Bidentate-Benzimidazolylidene-Group 10 Metal Complexes and Related Main-Chain Organometallic Polymers	14
2.1	Introduction	14
2.2	Synthesis and characterization of bidentate-benzimidazolylidene- group 10 metal complexes	21
2.3	Synthesis and characterization of bidentate-benzimidazolylidene- group 10 main-chain organometallic polymers	33
2.4	Conclusions	39
2.5	Experimental Section	42
Chapter 3:	Highly Efficient Synthesis and Solid-State Characterization of 1,2,4,5- Tetrakis(alkyl- and arylamino)benzenes and Cyclization to their Respective Benzobis(imidazolium) Salts	52
3.1	Introduction	52
3.2	Four-fold aryl amination	53
3.3	Formylative cyclization to produce benzobis(imidazolium) salts	58
3.4	Conclusions	59
3.5	Experimental Section	60
Chapter 4:	Synthesis of Benzobis(imidazolium) Salts via Tandem Cyclization- Oxidation of 2,5-Diamino-1,4-benzoquinonediimines	67
4.1	Introduction	67
4.2	Tandem cyclization-oxidation of 2,5-diamino-1,4-benzoquinonediimines	67
4.3	Conclusions	71
Chapter 5:	Synthesis and Study of Janus Bis(carbene)s and Their Transition Metal Complexes	72
5.1	Introduction	72
5.2	Synthesis and characterization of free bis(N-heterocyclic carbene)s	73
5.3	Synthesis and characterization of bimetallic complexes of bis(N- heterocyclic carbene)s	75
5.4	Conclusions	79
5.5	Experimental Section	79

Chapter 6:	Ionic Liquids via Efficient, Solvent-Free Anion Metathesis	87
6.1	Introduction	87
6.2	Solvent-free anion metathesis	88
6.3	Conclusions	91
6.4	Experimental Section	91
Chapter 7:	Phase-Tunable Fluorophores Based Upon Benzobis(imidazolium) Salts	98
7.1	Introduction	98
7.2	Synthesis of benzobis(imidazolium) salts with low T _g s	99
7.3	Synthesis of liquid crystalline benzobis(imidazolium) salts	102
7.4	Conclusions	103
7.5	Experimental Section	104
Chapter 8:	Fluorescent Benzobis(imidazolium) Salts: Synthesis and Photophysical Analyses	125
8.1	Introduction	125
8.2	Syntheses of benzobis(imidazolium) salts	128
8.3	Photophysical analyses	133
8.4	Effects of incorporating functional N-aryl groups	135
8.5	Solvent effects on absorption and emission properties	139
8.6	Red-edge effects	145
8.7	pH stability of benzobis(imidazolium) salts	148
8.8	Conclusions	150
8.9	Experimental Section	151
References		167
Vita.....		191

Chapter 1: A Modular Approach to Main-Chain Organometallic Polymers

1.1 Introduction

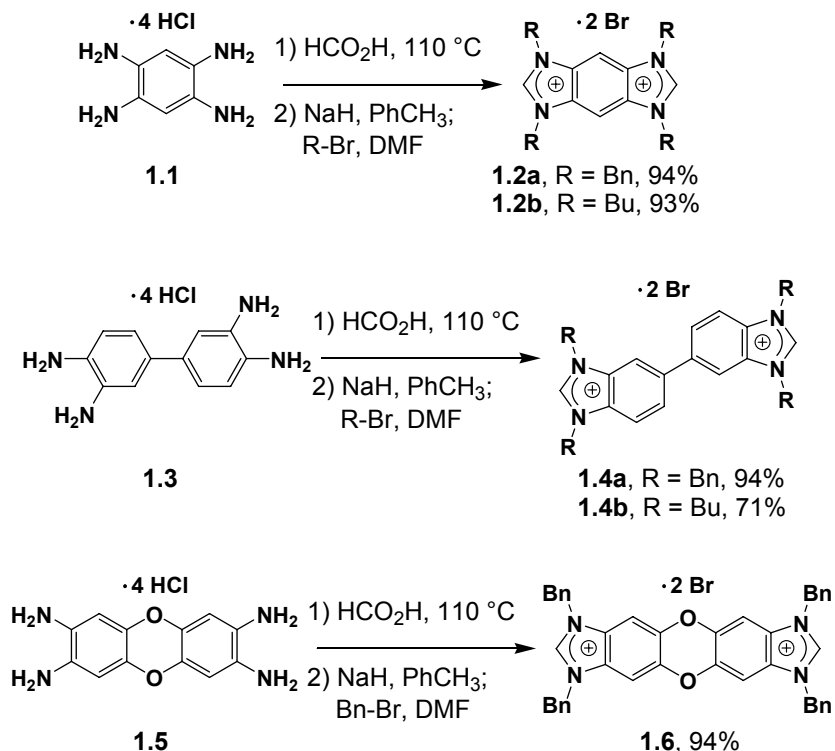
Main-chain conjugated organometallic polymers (COMPs) are an interesting class of materials with desirable electronic and mechanical properties.¹ Unfortunately, access to these materials is often challenged by factors such as the need for inert atmospheres and anhydrous conditions, restrictive compatibilities of transition metals with contemporary polymerization protocols, and limited polymer stabilities and/or solubilities. Overcoming these restraints, which have prevented COMPs from reaching their full potential, requires development of new building blocks and polymerization strategies. Although a variety of binding interactions have been employed for integrating metals into organic polymers, Arduengo-type N-heterocyclic carbenes² (NHCs) remain an untapped resource. This is surprising considering NHCs offer broad structural diversity and generally display high affinities toward a wide range of transition metals.³ We sought a versatile, direct, and simple route to bis(NHC)s connected *via* conjugated arenes. With the availability of these difunctional NHCs, we envisaged a new class of COMPs could be readily accessed.

1.2 Synthesis of annulated bis(imidazolium) salt monomers

We targeted rigid benzimidazole-based arene spacers to inhibit intramolecular metal chelation⁴ and to ensure regio-control over metallation.⁵ Toward this end, commercially available 1,2,4,5-tetraaminobenzene (**1.1**), 3,3'-diaminobenzidine (**1.3**), and known dioxin-tetraamine **1.5**,⁶ were condensed with formic acid⁷ to provide the

corresponding bis(imidazole)s. This cyclization protocol was conducted under ambient atmosphere and provided products in high purity (>95%) and high yields (>90%) after neutralization. As shown in Scheme 1.1, direct access to the respective bis(imidazolium) salts was accomplished *via* a single-step, four-fold alkylation. Thus, the bis(imidazole)s described above were each treated with NaH in PhCH₃ followed by addition of alkyl bromide. After 1 h at 110 °C, DMF was introduced as a co-solvent (50% v/v) which facilitated dissolution of partially alkylated intermediates. After an additional 6 h at 110 °C, introduction of excess PhCH₃ precipitated the desired bis(imidazolium) bromides (**1.2**, **1.4**, and **1.6**) in good to excellent yields (74 – 99%).

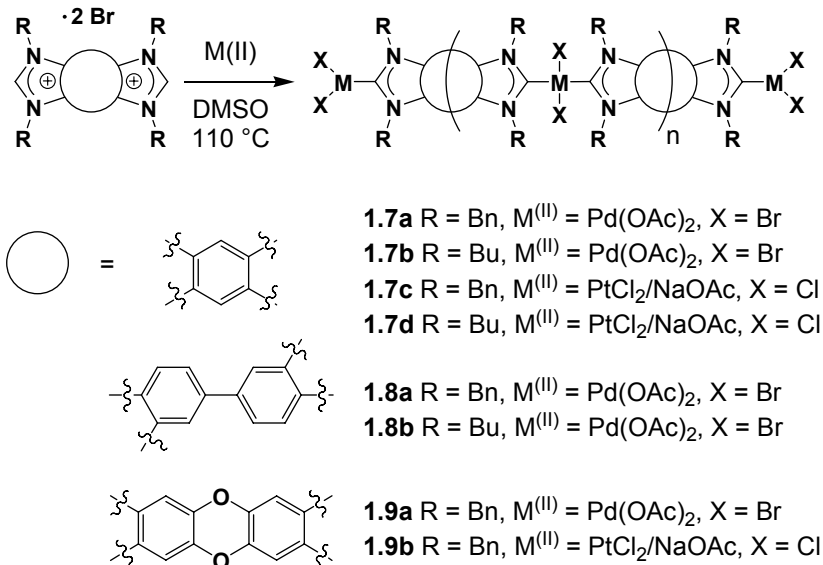
Scheme 1.1 Synthesis of bis(imidazolium) salt monomers



1.3 Synthesis of main-chain organometallic polymers

As shown in Scheme 1.2, polymerization and metal incorporation was carried out *via* a modified Herrmann-Schwarz-Gardiner method⁸ by treatment of bis(imidazolium) bromides **1.2**, **1.4**, or **1.6** with Pd(OAc)₂ in DMSO at 110 °C. After one hour, the reaction solutions were precipitated into an excess of MeOH or H₂O which afforded polymers **1.7** – **1.9** in high yields (84 – 99%). As expected, signals in the ¹H NMR spectra were relatively broad and shifted upfield in comparison with their respective bis(imidazolium) salt precursors. ¹³C NMR spectroscopy was used to verify Pd was successfully incorporated into the backbones of the polymer chains. For example, the ¹³C NMR spectrum of **1.8a** exhibited a resonance at 172 ppm which was diagnostic of an imidazol-2-ylidene-Pd bond.^{4,9} As summarized in Table 1, absorption maxima for the polymer systems were clustered around 320 nm and molar absorptivities (normalized per repeat unit) as high as 8.4 × 10⁴ M⁻¹•cm⁻¹ were observed. Analysis of the polymers by gel permeation chromatography¹⁰ (GPC) indicated their polydispersities were typical of step-growth polymerizations with number-average molecular weights (M_ns), ranging from 8.0 × 10³ – 1.1 × 10⁵ Da, dependent on the N-substituent and the bis(imidazole) structure. Likewise, the thermal stabilities of the polymers exhibited similar dependencies and began to degrade at 280 – 300 °C, as determined by thermogravimetric analysis.

Scheme 1.2 Polymerization of bis(imidazolium) salts with Pd(II) and Pt(II)



Copolymerization of **1.4a** with PdCl_2 in the presence of NaOAc (2.0 eqv) successfully produced a polymeric material with comparable molecular weight and yield as when prepared with $\text{Pd}(\text{OAc})_2$. No reaction was observed when **1.4a** was treated with NaOAc in DMSO at 110°C in the absence of metal. These results prompted us to explore the incorporation of other group 10 metals under similar reaction conditions. As shown in Scheme 1.2 and summarized in Table 1.1, copolymerizations of the bis(imidazolium) salts with $\text{PtCl}_2/\text{NaOAc}$ afforded materials with remarkably high molecular weights; for example, the M_n of **1.7c** was found to be 1.8×10^6 Da. As with Pd, molecular weights were found to be dependent on the organic moiety, however the transition metal obviously played a dominant role. Unfortunately, no polymeric materials were obtained with $\text{Ni}(\text{OAc})_2 \cdot 4\text{H}_2\text{O}$, which may reflect the reduced affinity of NHCs for Ni.¹¹

Table 1.1. Physical characteristics of polymers **1.7 – 1.9**

Polymer	Yield (%) ^a	M _n (kDa) ^b	M _w /M _n	T _d (°C) ^c	λ _{max} (nm) ^e	Log(ε) ^{e,f}
1.7a	90	18.4	1.9	291	316	4.72
1.7b	84	103	1.8	^d	314	4.72
1.7c	99	1760	1.3	294	329	4.45
1.7d	76	766	1.7	295	322	4.51
1.8a	85	26.1	2.0	284	308	4.80
1.8b	84	8.00	1.4	^d	308	4.93
1.9a	98	106	1.5	299	323	4.63
1.9b	93	408	2.6	^d	329	4.92

^aIsolated yield. ^bDetermined by GPC relative to polystyrene standards in DMF. ^cThe decomposition temperature (T_d) is defined as the temperature at which 10% weight loss occurs determined by thermogravimetric analysis under N₂, rate = 10 °C/min. ^dNot determined. ^eDetermined in DMF under ambient conditions. ^fPer repeat unit.

1.4 Metal-center coordination and structural dynamicity

Since the metal centers in the main-chain of the polymers are coordinatively unsaturated, we envisioned altering the physical properties of the macromolecules *via* a post-polymerization modification.¹² For example, treatment of **1.8a**, which is virtually insoluble in THF, with two equivalents of PCy₃ or PPh₃ resulted in rapid dissolution. GPC and ¹H NMR analysis of the phosphine-bound polymer confirmed the macromolecular structure was not compromised. Phosphine ligation to Pd was confirmed by ³¹P NMR spectroscopy (δ = 25 ppm).¹³

As bulk properties of polymeric materials are intimately related to molecular weight, methods for its precise control are essential for tailoring or fine-tuning physical characteristics.¹⁴ Chain transfer agents (CTAs) have been used extensively to control molecular weights of polymers obtained from equilibrium polymerizations.¹⁵ Since coordination of NHCs to group 10 metals is dynamic,¹⁶ inclusion of monofunctional

NHCs as CTAs during these polymerizations should provide an effective handle for controlling molecular weight. As shown in Scheme 1.3, copolymerization of **1.4b** with Pd(OAc)₂ in the presence of various amounts of *N,N'*-dibenzylbenzimidazolium bromide (**1.10**)¹⁷ provided the corresponding end-functionalized polymers **1.11**. Integration of the benzyl end-groups (PhCH₂- δ = 6.2 ppm) with respect to the butyl groups (ArNCH₂- δ = 4.8 ppm) along the polymeric backbone indicated the molecular weights of the polymers were in excellent agreement with their theoretical values based on complete incorporation of the CTA (Table 1.2).

Scheme 1.3 Incorporation of chain-transfer agents

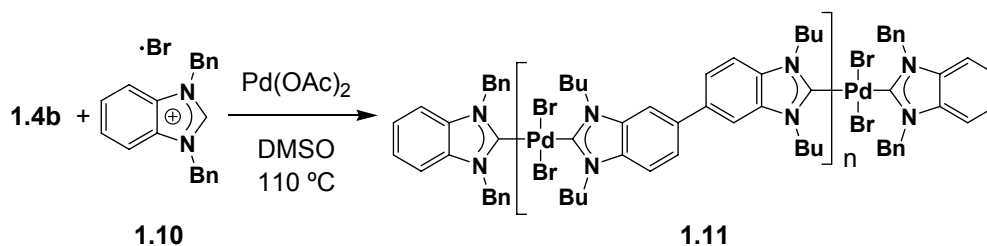


Table 1.2 Experimental and theoretical molecular weight data for **11**

Polymer	X_n , theo ^a	X_n , NMR ^b	M_n , NMR (kDa) ^b	M_n , GPC (kDa) ^c
1.11a	10	8.9	6.4	4.8
1.11b	20	23	17	8.5
1.11c	40	47	34	11

^aTheoretical number average of monomer units per polymer chain given by $2[\mathbf{1.4b}]_0/[\mathbf{1.10}]_0$. ^bDetermined by ¹H NMR spectroscopy. ^cDetermined by GPC relative to polystyrene standards in DMF.

1.5 Conclusions

In conclusion, we have developed a highly efficient route to a new class of organometallic polymers with metal centers linked together via conjugated, difunctional NHCs. The polymerizations did not require anhydrous conditions or inert atmospheres and the entire process, from commercial materials to polymeric products, was accomplished in three simple manipulations with minimal technical difficulty. The physical properties of the polymers were found to be dependent on both the transition metal and the modular structural characteristics of the NHC, and could be further modified through post-polymerization ligation. Control over both molecular weight and end-groups was also demonstrated through the inclusion of chain transfer agents during polymerization. Combined with the ability to prepare polymers with high molecular weights, these modular building blocks should open new opportunities in polymer synthesis, conductive polymers, non-linear optics, and electronic devices. Full investigation of the electronic and physical characteristics of the polymers presented herein will be reported in due course.

1.6 Experimental Section

General Considerations: ^1H and ^{13}C NMR spectra were recorded using a Varian Unity Plus 300 or 400 spectrometer. Chemical shifts (δ) are expressed in ppm downfield from tetramethylsilane using the residual protonated solvent as an internal standard (DMSO- d_6 , ^1H 2.49 ppm and ^{13}C 39.5 ppm). Coupling constants are expressed in hertz. HRMS (ESI, CI) were obtained with a VG analytical ZAB2-E instrument. UV-vis spectra were recorded using a Perkin Elmer Instruments Lambda 35 spectrometer. GPC data was

recorded using an Agilent 1100 HPLC with an Agilent PLgel 5 μ m MIXED-C column. Molecular weight data is reported relative to polystyrene standards in DMF. T_d s were determined using a TA Instruments TGA-Q500 under nitrogen atmosphere. PhCH₃ was distilled from CaH₂ or sodium and benzophenone under N₂ atmosphere prior to use. DMF was used from a solvent purification column under an atmosphere of argon. DMSO for polymerization reactions was of reagent quality and used as obtained from commercial sources.

General Procedure for formation of bis(imidazole)s via condensation of tetraamino arenes with formic acid: A round bottom flask was charged with a magnetic stir bar and the tetraamine. Formic acid (88-99%) was added and the flask was fitted with an air-jacketed condenser. The reaction mixture was placed in an oil bath at 100 – 110 °C for 2-36 h. The reaction mixture was then allowed to cool, poured into ice-cold water (equal volume to formic acid) and neutralized with 10% NaOH solution or saturated K₂CO₃ solution. Neutralization caused precipitation of the product which was collected via vacuum filtration, rinsed with cold water, and dried under vacuum over P₂O₅.

Benzo-bis(imidazole): 1,2,4,5-Benzenetetraamine tetrahydrochloride **1.1** (284 mg, 1.00 mmol) was treated with formic acid (10 mL) for 36 h according to the General Procedure to provide 152 mg (96%) of the desired product as a brown solid: mp > 300 °C; ¹H NMR (400 MHz, DMSO-*d*₆) δ 8.16 (s, 2H), 7.67 (s, 2H); ¹³C NMR (100 MHz, DMSO-*d*₆) δ 142.5, 135.6, 99.2; HRMS *m/z* calcd for C₈H₇N₄ [M+H⁺] 159.0671, found 159.0665.

3,3'-bibenzimidazole: 3,3'-diaminobenzidine **1.3** (4.71 g, 21.98 mmol) was treated with formic acid (25 mL) for 2 h according to the General Procedure to provide 4.92 g (96%) of the desired product as a tan powder. mp 262-267 °C (dec); ¹H NMR (400 MHz, DMSO-*d*₆) δ 8.23 (s, 2H), 7.82 (d, *J* = 1.1 Hz, 2H), 7.65 (d, *J* = 8.3 Hz, 2H), 7.51 (dd, *J* = 8.3, 1.1 Hz, 2H); ¹³C NMR (100 MHz, DMSO-*d*₆) δ 143.0, 138.7, 137.9, 135.9, 122.0, 116.1, 113.5; HRMS *m/z* calcd for C₁₄H₁₁N₄ [M+H⁺] 235.0984, found 235.0985.

Dioxin-bis(imidazole): Dioxin-2,3,7,8-tetraamine tetrahydrochloride (**1.5**) (525 mg, 1.35 mmol) was treated with formic acid (15 mL) according to the General Procedure (complete dissolution was not achieved, and the reaction mixture remained a suspension) to provide 303 mg (85%) of the desired product as a tan powder: mp >300 °C (dec); ¹H NMR (400 MHz, DMSO-*d*₆) δ 8.13 (s, 2H), 8.11 (s, 2H), 7.21 (s, 4H); ¹³C NMR (100 MHz, DMSO-*d*₆) δ 163.2, 142.7, 138.4, 101.8; HRMS *m/z* calcd for C₁₄H₉N₄O₂ [M+H⁺] 265.0726, found 265.0725.

Tetrabenzyl benzo-bis(imidazolium) bromide (1.2a): To a solution of NaH (298 mg, 60 wt %, 7.46 mmol) in PhCH₃ (30 mL) was added the corresponding bis(imidazole) (576 mg, 3.64 mmol) under dry nitrogen. The solution was heated to 110 °C for 1 h, allowed to cool to ambient, and benzylbromide (2.61 mL, 21.84 mmol) was added via syringe. The suspension was placed in an oil bath at 110 °C for 1 h, then dry DMF (30 mL) was added via syringe and the reaction was maintained at 110 °C for 6 h, then 60 °C for 4 h. Upon completion, the suspension was allowed to cool, diluted with PhCH₃ (50 mL) and the solids were collected by vacuum filtration, rinsed with water and THF

successively, and dried under vacuum over P_2O_5 to give 2.42 g (98%) as a tan powder: mp 280-282 °C (dec); ^1H NMR (400 MHz, $\text{DMSO}-d_6$) δ 10.54 (s, 2H), 8.93 (s, 2H), 7.60-7.58 (m, 8H), 7.39-7.34 (m, 12H), 5.87 (s, 8H); ^{13}C NMR (100 MHz, $\text{DMSO}-d_6$) δ 146.1, 133.4, 129.9, 128.9, 128.8, 128.6, 99.8, 50.5; HRMS m/z calcd for $\text{C}_{36}\text{H}_{31}\text{N}_4$ [$\text{M}-\text{H}^+$] 519.2549, found 519.2543.

Tetrabutyl benzo-bis(imidazolium) bromide (1.2b): It should be noted that **2b** is H_2O -soluble. To a solution of NaH (415 mg, 60 wt %, 10.37 mmol) in PhCH_3 (20 mL) was added the corresponding bis(imidazole) (800 mg, 5.06 mmol) under argon and the resulting suspension was placed in an oil bath at 110 °C for 1 h. To the cooled suspension was added 1-bromobutane (3.26 mL, 30.36 mmol) via syringe and the mixture was heated at 110 °C for 1 h, then dry DMF (20 mL) was added via syringe and the mixture was stirred at 110 °C for 8 h, then 60 °C for 4 h. The cooled reaction mixture was then concentrated under vacuum and the residue taken up in 1:1 $\text{CH}_2\text{Cl}_2/\text{MeOH}$ and the insoluble NaBr was removed via filtration. To the filtrate was added EtOAc until precipitation of the product occurred. The solids were collected via vacuum filtration and dried under vacuum to provide 2.66 g (97%) of the product as a tan powder: mp 194-198 °C (dec); ^1H NMR (300 MHz, $\text{DMSO}-d_6$) δ 10.25 (s, 2H), 9.11 (s, 2H), 4.62 (t, $J = 7.4$ Hz, 8H), 1.97 (p, $J = 7.4$ Hz, 8 H), 1.38 (sext, $J = 7.4$ Hz, 8H), 0.93 (t, $J = 7.4$ Hz, 12H); ^{13}C NMR (75 MHz, $\text{DMSO}-d_6$) δ 145.5, 130.2, 99.3, 47.1, 30.4, 19.1, 13.5; HRMS m/z calcd for $\text{C}_{24}\text{H}_{39}\text{N}_4$ [$\text{M}-\text{H}^+$] 383.3175, found 383.3180.

Tetrabenzyl bis(benzimidazolium) bromide (1.4a): In a manner analogous to **1.2a**, 3.05 g (98%) of compound **1.4a** was obtained as a tan solid: mp 179-183 °C (dec); ¹H NMR (400 MHz, DMSO-*d*₆) δ 10.29 (s, 2H), 8.67 (s, 2H), 8.1 (d, J = 8.8 Hz, 2H), 8.04 (d, J = 8.8 Hz, 2H), 7.66 (d, J = 7.2 Hz, 4H), 7.57 (d, J = 7.2 Hz, 4H) 6.00 (s, 4H), 5.87; ¹³C NMR (100 MHz, DMSO-*d*₆) δ 143.5, 137.7, 134.1, 134.0, 131.9, 130.8, 129.01, 128.97, 128.7, 128.5, 128.3, 126.5, 114.7, 112.9, 50.1, 50.0; HRMS m/z calcd for C₄₂H₃₅N₄ [M-H⁺] 595.2862, found 595.2858.

Tetrabutyl bis(benzimidazolium) bromide (1.4b): It should be noted that **1.4b** is H₂O-soluble. In a manner analogous to **1.2b**, 1.96 g (74%) of compound **4b** was obtained as a tan solid: mp 248-255 °C (dec); ¹H NMR (400 MHz, DMSO-*d*₆) δ 10.05 (s, 2H), 8.71 (s, 2H), 8.28 (d, J = 8.7 Hz, 2H), 8.2 (dd, J = 8.7, 1.4 Hz, 2H), 4.66 (t, J = 7.2 Hz, 4H), 4.57 (t, J = 7.2 Hz, 4H), 1.97-1.90 (m, 8H), 1.41-1.32 (m, 8H), 0.93 (t, J = 7.2 Hz, 12H); ¹³C NMR (100 MHz, DMSO-*d*₆) δ 142.9, 137.5, 132.0, 130.9, 126.3, 114.3, 112.6, 46.6, 34.2, 30.67, 30.65, 19.09, 19.07, 13.5, 13.4; HRMS m/z calcd for C₃₀H₄₅N₄ [M+H⁺] 461.3644, found 461.3643.

Tetrabenzyl dioxin-bis(imidazolium) bromide (1.6): In a manner analogous to **1.2a**, 707 mg (90%) of the compound **6** was obtained as a yellow-tan powder: mp 252-258 °C (dec); ¹H NMR (400 MHz, DMSO-*d*₆) δ 10.09 (s, 2H), 7.77 (s, 4H), 7.56-7.55 (m, 8H), 7.44-7.38 (m, 12H), 5.73 (s, 8H); ¹³C NMR (100 MHz, DMSO-*d*₆) δ 142.8, 140.7, 133.8, 129.0, 128.8, 128.4, 127.4, 101.2, 50.1; HRMS m/z calcd for C₄₂H₃₃N₄O₂ [M-H⁺] 625.2604, found 625.2601.

Typical procedure for polymerization: Polymerizations were conducted on 0.1-2.0 g scale. Bis(imidazolium) bromide (1.0 equiv) was dissolved in DMSO (ca. 0.1-0.2 M) and either M(II)(OAc)₂ (1.0 equiv), or a combination of M(II)Cl₂ (1.0 equiv) and NaOAc (2.0 equiv), was added in one portion. The solution was placed in a preheated oil bath at 110 °C and stirred open-air for 1-5 h. The reaction mixtures typically darkened in color (to orange-brown) as the reaction progressed. The cooled reaction mixture was precipitated into either MeOH or H₂O and the solids were collected via vacuum filtration and dried under vacuum.

1.7a: Light brown solid. ¹H NMR (400 MHz, DMSO-*d*₆) δ 7.80-6.80 (m, 22H), 6.40-5.41 (m, 8H); T_d = 291 °C; M_n = 18.4 kDa; PDI = 1.9.

1.7b: Tan solid. ¹H NMR (400 MHz, DMSO-*d*₆) δ 8.20-8.04 (m, 2H), 4.95-4.76 (m, 8H), 2.18-2.10 (m, 8H), 1.48-1.40 (m, 8H), 1.01-0.92 (m, 12H); M_n = 103 kDa; PDI = 1.8.

1.7c: Tan solid. ¹H NMR (400 MHz, DMSO-*d*₆) δ 7.60-6.45 (m, 26H), 6.40-5.20 (m, 8H); T_d = 294 °C; M_n = 1760 kDa; PDI = 1.3.

1.7d: Tan powder. ¹H NMR (400 MHz, DMSO-*d*₆) δ 8.18 (br s, 2H), 4.91-4.55 (m, 8H), 2.18-1.99 (m, 8H), 1.47 (br s, 8H), 1.00-0.91 (m, 12H); T_d = 295 °C; M_n = 766 kDa; PDI = 1.7.

1.8a: Light green powder. ^1H NMR (400 MHz, $\text{DMSO-}d_6$) δ 7.62 (br s, 7H), 7.40-6.90 (m, 19H), 6.13 (br s, 4H), 6.07 (br s, 4H); $T_d = 284\text{ }^\circ\text{C}$; $M_n = 26.1\text{ kDa}$; PDI = 2.0.

1.8b: Yellow solid. ^1H NMR (400 MHz, $\text{DMSO-}d_6$) δ 7.97-7.92 (m, 2H), 7.77-7.60 (m, 4H), 4.83-4.54 (m, 8H), 2.18-2.14 (m, 8H), 1.50 (br s, 8H), 0.99 (br s, 12H); $M_n = 8.00\text{ kDa}$; PDI = 1.4.

1.9a: Green powder. ^1H NMR (400 MHz, $\text{DMSO-}d_6$) δ 7.80-6.90 (m, 26H), 6.20-5.90 (m, 8H); $T_d = 299\text{ }^\circ\text{C}$; $M_n = 106\text{ kDa}$; PDI = 1.5.

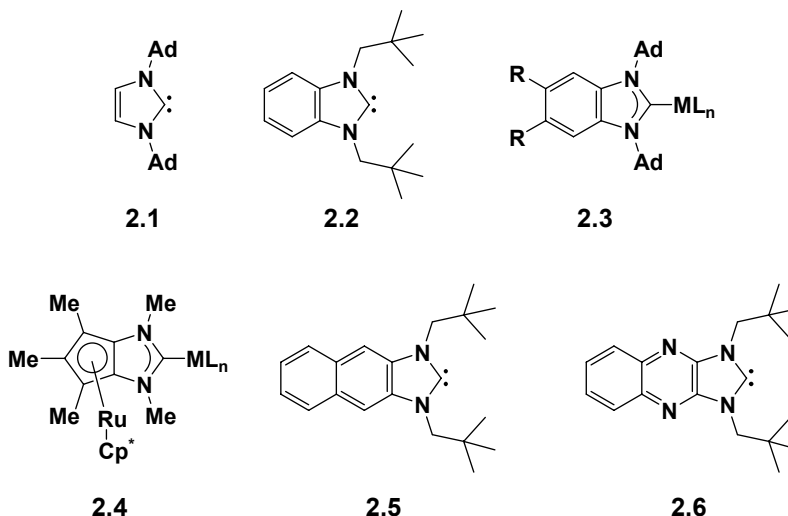
1.9c: Tan powder. ^1H NMR (400 MHz, $\text{DMSO-}d_6$) δ 7.80-7.00 (m, 26H), 6.40-5.40 (m, 8H); $M_n = 408\text{ kDa}$; PDI = 2.6.

Chapter 2: Synthesis and Study of Bidentate-Benzimidazolylidene-Group 10 Metal Complexes and Related Main-Chain Organometallic Polymers

2.1 Introduction

Since the synthesis and isolation of the first stable, crystalline N-heterocyclic carbene (NHC) was disclosed² by Arduengo in the early 1990s (**2.1**, Figure 2.1), the development of new functional organometallic complexes has witnessed tremendous growth.^{2,3} During this time, an impressively broad structural range of NHCs, and their complexes with various transition metals, have been studied and employed in a wide range of synthetic reactions.³ The electronic nature of NHC systems is important in both synthetic and materials chemistry, and quantum chemical studies have shown that annulation significantly impacts this aspect of NHCs.¹⁸ Experimentally, key advances with annulated NHCs have been made in the areas of benzimidazolylidenes¹⁹ (e.g., **2.2**²⁰ and **2.3**²¹), fused metallocenes (e.g., **2.4**),²² extended annulated systems (e.g., **2.5**),²³ and heterocycle-fused²⁴ NHCs (e.g., **2.6**²⁵). Collectively, these compounds exhibit remarkable structural tunability and broad metal compatibility which often results in considerable performance enhancement in the respective metal-catalyzed reactions. Prime examples of such effects have been observed in Pd mediated carbon-carbon and carbon-heteroatom bond forming reactions and in Ru mediated olefin metathesis reactions.²⁶

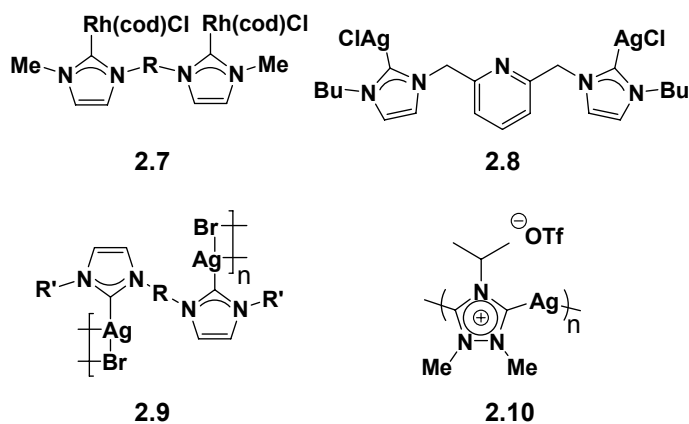
Figure 2.1 Representative examples of NHCs and NHC-metal complexes



In contrast, relatively little attention has been directed toward using NHCs as a means to construct organometallic polymeric materials.¹ Considering the large amount of synthetic and functional diversity inherent to NHCs coupled with their high affinity toward a wide range of transition metals, they are ideally suited for this purpose. However, to obtain polymeric materials, access to multitopic NHCs capable of binding at least two transition metals with high fidelity is essential. Although many di-, tri-, and multitopic NHC-based ligands are known,^{8,27} they are often poised (and designed) to preferentially bind to one metal center in a chelating or pincer-type fashion. Notable exceptions (Figure 2.2) include systems from Herrmann (**2.7**),²⁸ Youngs (**2.8**),²⁹ and Lee (**2.9**)^{4a} who have each shown that some pincer-type bis(carbene)s form bimetallic structures (with 1:1 NHC/metal stoichiometry). In particular, with Ag(I) salts, materials could be obtained that were polymeric in the solid-state. However, dissolution of these materials affords the respective discrete bimetallic complexes. In a related example,

Bertrand³⁰ reported that non-chelating bis(carbene)s based on dialkylated 1,2,4-triazoles (**2.10**) also afforded solid-state polymers with Ag(I) salts. These results suggested that tuning the NHC-metal interaction in corresponding organometallic polymers may ultimately lead to new advances in responsive materials, analogous to those of Craig³¹ and Rowan.³²

Figure 2.2 Representative examples of NHC-based bimetallic complexes and related solid-state polymers

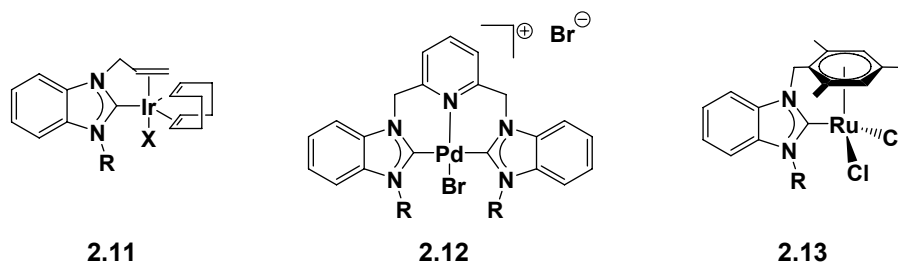


One limitation of our initial approach to metal-containing polymers was that the range of compatible transition metals was confined to Pd(II) and Pt(II) salts (see Chapter 1). Use of other metals (e.g., Ni) resulted in labile polymeric materials that rapidly underwent solvolysis in the presence of protic media (e.g., H₂O and MeOH). To increase control over material, physical, and electronic properties, we desired a method for overcoming this constraint and expanding the scope of compliant transition metals in NHC-based organometallic polymers. This required the design and synthesis of a new ditopic NHC-based monomer that was appropriately functionalized to exhibit enhanced

affinities toward transition metals. In addition, we sought a design that was flexible and would not compromise the ability to independently tune other characteristics of the resulting polymeric materials (e.g., solubilities, electronics, etc.)

An exemplary strategy for enhancing the chemical stability of metal-NHC interactions is to incorporate a bidentate, or chelating, scaffold into the NHC architecture. For example, enhanced stability of a Cu-NHC complex was demonstrated in Hoveyda's³³ use of imidazolyliene ligands containing N-aryloxy units. Similarly, Grubbs³⁴ utilized N-(2-hydroxyphenyl) substituted imidazolium salts to complex to Pd(II) species in a chelating-type fashion. While many other examples of mixed multidentate carbene ligands built on various types of imidazole-based frameworks are known,³⁵ related bidentate benzimidazolylienes have received considerably less attention. Key examples are depicted in Figure 2.3 and include Ir-based complexes using chelating olefinic groups (**2.11**),³⁶ Pd-pincer complexes comprised of a difunctional pyridine bridge (**2.12**),³⁷ and a Ru-containing complex that exhibits intramolecular chelation through metallocene formation (**2.13**).³⁸ For the purpose of forming macromolecular materials suitable for use in electronic applications, benzannulated systems are particularly attractive since the arene linkers maintain formal conjugation within the corresponding main-chains of the polymeric materials and should permit electronic tuning through further derivatization.²¹ However, incorporation of chelating groups into multitopic, annulated frameworks designed for macromolecular applications presents specific synthetic challenges.

Figure 2.3 Representative examples of chelating benzimidazolylidene-metal complexes



The formation of main-chain polymers with transition metals that prefer four coordinate geometries, e.g. Ni(II), requires a ditopic NHC ligand where each carbene “face” of the monomer is desymmetrized³⁹ to contain only one chelating N-substituent. Installation of the appropriate (i.e., chelating) N-substituents in a regiospecific manner about the benzobis(imidazole) system, however, can be nontrivial. Aryl-amination, a method that has been successfully used for the synthesis of desymmetrized benzimidazolium compounds,^{19c} is reluctant to give high yields of regioselective amination products when tetrahalobenzenes are used. Likewise, regioselective alkylation of benzobis(imidazole) would be expected to be challenged by similar difficulties. Thus, a new synthetic route to ditopic bis(bidentate) NHC systems was needed in order to facilitate formation of well-defined chelated metal centers at each terminus of the ditopic ligand.

Synthetic methods used to prepare NHC-metal complexes typically utilize one of three strategies: 1) reaction of an azolium salt with an electrophilic metal species possessing basic counterions or coordinating anions,^{27d,40} 2) generation of the free carbene followed

by introduction of an electrophilic metal species, or 3) formation of a Ag(I)-NHC complex followed by ligand transfer to the desired transition metal.⁴¹ While each of the aforementioned methods are excellent for constructing small-molecule systems, none seemed directly amenable to forming stable, high molecular weight polymers with metals other than Pd and Pt. Examples of specific challenges can be found by surveying known Ni-NHC complexes. For example, Herrmann demonstrated that imidazolylidene-Ni(II) complexes can be obtained directly from their respective imidazolium salts in 30% yield using Ni(OAc)₂.⁴² While this was an outstanding synthetic achievement, this yield is too low for forming high polymer and the reaction must be conducted in the melt under vacuum using anhydrous reagents. Synthesis of benzimidazolylidene-based Ni complexes using this methodology was found to be challenged by the fact that the resulting complexes decompose at the high reaction temperatures required (150 °C).^{19a} Recently, Hahn accomplished the first synthesis of benzimidazolylidene-Ni(II) complexes^{19a} using an elegant adaptation of Herrmann's procedure. By combining benzimidazolium salts with tetrabutylammonium salts at elevated temperatures under vacuum, the ammonium salts were melted to give an ionic liquid solvent system. This ultimately allowed for reduced reaction temperatures (120 °C) and afforded the desired Ni complexes in 28 – 60% yield. Since reaction yields of >95% are typically necessary to obtain high molecular weight polymer,⁴³ and mild polymerization reaction conditions are desirable, the development of a new protocol for forming benzimidazolylidene-transition metal complexes was needed.

Considering alternatives to direct metallation of azolium salts, free carbene generation is compatible with essentially all transition metals known to form complexes

with NHCs. Caveats of this approach, however, include a two-step procedure under an inert atmosphere and the use of dry solvents to avoid destruction of the free carbene. When carbene dimerization can occur, the resulting enetetraamines^{19d,44} are extremely sensitive toward oxygen and often subject to rearrangement or fragmentation, depending on the nature of the N-substituent.⁴⁵ Although benzobis(imidazolylidene)s can be manipulated as either their free carbenes or respective homopolymers⁴⁶ en route to bimetallics and metallo-polymers, this imposes limitations on compatible solvents. Furthermore, high molecular weight materials are generally precluded by limited solubilities in common organic solvents (e.g., THF, benzene, PhCH₃, etc.) One method that has been employed with a diverse array of conditions, solvents, and substrates is Lin's NHC-transfer method.^{33,41,47} However, disposal of stoichiometric Ag salts and confirmation of quantitative Ag exchange is not ideal for macromolecular applications.

With these considerations in mind, we targeted a ligand design that alleviated the need for strict use of inert atmospheres and allowed access to stable NHC complexes via direct metallation of benzimidazolium salts in a single step and in high yields. Herein, we report our efforts to expand the range of transition metals that can be incorporated into NHC-based main-chain organometallic polymers via direct metallation of bis(azolium) salts bearing chelating N-(o-phenol) moieties. In particular, we aimed to increase the binding affinity within bis(NHC)-metal systems without compromising control over electronic properties. Our initial efforts focused on the synthesis and study of discrete complexes designed to mimic the repeating metal centers in their corresponding main-chain polymers. Building from these results, we turned our attention toward designing

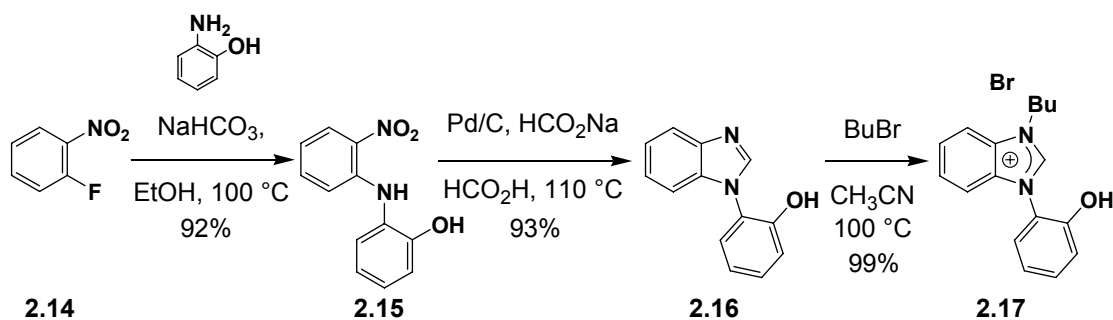
and deploying analogous ditopic systems that were prone to polymerize. The results of these investigations follow.

2.2 Synthesis and characterization of bidentate-benzimidazolylidene-group 10 metal complexes

Prior to engaging in the synthesis of polymeric materials, we first investigated the propensity of a phenol-substituted benzimidazolium salt to undergo metallation and chelation with group 10 metal(II) species. This would provide insight into the chelation event and allow for characterization of model complexes representative of the repeat units of their respective polymer chains. Thus, a benzimidazolium salt containing a pendant N-(*o*-phenol) group was synthesized as shown in Scheme 2.1. Aryl amination of 1-fluoro-2-nitrobenzene (**2.14**) with 2-aminophenol under basic conditions⁴⁸ provided the respective diarylamine **2.15** in 92% yield.⁴⁹ We envisioned that reduction of the nitro group followed by formylative cyclization of the resulting diamino intermediate could be accomplished using a “one-pot” protocol. This was successfully executed by using a mixture of NaO₂CH/HO₂CH in the presence of catalytic amounts of Pd/C which effectively hydrogenated the nitro group in situ. Within 1-2 h, the intense red-orange color associated with nitroarene **2.15** had dissipated indicating complete reduction had been accomplished. Continued heating (up to 10 h) ultimately provided the formylatively cyclized product **2.16**, which was obtained after removal of Pd/C via filtration and neutralization of the filtrate with aqueous base.⁵⁰ The crude benzimidazole was collected and alkylated with 1-bromobutane in CH₃CN followed by removal of volatiles under vacuum to give benzimidazolium bromide **2.17**. Due to the solubilizing butyl group, this

hydroscopic azolium salt was soluble in polar organic solvents (e.g., CH₂Cl₂, CHCl₃, THF, CH₃CN, and DMSO).

Scheme 2.1 Synthesis of phenol-substituted benzimidazolium salt **2.17**



With **2.17** in hand, we were poised to investigate the efficiency of metal complexation. Given that direct metallation of azolium salts with Pd(II) species is a well-established protocol that gives rise to stable metal complexes, we targeted a chelated Pd(II) model system. Benzimidazolium salt **2.17** was thus treated with 0.5 equiv Pd(OAc)₂ in THF at 50 °C for 2 h. Analysis of the crude product mixture by ¹H NMR spectroscopy confirmed that no residual azolium species remained (diagnostic azolium ¹H signal: δ = 10.8 ppm in DMSO-*d*₆). However, the phenol moieties did not appear to be chelated to the metal center as broad singlets were observed at δ = 10.0 and 9.9 ppm in the ¹H NMR spectrum (solvent = DMSO-*d*₆) and a strong signal was observed at 3331 cm⁻¹ in the IR spectrum of this complex. Mass spectral analysis supported a palladium dibromide species ligated by two NHC ligands consistent with structure (**2.18**•Pd) shown in Scheme 2.2. The methylene units of the butyl groups appeared in the ¹H NMR spectrum as complex multiplets which, in combination with the observation of two

distinct hydroxyl signals, suggested that isomeric structures may be present in solution (e.g., relative syn and anti conformations may exist from possible cis and trans isomers). To investigate, X-ray quality crystals were obtained as light brown prisms by diffusion of hexanes into a THF solution of the product mixture. Although selected crystal data are summarized in Table 2.1, the ORTEP diagram shown in Figure 2.4 confirmed the non-chelated structure of this complex. The crystallized product existed in a relative trans confirmation about the square-planar metal center (C1-Pd-C1* and C1-Pd-Br bond angles = 180.0 and 88.9°, respectively) with each butyl group experiencing a π -facial interaction with the phenol ring of the complementary NHC ligand (nearest interatomic distance: C11-C16, 3.97 Å). Most notably, the phenol rings were twisted nearly perpendicular to the plane of the benzimidazolylidene (average dihedral angle = 68°) with essentially no discernible interaction between either phenol oxygen and the Pd atom (avg. distance = 3.99 Å). The complex exhibited a ^{13}C resonance at $\delta = 181$ ppm and a Pd-C_{carbene} bond length of 2.02 Å, which were each consistent with other benzimidazolylidene-Pd(II) complexes.^{4b,23,51} The complex appeared to be stable to air and moisture, and thermogravimetric analysis (TGA) revealed a $T_d = 287$ °C under an atmosphere of nitrogen. Finally, the complex showed good solubility in most polar organic solvents (e.g., CH₂Cl₂, CHCl₃, THF, MeOH).

Scheme 2.2 Synthesis of model complexes **2.18·Pd** and **2.19** (yields of **2.19** represent the direct conversion from **2.17**)

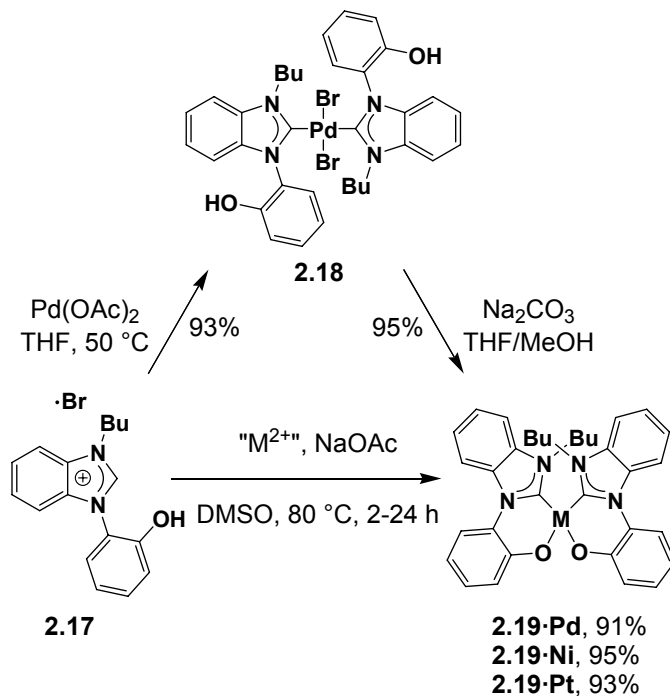


Figure 2.4 ORTEP diagram of the molecular structure of **2.18·Pd** (selected bond lengths, angles, and crystal data are summarized in Table 2.1; ellipsoids are drawn at the 50% probability level, hydrogen atoms and solvent molecules have been removed for clarity).

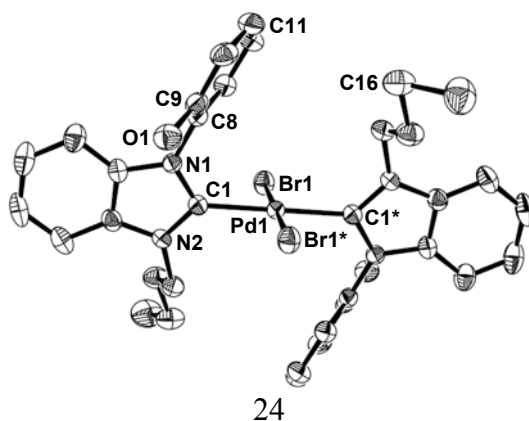


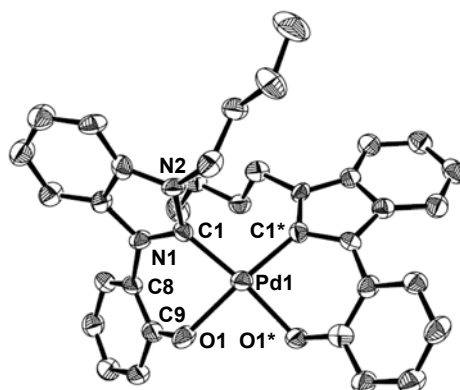
Table 2.1 Selected bond lengths, angles, and crystal data for **2.18·Pd** and **2.19**.

	2.18·Pd·2 DMSO	2.19·Pd·H₂O	2.19·Ni	2.19·Pt·H₂O
Bond Lengths (Å)				
M-C1	2.024(3)	1.937(6)	1.839(2)	1.941(11)
N1-C1	1.353(4)	1.372(7)	1.367(2)	1.376(16)
M-X (O, Br, Cl)	2.4461(4)	2.044(4)	1.895(5)	2.040(8)
Angles (°)				
N1-C1-N2	106.7(3)	105.6(5)	106.2(7)	106.6(9)
C1-M-C1*	180.00(18)	99.3(3)	94.5(3)	100.9(5)
C1-M-O1	--	86.5(2)	88.3(9)	86.7(4)
C1-M-O1*	--	173.2(2)	168.9(6)	171.9(4)
C1-N1-C8-C9	110.3(4)	-34.4(8)	26.7(3)	-33.6(18)
Crystal Data				
empirical formula	C ₃₄ H ₃₆ Br ₂ N ₄ O ₂ Pd·2(CH ₃) ₂ SO	C ₃₄ H ₃₄ N ₄ O ₂ Pd·H ₂ O	C ₃₄ H ₃₄ N ₄ NiO ₂	C ₃₄ H ₃₄ N ₄ O ₂ Pt·H ₂ O
formula weight	955.14	655.07	589.36	743.76
cryst syst	monoclinic	triclinic	monoclinic	triclinic
space group	P21/c	P-1	P21/n	P-1
a, Å	9.5039(3)	12.4990(4)	12.8694(2)	12.5210(5)
b, Å	10.6594(4)	13.8210(5)	10.3815(2)	13.8700(6)
c, Å	20.8233(9)	18.5590(7)	21.7249(4)	18.6940(10)
α, deg	90	90.2940(15)	90	90.248(2)
β, deg	101.660(2)	102.5920(14)	96.904(1)	102.670(2)
γ, deg	90	99.4230(14)	90	99.0040(17)
V, Å ³	2065.99(14)	3083.93(19)	2881.48(9)	3125.9(2)
T, K	153(2)	153(2)	233(2)	153(2)
Z	2	4	4	4
D _{calc} , Mg/m ³	1.535	1.411	1.359	1.580
cryst size (mm)	0.22 × 0.21 × 0.17	0.20 × 0.06 × 0.05	0.20 × 0.16 × 0.12	0.14 × 0.13 × 0.05
reflections collected	7923	12704	13775	11823
independent reflections	4689	12706	13779	6579
R ₁ , wR ₂ {I > 2σ(I)}	0.0401, 0.0894	0.0683, 0.1011	0.0407, 0.0891	0.0654, 0.1355
goodness of fit	1.054	1.140	1.017	1.018

To facilitate chelation, crystals of **2.18·Pd** were redissolved in THF and treated with a methanolic solution of Na₂CO₃ for 1 h under ambient conditions. After aqueous workup, spectroscopic analysis of the product suggested successful chelation and clean formation of complex **2.19·Pd**. Signals corresponding to hydroxyl groups were not observed in either the ¹H NMR or IR spectrum of this complex. In contrast to **2.18·Pd**, the ¹H NMR spectrum of **2.19·Pd** represented a single isomer with a NCH₂ triplet at δ =

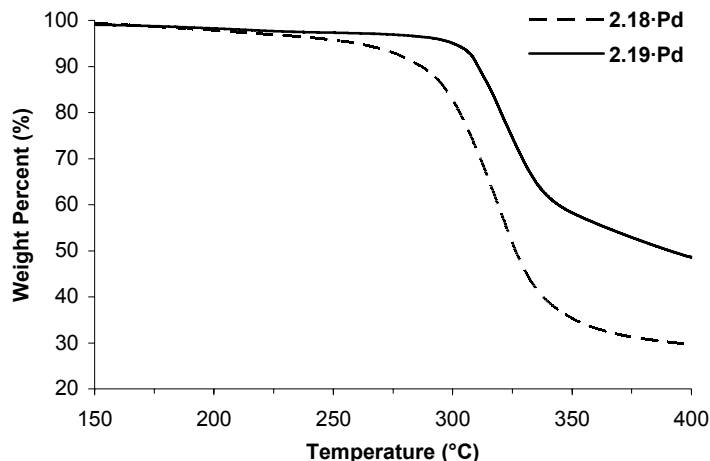
4.9 ppm. To confirm and study its molecular structure, X-ray quality crystals of **2.19-Pd** were obtained as yellow laths by slow evaporation of a THF/hexanes solution of the complex. Surprisingly, the X-ray data (represented as an ORTEP diagram in Figure 2.5) revealed that the relative geometry about the metal center was now cis.⁵² The metal center remained square-planar as expected with C1-Pd-O1* and C1-Pd-C1* bond angles of 173.2 and 99.3°, respectively. The Pd-C_{carbene} bond length (1.94 Å) was slightly shorter than those typically observed in benzimidazolylidene-Pd(II) complexes (1.97 – 2.02 Å).^{23,51} It is important to note, however, that the majority of related benzimidazolylidene-Pd(II) complexes contain Pd-halide bonds whereas **2.19-Pd** contains Pd-O bonds; thus, different trans influences may be expected. In addition, chelation effects may also contribute to the relative shortening of the Pd-C_{carbene} bond. The N-C-N bond angle (105.6°) and ¹³C NMR resonance at δ = 178 ppm were consistent with other known benzimidazolylidene-Pd(II) complexes.^{23,51} The slight upfield shift of the carbenoid signal (relative to **2.18-Pd**, δ = 181 ppm) may reflect increased electron density at the metal center as a result of the Pd-O bonds. Interestingly, chelation appeared (qualitatively) to impart greater solubility (relative to **2.18-Pd**) and complex **2.19-Pd** readily dissolved in common organic solvents such as CH₂Cl₂, THF, CHCl₃, MeOH, PhH, PhCH₃, EtOAc, and 1,4-dioxane.

Figure 2.5 ORTEP diagram of the molecular structure of **2.19•Pd** (selected bond lengths, angles, and crystal data are summarized in Table 2.1; ellipsoids are drawn at the 50% probability level, hydrogen atoms and solvent molecules have been removed for clarity).



It was desirable to have a “one-pot” complexation/chelation sequence to afford chelated complexes directly from benzimidazolium salt **2.17**. This was accomplished by simply adding exogenous base during the metallation procedure. Thus, treatment of benzimidazolium salt **2.17** with Pd(OAc)₂ and NaOAc provided the chelated complex **2.19•Pd** in 91% yield. Reactions were routinely conducted in DMSO or THF, however other polar organic solvents (e.g., EtOH, CH₃CN, etc.) were also found to facilitate efficient complexation.⁵³ The effects of chelation on thermal stability were probed using TGA. Complex **2.18•Pd** exhibited a T_d = 287 °C whereas complex **2.19•Pd** exhibited a T_d = 311 °C (both under nitrogen) (Figure 2.6). The 24 C° increase in decomposition temperature is believed to be predominately due to chelation effects.

Figure 2.6 TGA data for complexes **2.18·Pd** (---) and **2.19·Pd** (—) taken under nitrogen atmosphere heating rate = 10 °C/min.



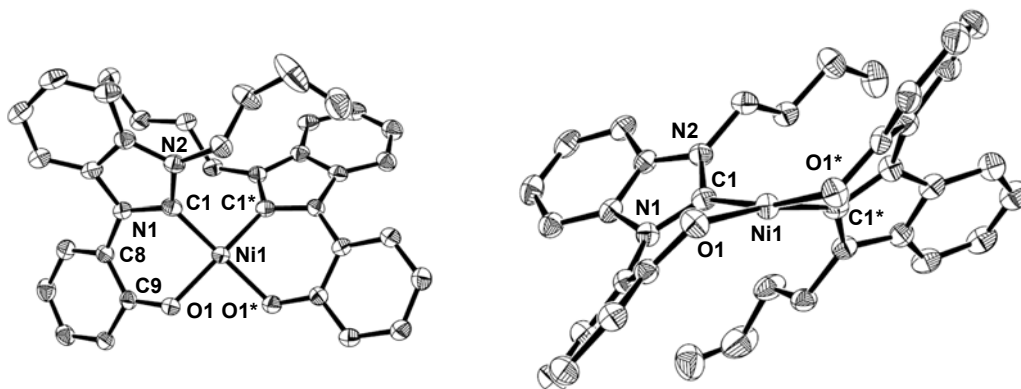
Having confirmed chelation, and enhanced thermal stability as a result of these extra intramolecular interactions, we investigated the susceptibility of other transition metals to undergo chelation to provide stable complexes. In particular, incorporation of Ni(II) would expand the relatively narrow scope of synthetic methodologies for accessing benzimidazolylidene-Ni(II) complexes. Thus, in analogy with the synthesis of **2.19·Pd**, benzimidazolium salt **2.17** was reacted with 0.5 equiv of Ni(OAc)₂·4H₂O in the presence of NaOAc in DMSO at 80 °C. Gratifyingly, this provided the corresponding Ni complex **2.19·Ni** in excellent yield (95%). Attempts to isolate a ligated, non-chelated Ni-complex in analogy to **2.18·Pd** were met with limited success which can likely be ascribed to a more favorable cyclization geometry and/or relative greater oxophilicity of Ni. Similar to the Pd-complex **2.19·Pd**, **2.19·Ni** was found to be stable toward air and moisture, and exhibited similar solubilities as well. The thermal stability of **2.19·Ni** was investigated

through TGA and revealed a $T_d = 286\text{ }^{\circ}\text{C}$ (under nitrogen) which reiterates the positive effects of chelation. Similar to the Pd analogue **2.19-Pd**, the Ni-complex appeared to be stable indefinitely in solution and in the solid-state under ambient conditions, and could be purified by chromatography on neutral alumina.

NMR, IR, and mass spectral analyses of **2.19-Ni** supported formation of a chelated 2:1 ligand/metal complex. The ^{13}C NMR was unremarkable and displayed a single NCN resonance at $\delta = 173\text{ ppm}$, which was intermediate with known benzimidazolylidene ($\sim 184\text{ ppm}$) and imidazolylidene ($\sim 164 - 170\text{ ppm}$)^{35e,54} Ni(II) complexes. Interestingly, and in contrast to **2.19-Pd**, the butyl groups in **2.19-Ni** showed diastereotopic signals in the ^1H NMR spectrum with some signals appearing markedly upfield in comparison with other NHC-Ni complexes.^{35,42} In particular, NCH_2 resonances typically appear between $\delta = 4.5$ and 6.5 ppm , depending on the nature of the alkyl groups. In **2.19-Ni** however, the diastereotopic protons associated with the NCH_2 fragment appeared at $\delta = 4.2$ and 3.6 ppm . One plausible explanation for the observed diastereotopicity in the ^1H NMR spectrum can be drawn from the X-ray data (see below) which revealed a π -facial interaction between each butyl group and the benzimidazolylidene moiety of its complementary ligand. Although this arrangement is superficially similar to that of **2.19-Pd**, the distances between the methylene units and the complementary benzimidazolylidene moiety in **2.19-Ni** are shorter than in the Pd analogue. For example, the interatomic distance between the NCH_2 carbon and the nearest atom of the complimentary benzimidazolylidene moiety (i.e., C1) in **2.19-Ni** is 3.20 \AA . The same interatomic measurement in **2.19-Pd** is 3.54 \AA .

Quality crystals suitable for X-ray diffraction analysis were obtained as yellow plates by slow diffusion of hexanes into a saturated THF solution of **2.19·Ni**. As shown in the ORTEP diagram in Figure 2.7, the molecular structure of **2.19·Ni** revealed that the complex adopted a cis geometry about the metal center, which to the best of our knowledge is the first Ni complex comprised of two benzimidazolyldenes of this relative configuration. The metal center displayed a distorted square-planar arrangement with C1-Ni-C1*, C1-Ni-O1 (cis), and O1-Ni-O1* bond angles of 94.5, 89.0, and 90.5°, respectively. Analogous to the Pd-complex, the Ni-C_{carbene} bond lengths were shortened (1.84 Å) relative to known bis(benzimidazolyldene)-Ni(II) halide complexes (1.89 – 1.91 Å), again likely due to chelation in conjunction with trans effects. The N-C-N bond angles of complex **2.19·Ni** (106.2°) were as expected for azolyldene-Ni(II) complexes.⁴²

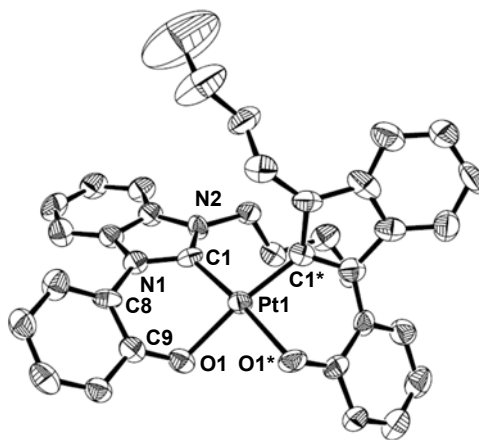
Figure 2.7 ORTEP diagram of the molecular structure of **2.19·Ni** (selected bond lengths, angles, and crystal data are summarized in Table 2.1; ellipsoids are drawn at the 50% probability level, hydrogen atoms and solvent molecules have been removed for clarity).



To complete the series of group 10 model systems, we targeted Pt-based complex **2.19•Pt** (Scheme 2.2). Chelation to form **2.19•Pt** required additional reaction periods at elevated temperatures, relative to its Ni- and Pd-analogues, which may be ascribed to the reduced oxophilicity of Pt. More specifically, whereas chelation from **2.18•Pd** could be completed within 1 h using Na₂CO₃ at room temperature, complete formation of **2.19•Pt** (monitored by ¹H NMR spectroscopy) in the presence of Na₂CO₃ in DMSO required 8 h at 80 °C (up to 24 h when NaOAc was used in lieu of Na₂CO₃).⁵⁵ Upon completion, the desired Pt complex was isolated as a single isomer in 93% yield. Full chelation was confirmed through IR and NMR spectroscopy, as well as mass spectral analysis, and solubilities resembled those of the Ni- and Pd-analogues. Although the solid-state structure (see below) was isostructural with **2.19•Pd**, the ¹H NMR spectrum more closely resembled the Ni analogue with regard to chemical shifts and splitting patterns for the butyl groups. Specifically, diastereotopic NCH₂ resonances appeared at δ = 4.0 and 3.8 ppm in the ¹H NMR spectrum of **2.19•Pt**. The ¹³C NMR spectrum of this same complex showed resonances at δ = 161 and 158 ppm, either of which could reasonably be assigned to the carbene NCN signal.⁵⁶ Considering that there are very few benzimidazolylidene-Pt(II) complexes known,^{19b,57} and that the range NCN ¹³C NMR resonances of known imidazolylidene- and imidazolinylidene-Pt(II) complexes varies from 143 – 191 ppm,⁵⁸ full assignment of the ¹³C signals in **2.19•Pt** cannot be made at this time. To confirm and study the structure of **2.19•Pt**, X-ray quality crystals were obtained as colorless plates by slow evaporation of a THF solution of the complex. An ORTEP diagram of the molecular structure of **2.19•Pt** is shown in Figure 2.8. Although N-C-N bond angle (106.7°) was consistent with other Pt(II)-based azolylidene complexes, the Pt-C_{carbene} bond length

(1.94 Å) was shorter than typically observed (1.96 – 2.04 Å).^{19b,57-59} Similar to chelated complexes **2.19·Pd** and **2.19·Ni**, the Pt-analogue showed a T_d of 314 °C by TGA.

Figure 2.8 ORTEP diagram of the molecular structure of **2.19·Pt** (selected bond lengths, angles, and crystal data are summarized in Table 2.1; ellipsoids are drawn at the 50% probability level, hydrogen atoms and solvent molecules have been removed for clarity).



Overall, the model systems provide a comprehensive view of chelation effects in group 10 metals and key characterization data are summarized in Table 2.2. Chelation from the phenol moieties was qualitatively observed to be progressively slower from Ni to Pd to Pt, a reflection of their relative oxophilicities. The respective metal- $C_{carbene}$ bond lengths were generally shorter in complexes **2.19** when compared to known azolylidene complexes with the same metal(II) species. Chelation resulted in a change in the geometry of the metal center from trans (**2.18·Pd**) to cis (**2.19·Pd**), as well as increased thermal stability as determined using TGA. Interestingly, the cis conformation observed for each model system resulted in C_2 -symmetric planar chiral complexes.

Although the crystals formed as racemates, separation of these enantiomers may ultimately open new avenues to optically active metal species with potential application in asymmetric catalysis.

Table 2.2 Key characterization data for complexes **2.18·Pd** and **2.19**

Complex	Yield (%) ^a	T _d (°C) ^b	λ _{max} (nm) ^c	δ NCN (ppm)
2.18·Pd	93	287	285	181
2.19·Pd	91	311	315	178
2.19·Ni	95	286	359	173
2.19·Pt	93	314	314	161 or 158 ^d

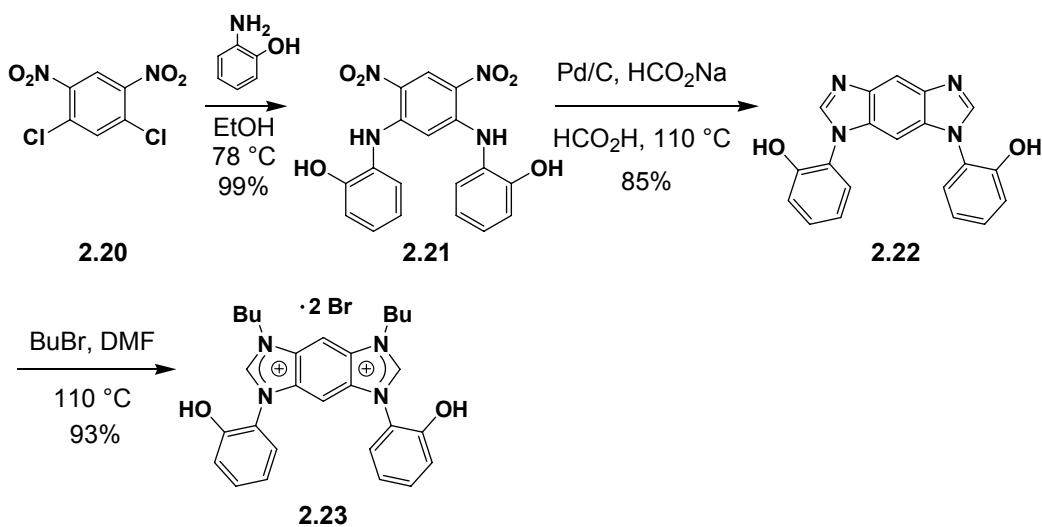
^aIsolated yields based on **2.17**. ^bThe decomposition temperature (T_d) is defined as the temperature at which 10% weight loss occurs, as determined by thermogravimetric analysis under N₂ with a rate = 10 °C/min. ^cDetermined in DMF under ambient conditions. ^dSee discussion in the text.

2.3 Synthesis and characterization of bidentate-benzimidazolylidene-group 10 main-chain organometallic polymers

Having confirmed chelation and proof of structure in each of the group 10 model complexes, we turned our attention toward synthesizing main-chain organometallic polymers containing chelating benzimidazolylidenes. Considering that benzobis(imidazolylidene)s have a high propensity to form metal adducts at each carbene moiety of the ditopic ligand, installation of a single chelating N-substituent on each imidazole moiety should provide a monomer capable of forming chelated metal centers at each terminus. As shown in Scheme 2.3, the corresponding ditopic bis(bidentate) benzobis(imidazolium) monomer was synthesized by the same general reaction sequence that was used for the synthesis of **2.17**: S_NAr, reduction/cyclization, and alkylation. In

particular, treatment of readily available 1,5-dichloro-2,4-dinitrobenzene **2.20** with 2-aminophenol (4.0 equiv) in refluxing EtOH provided 1,5-bis[(2-hydroxyphenyl)amino]-2,4-dinitrobenzene **2.21** in nearly quantitative yield. The in situ reductive cyclization protocol described above was successfully applied to **2.21** and provided benzobis(imidazole) **2.22** in 85% yield. Finally, alkylation with 1-bromobutane provided bis(azolium) dibromide **2.23** in 93% yield (78% overall yield from **2.21**).

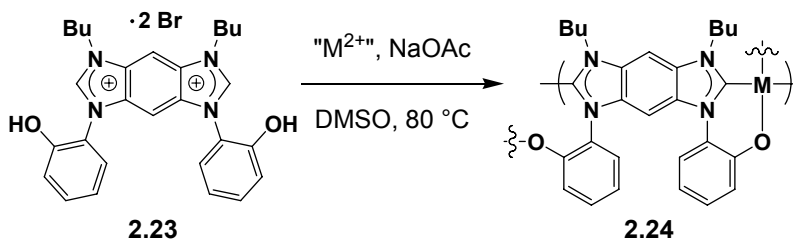
Scheme 2.3 Synthesis of bis(phenolic) benzobis(imidazolium) monomer **2.23**



As shown in Scheme 2.4, polymerizations were conducted using the conditions optimized for the synthesis of model complexes **2.19**. Combining a stoichiometric amount of metal salt⁶⁰ with **2.23** and NaOAc⁶¹ in DMSO at 80 °C gave polymers **2.24·Pd**, **2.24·Ni** and **2.24·Pt** in 99, 95, and 96% yields, respectively.⁶² The Pd- and Pt-based systems **2.24·Pd** and **2.24·Pt** were tan powders whereas the Ni-based polymer **2.24·Ni** was a dark brown powder. Each of the polymers noted above were characterized

by IR spectroscopy, NMR spectroscopy, gel permeation chromatography (GPC), UV-Vis spectroscopy, and TGA; key information is summarized in Table 2.3.

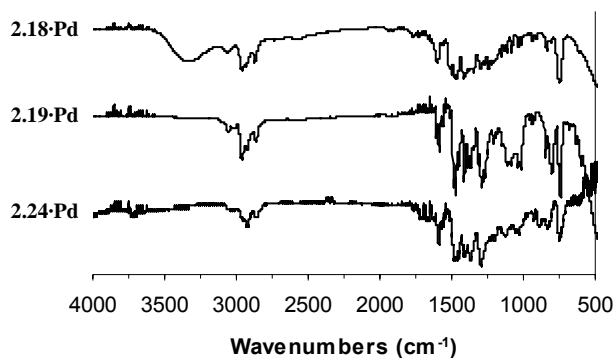
Scheme 2.4 Copolymerization with various transition metals to form organometallic polymers **2.24**



The availability of non-chelated complex **2.18·Pd** allowed for direct comparison of IR spectra obtained for the corresponding chelated monomer (**2.19·Pd**) and its respective polymer (**2.24·Pd**) (Figure 2.9). It was clear that the signal corresponding to the OH stretching frequency at approximately 3330 cm^{-1} was absent in both (small molecule and polymeric) chelated systems. Similar spectra were observed for polymers **2.24·Ni** and **2.24·Pt**, which also supported chelated structures. This was further supported by ^1H NMR spectroscopy as polymers **2.24** did not show any signals indicative of free phenol hydroxyl groups (e.g., $\delta \sim 10\text{ ppm}$ in $\text{DMSO-}d_6$). In general, the ^1H NMR spectra of the polymers **2.24** were broadened and shifted upfield relative to their respective monomer **2.23**. The ^1H NMR signals corresponding to the butyl groups in **2.24** were suggestive of diastereotopic signals for each of the metals used. Specifically, the NCH_2 signals were broad multiplets appearing between 4.1 and 5.0 ppm. Considering the NMR

data in combination with the rapid and exclusive formation of cis isomers in the model systems (**2.19**), the metal centers in **2.24** are assumed to be of high cis content.

Figure 2.9 IR spectra of (top to bottom): **2.18·Pd**, **2.19·Pd**, and **2.24·Pd**



Polymer **2.24·Ni** was only slightly soluble in common polar solvents (e.g., DMSO, DMF, and NMP) which manifested in low molecular weight material as determined by GPC ($M_n = 7.68$ kDa, relative to polystyrene standards). The polydispersity of this polymer was also extraordinarily narrow (PDI = 1.09) which was believed to be due to selective fractionation of insoluble high molecular weight material. In contrast, the Pd- and Pt-based polymers **2.24** were highly soluble in polar solvents and afforded polymers with M_n s of 67.5 and 363 kDa, respectively. The polydispersity indices (PDIs) of these materials were 1.6 and 2.2, respectively and typical of step-growth polymerizations, as expected. Qualitatively, each of the polymers (**2.24·Pd**, **2.24·Ni** and **2.24·Pt**) were found to be stable toward water and oxygen as no signs of degradation (as determined by ¹H NMR spectroscopy and GPC analysis) were observed

upon prolonged standing in wet, aerated solvents. Quantitative thermal gravimetric analysis of polymers **2.24** indicated that their T_d s ranged from 340 to 362 °C. This represented a 50 – 80 °C increase in thermal stability in comparison with their analogous organometallic polymers containing (non-chelating) N-alkyl substituents (e.g., **1.7**, **1.8**, and **1.9**).

Table 2.3 Physical characterization and absorption maxima of polymers **2.24**

Metal	Yield (%) ^a	M_n (kDa) ^b	M_w/M_n	T_d (°C) ^c	λ_{\max} (nm) ^d
Pd	99	67.5	2.20	342	312
Ni	96	7.68 ^e	1.09 ^e	362	322
Pt	95	363	1.59	340	316, 372 (sh)

^aIsolated yields. ^bDetermined by GPC relative to polystyrene standards in DMF with 0.01 M LiBr at 40 °C. ^cThe decomposition temperature (T_d) is defined as the temperature at which 10% weight loss occurs, as determined by thermogravimetric analysis under N₂ with a rate = 10 °C/min. ^dDetermined in DMF under ambient conditions. ^ePoor solubility of **2.24-Ni** resulted in fractionation.

After model metal complexes **2.19** and their respective polymers **2.24** were synthesized, it was possible to independently study and compare the electronic effects resulting from chelation as well as polymerization using UV/Vis spectroscopy (Figure 2.10). The effects of chelation on the overall electronic properties were investigated by comparing non-chelated **2.18-Pd** with chelated analogue **2.19-Pd** (Figure 2.10A). The two spectra nearly overlap which suggested that chelation had minimal impact on the electronic characteristics of the chromophore. Ultimately, this may provide a general means to adjust physical characteristics of NHC-based metal complexes without compromising control over their electronic properties. Additional support was obtained after analyzing polymers **2.24-Pd** (λ_{\max} = 312 nm) values and **2.24-Pt** (λ_{\max} = 316 nm);

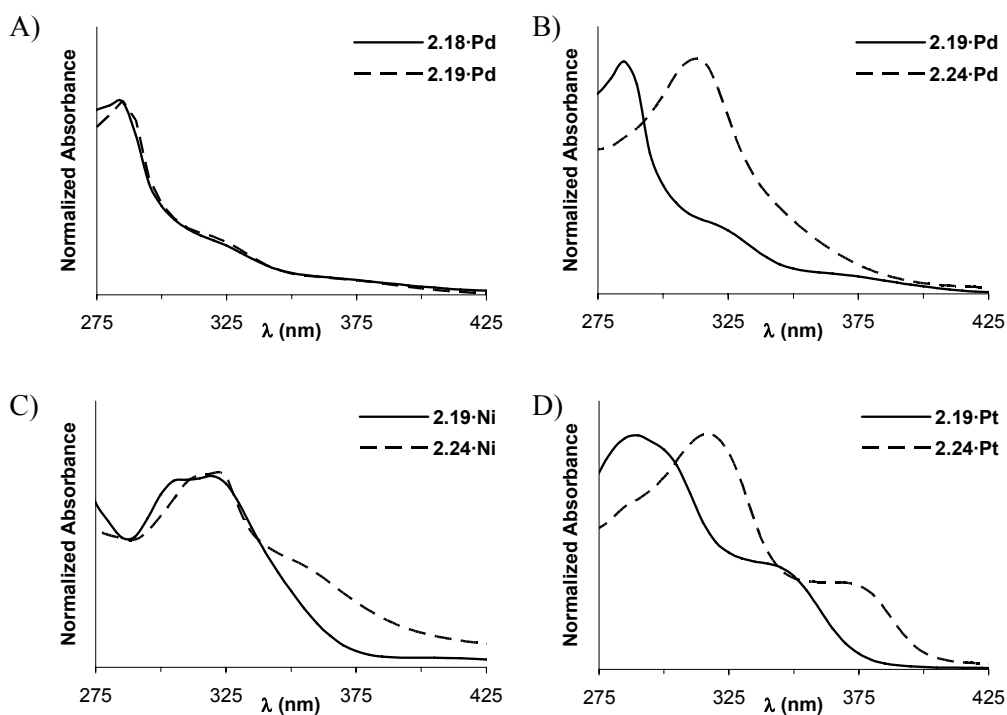
these polymer exhibit λ_{max} values in the same range as similar Pd- and Pt-based polymer that do not contain chelating N-substituents (λ_{max} values from 314 – 329 nm).

To determine if delocalization occurred along the main-chain of polymers **2.24**, we compared each model complex with its corresponding polymer (Figure 2.10B-C). In general, the λ_{max} values of the polymers were bathochromically shifted from their respective model complexes. In particular, Pd- and Pt-based polymers were red-shifted 27 and 26 nm when compared to **2.19-Pd** (Figure 2.11B) and **2.19-Pt** (Figure 2.10C), respectively. In contrast, polymer **2.24-Ni** was red-shifted by only 3 nm relative to model complex **2.19-Ni**, which may be partially explained by fractionation and detection of only low-molecular weight material (see above). The Ni polymer does, however, show increased relative absorption intensities at longer wavelengths (> 335 nm) in comparison with the model system. The electronic fine structures of polymers **2.24** were also in good agreement with those of model complexes **2.19**, as concluded by comparing the topologies of the corresponding spectra. For example, vibronic contributions in the Ni-based systems were manifested in two distinguishable local maxima (Figure 2.10C) between 300 and 325 nm.

The general order of absorption maxima for both the models and polymers was found to be: Ni > Pt ~ Pd. The increased electronic communication between the NHC moiety and the Ni(II) center may be due to the lower electronegativity of Ni in combination with better orbital overlap between the NHC and the smaller Ni center (relative to Pd and Pt). In both the models and the polymers, the Pd- and Pt-based compounds showed similar absorption maxima. This is as would be expected given their nearly identical electronegativities and the observation that **2.19-Pd** and **2.19-Pt** were

isostructural in the solid-state. Overall, the electronic absorption data was encouraging because it supported the possibility of these materials exhibiting long-range, through-metal electron communication.

Figure 2.10 Electronic absorption spectra of metal complexes and related polymers in DMF at room temperature



2.4 Conclusions

In summary, we describe the synthesis and characterization of a series of group 10 metal-carbene complexes and organometallic polymers comprised of a new chelating benzimidazolyliidene. The model complexes were prepared in 91 – 95% yields via direct

metallation of a N-(*o*-phenol) substituted benzimidazolium bromide using Pd(II), Ni(II), or Pt(II) salts. The synthesis of the requisite benzimidazolium salt was completed in three steps in 85% yield from commercial material. This synthesis was borne out through the development of a one-pot reduction/cyclization protocol which converted *o*-nitroanilines to benzimidazoles in high yields. A modular feature of this ligand design is that the final N-substituent (i.e., the butyl group) may be varied to control physical characteristics such as solubility and processability. A ligated but non-chelated Pd(II) complex (**2.18·Pd**) was also obtained which allowed for direct comparison of the effects of chelation on bonding geometry, thermal stability, and electronic characteristics. Interestingly, it was observed that the non-chelated trans Pd complex was converted into the corresponding cis isomer upon chelation, a geometry that was observed for each of the chelated complexes. In addition, chelation provided increased thermal stability which was manifested in a 24 °C increase in T_d in going from **2.18·Pd** to **2.19·Pd**. The structures of the model complexes were supported by NMR and IR spectroscopy, and unambiguously confirmed through X-ray crystallographic analysis. The ^1H NMR spectra of the Ni- and Pt-based complexes displayed diastereotopic butyl groups whereas the Pd complex exhibited no diastereotopicity. Each of the model complexes contained shorter metal- $\text{C}_{\text{carbene}}$ bonds than generally observed for NHC complexes of the same metal species.

These results formed the basis for the design of a new class of organometallic polymers. An annulated benzobis(imidazolium) salt bearing N-(*o*-phenol) substituents was synthesized by a short $\text{S}_{\text{N}}\text{Ar}$, reduction/cyclization, alkylation sequence in 78% overall yield without the need for chromatography. Direct metallation with Pd(II), Ni(II), or Pt(II) salts afforded the respective main-chain organometallic polymers in 95 – 99%

isolated yields. The resulting organometallic polymers contained a benzobis(imidazolylidene) with pendant N-(*o*-phenol) groups that were found to coordinate to transition metals in a chelating type fashion, as confirmed by ^1H NMR and IR spectroscopies. This resulted in polymeric materials with molecular weights up to 363 kDa (relative to polystyrene standards) and PDIs typical of step-growth polymerizations. The polymers showed excellent moisture- and air-stability in both solution and solid-state. TGA analysis of the polymers revealed T_d s ranged from 340 – 362 °C (under nitrogen), which correspond to a 50 – 80 °C increase in thermal stability relative to previously reported, non-chelating polymers of similar composition.

The electronic absorption spectra of the model complexes and their corresponding polymeric materials revealed several promising features. First, chelation has a minimal overall impact on the electronic characteristics of the complexes and polymers. This was confirmed through the comparison of **2.18•Pd** and **2.19•Pd** which displayed nearly overlapping electronic absorption spectra. The λ_{max} values for the model complexes and polymers ranged from 285 - 319 nm and 312 - 322 nm, respectively, depending on the incorporated metal. In each series, λ_{max} increased in the order of Ni > Pt ~ Pd. The polymers each displayed electronic absorption spectra consistent in shape with the corresponding model complexes. The electronic absorption spectra of the polymers were also bathochromically shifted by 3 – 27 nm relative to their respective model systems which suggested an increased delocalization character in the former. Collectively, the data suggested that the thermal stabilities of our previously reported materials were increased without a compromise in their electronic characteristics.

This new series of main-chain NHC-based polymers builds upon our recently reported procedure for preparing analogous polymers by extending the range of transition metals that may be incorporated into the main-chains. Importantly, the new ligand design facilitated the synthesis and characterization of each group 10 system, ultimately revealing that the greatest degree of electronic communication may in fact be in the Ni-based materials. Future efforts will focus on exploring the utility of these materials in catalysis and further examining their physical characteristics with an emphasis on their potential in electronic applications

2.5 Experimental Section

General Considerations: ^1H and ^{13}C NMR spectra were recorded using a Varian Unity Plus 300 or 400 spectrometer and were routinely run using broadband decoupling. Chemical shifts (δ) are expressed in ppm downfield from tetramethylsilane using the residual protonated solvent as an internal standard (DMSO- d_6 , ^1H : 2.49 ppm and ^{13}C : 39.5 ppm; CDCl_3 ^1H : 7.26 ppm and ^{13}C : 77.0 ppm). Coupling constants are expressed in hertz (Hz). HRMS (CI) were obtained with a VG analytical ZAB2-E instrument. UV-vis spectra were recorded using a Perkin Elmer Instruments Lambda 35 spectrometer. Infrared spectra were recorded a Thermo IR200. GPC data was obtained using a Waters HPLC system consisting of HR-1, HR-3, and HR-5E Styragel® columns arranged in series, a 1515 pump, and a 2414 RI detector. Molecular weight data is reported relative to polystyrene standards in DMF (0.01 M LiBr) at 40 °C (column temperature). Decomposition temperatures (T_d s) were determined using a TA Instruments TGA-Q500 under nitrogen atmosphere and were defined as the temperature at which 10% mass loss

occurred. All solvents and reagents were of reagent quality and used as obtained from commercial sources. Chromatography was performed with neutral alumina (Brockmann I, 60-325 mesh).

2-(2-Nitro-phenylamino)-phenol (2.15): 1-Fluoro-2-nitrobenzene (**2.14**) (1.34 g, 9.48 mmol), 2-aminophenol (2.59 g, 23.7 mmol), NaHCO₃ (1.59 g, 18.96 mol), EtOH (10 mL) and a magnetic stirbar were combined in a 20 mL Schlenk flask. The mixture was stirred in an oil bath at 100 °C for 20 h. The cooled reaction mixture was filtered through Celite with the aid of 10 mL CH₂Cl₂ and concentrated. The crude material was taken up in CH₂Cl₂ and filtered through a plug of silica gel (eluting with CH₂Cl₂). Concentration of the resulting red-orange filtrate provided 2.00 g (92% yield) of the desired material. Although this compound was previously reported, complete spectral data were not provided.⁴⁹ ¹H NMR (400 MHz, CDCl₃): δ 9.01 (br s, 1H), 8.21 (dd, *J* = 8.4, 1.6 Hz, 1H), 7.40-7.35 (m, 1H), 7.28-7.20 (m, 2H), 7.07 (dd, *J* = 8.0, 1.2 Hz, 1H), 6.99 (ddd, *J* = 7.8, 7.6, 1.2 Hz, 1H), 6.84-6.79 (m, 1H), 6.77 (dd, *J* = 8.6, 1.4 Hz, 1H), 5.63 (br s, 1H). ¹³C NMR (100 MHz CDCl₃): δ 152.2, 144.0, 136.1, 133.6, 128.9, 127.8, 126.5, 124.9, 121.4, 118.1, 116.3, 116.2. HRMS *m/z* calcd for C₁₂H₁₁N₂O₃ [M+H⁺] 231.0770, found 231.0775.

N-(2-hydroxyphenyl)-benzimidazole (2.16): A 100 mL flask was charged with a magnetic stirbar, formic acid (88%, 60 mL), NaO₂CH (1.77 g, 26.1 mmol), and 10% Pd/C (460 mg, 0.43 mmol Pd). After adding nitroarene **2.15** (2.00 g, 8.69 mmol) to this mixture, this flask was fitted with a H₂O-jacketed condenser and stirred in an oil bath at

110 °C for 7 h. Upon completion, the cooled reaction mixture was filtered through Celite with the aid of 25 mL H₂O and the volume of the filtrate was reduced to approximately 10 mL, under reduced pressure. The acidic solution was then slowly added to a vigorously stirred aqueous solution of saturated Na₂CO₃ (250 mL). The resulting solids were collected by vacuum filtration, rinsed with H₂O, and dried under vacuum to give 2.12 g (93% yield) of monosubstituted benzimidazole **2.16** as a tan solid. This material was routinely used without additional purification. Although this compound was previously reported, complete spectral data were not provided. ¹H NMR (400 MHz, DMSO-*d*₆): δ 8.29 (s, 1H), 7.72 (br s, 1H), 7.34 (d, *J* = 7.6 Hz, 1H), 7.29-7.22 (m, 4H), 7.11 (d, *J* = 8.4 Hz, 1H), 6.89 (t, *J* = 7.2 Hz, 1H); ¹³C NMR (100 MHz, DMSO-*d*₆): δ 152.2, 144.4, 143.0, 134.3, 129.7, 127.5, 122.9, 122.9, 121.9, 119.6, 119.5, 117.0, 111.1. HRMS *m/z* calcd for C₁₃H₁₁N₂O [*M*+H⁺] 211.0871, found 211.0873.

N-Butyl-*N'*-(2-hydroxyphenyl)-benzimidazolium bromide (2.17): In a 20 mL screw-cap vial, benzimidazole **2.16** (347 mg, 1.65 mmol) was dissolved in a mixture of CH₃CN (5.0 mL) and 1-bromobutane (0.53 mL, 4.95 mmol). After adding a magnetic stirbar, the vial was sealed with a Teflon-lined cap, placed in an oil bath at 100 °C and then stirred for 12 h. After cooling to ambient temperature, the reaction mixture was transferred to a round-bottom flask with the aid of 3 mL MeOH. The crude material was then concentrated under reduced pressure to provide benzimidazolium bromide **2.17** as the sole detectable product in >99% yield. Recrystallization from hot CH₂Cl₂/hexanes gave colorless needles. ¹H NMR (400 MHz, DMSO-*d*₆): δ 10.75 (s, 1H), 10.11 (s, 1H), 8.21 (d, *J* = 8.0 Hz, 1H), 7.76-7.69 (m, 3H), 7.58-7.51 (m, 2H), 7.22 (d, *J* = 0.8 Hz, 1H), 7.11

(ddd, $J = 8.0, 7.6, 1.2$ Hz, 1H) 4.59 (t, $J = 7.2$ Hz, 2H), 1.96 (pent, $J = 7.2$ Hz, 2H), 1.39 (sext, $J = 7.2$ Hz, 2H), 0.95 (t, $J = 7.2$ Hz, 3H); ^{13}C NMR (100 MHz, DMSO- d_6): δ 152.2, 143.2, 132.1, 131.7, 130.8, 127.9, 127.2, 126.7, 112.0, 119.8, 117.3, 114.0, 46.8, 30.5, 19.1, 13.4; HRMS m/z calcd for $\text{C}_{17}\text{H}_{19}\text{N}_2\text{O}$ [M^+] 267.1497, found 267.1494.

Palladium dibromide complex 2.18·Pd: After suspending benzimidazolium bromide **2.17** (598 mg, 1.72 mmol) in THF (15 mL), $\text{Pd}(\text{OAc})_2$ (193 mg, 0.86 mmol) was added. The resulting mixture was then vigorously stirred at 50 °C for 2 h, allowed to cool, filtered through a thin pad of alumina, and then concentrated under vacuum to give 639 mg (93% yield) of complex **2.18·Pd** as a tan powder. Crystals suitable for X-ray analysis were obtained by dilution of an NMR sample (in DMSO- d_6) with THF (four-fold by volume) and diffusion of hexanes into this mixture. Anal. calcd for $\text{C}_{34}\text{H}_{36}\text{N}_4\text{O}_2\text{Br}_2\text{Pd}\cdot\text{H}_2\text{O}$: C, 49.99; H, 4.54; N, 7.04; found: C, 49.84; H, 4.43; N, 6.53; ^1H NMR (400 MHz, DMSO- d_6): δ 7.55-7.49 (m, 4H), 7.38 (d, $J = 8.0$ Hz, 2H), 7.33 (dd, $J = 8.2, 1.4$ Hz, 2H), 7.31-7.27 (m, 2H), 7.23-7.18 (m, 4H), 7.01-6.98 (m, 2H), 4.40-4.29 (m, 4H), 1.85-1.79 (m, 4H), 1.29-1.23 (m, 4H), 0.94 (t, $J = 7.4$ Hz, 6H); ^{13}C NMR (75 MHz DMSO- d_6): δ 181.2, 152.2, 136.2, 134.1, 131.1, 130.7, 126.2, 123.5, 121.9, 120.4, 111.3, 110.5, 109.7, 106.7, 48.3, 44.5, 31.4, 20.3, 14.0; IR (KBr): 3331, 3061, 2958, 2931, 2872, 1591, 1500, 1462, 1416, 1344 cm^{-1} ; HRMS m/z calcd for $\text{C}_{34}\text{H}_{36}\text{N}_4\text{O}_2\text{Br}_2\text{Pd}$ [M^+] 794.0245, found 794.0240.

Chelated palladium complex 2.19•Pd: Direct procedure: After dissolving benzimidazolium bromide **2.17** (200 mg, 0.58 mmol) in DMSO (10 mL), Pd(OAc)₂ (58 mg, 0.26 mmol) and NaOAc (48 mg, 0.58 mmol) were added. The reaction mixture was then placed in an oil bath thermostatted at 80 °C and stirred for 2 h at which time NMR spectroscopy revealed complete consumption of **2.17**. The solution was then allowed to cool to ambient temperature and poured into H₂O (25 mL). The resulting precipitates were collected via vacuum filtration and dried under vacuum to give 151 mg (91% yield) of the chelated complex. Step-wise procedure: After dissolving benzimidazolium bromide **2.17** (200 mg, 0.58 mmol) in THF (10 mL), Pd(OAc)₂ (58 mg, 0.26 mmol) was added. The reaction mixture was placed in an oil bath thermostatted at 50 °C and stirred for 2 h. After allowing the mixture to cool to ambient temperature, Na₂CO₃ (256 mg, 2.32 mmol) and MeOH (10 mL) were added. The resulting slurry was stirred for 1 h, poured into H₂O (25 mL), and extracted with EtOAc (3 × 10 mL). The organic extracts were washed with brine (50 mL), dried over Na₂SO₄, filtered through a thin pad of alumina, and concentrated. Flash chromatography on neutral alumina (eluent = Et₂O) provided the desired complex in 88% yield as a yellow-gold powder. Crystals suitable for X-ray analysis were obtained by slow evaporation of a THF/hexanes mixture of the crude product mixture. Anal. calcd for C₃₄H₃₄N₄O₂Pd•0.5H₂O: C, 63.21; H, 5.46; N, 8.55; found: C, 63.81; H, 5.42; N, 8.74; ¹H NMR (400 MHz, CDCl₃): δ 7.89 (dd, *J* = 7.4, 1.0 Hz, 2H), 7.59 (dd, *J* = 8.0, 1.6 Hz, 2H), 7.54 (dd, *J* = 7.4, 1.4 Hz, 2H), 7.39-7.31 (m, 4H), 7.07-6.99 (m, 6H), 6.76 (ddd appearing as td, *J* = 7.4, 1.8 Hz, 2H), 4.86 (t, *J* = 7.6 Hz, 4H), 2.20-2.13 (m, 4H), 1.68-1.58 (m, 4H), 1.03 (t, *J* = 7.6 Hz, 6H); ¹³C NMR (75 MHz CDCl₃): δ 177.7, 160.6, 135.4, 131.6, 130.6, 127.6, 123.5, 122.0, 121.5, 115.1, 112.9,

111, 46.0, 32.8, 20.4, 14.0; IR (KBr): 3057, 3022, 2960, 2929, 2860, 1585, 1473, 1288, 1115, 1084, 1018 cm^{-1} ; HRMS m/z calcd for $\text{C}_{34}\text{H}_{34}\text{N}_4\text{O}_2\text{Pd}$ [M^+] 636.1717, found 636.1721.

Nickel complex 2.19•Ni: The complex was synthesized in analogy to **2.19•Pd** from azolium salt **2.17** (347 mg, 1.0 mmol), $\text{Ni}(\text{OAc})_2 \cdot 4\text{H}_2\text{O}$ (124 mg, 0.50 mmol), and NaOAc (82 mg, 1.0 mmol) in DMSO (4.0 mL). Recrystallization of the crude material from CH_2Cl_2 /hexanes gave 280 mg (95% yield) of the desired product as a yellow solid. Alternatively, the crude material could be purified by flash chromatography on neutral alumina (eluent = Et_2O). Crystals suitable for X-ray analysis were obtained by slow diffusion of hexanes into a THF solution of the crude product mixture. Anal. calcd for $\text{C}_{34}\text{H}_{34}\text{N}_4\text{O}_2\text{Ni} \cdot \text{H}_2\text{O}$: C, 67.23; H, 5.97; N, 9.22; found: C, 67.23; H, 5.83; N, 9.17; ^1H NMR (400 MHz, CDCl_3): δ 7.91-7.89 (m, 2H), 7.67 (d, $J = 7.2$ Hz, 2H), 7.39 (d, $J = 8.4$ Hz, 2H), 7.30-7.29 (m, 6H), 7.17 (t, $J = 7.2$ Hz, 2H), 6.80 (t, $J = 7.4$ Hz, 2H), 4.23-4.16 (m, 2H), 3.64-3.57 (m, 2H), 2.32-2.28 (m, 2H), 1.32-1.24 (m, 4H), 1.11-1.04 (m, 2H), 0.55 (t, $J = 7.0$ Hz, 6H); ^{13}C NMR (75 MHz, CDCl_3): δ 172.5, 158.9, 135.3, 132.2, 128.2, 128.1, 123.72, 123.67, 122.4, 120.1, 113.9, 112.2, 109.9, 48.3, 32.1, 20.2, 13.3; IR (KBr): 3059, 3037, 2962, 2933, 2862, 1585, 1487, 1275, 1115, 1020 cm^{-1} ; HRMS m/z calcd for $\text{C}_{34}\text{H}_{35}\text{N}_4\text{O}_2\text{Ni}$ [$\text{M}+\text{H}^+$] 589.2113, found 589.2115.

Platinum complex 2.19•Pt: The complex was synthesized in analogy to **2.19•Pd** from azolium salt **2.17** (120 mg, 0.35 mmol), PtCl_2 (41 mg, 0.16 mmol), and NaOAc (62 mg, 0.76 mmol) in DMSO (3.0 mL). Recrystallization of the crude material from

CH₂Cl₂/hexanes gave 108 mg (93% yield) of the desired product as a white solid. Alternatively, the crude material could be purified by flash chromatography on neutral alumina (eluent = 10% CH₂Cl₂/Et₂O). Crystals suitable for X-ray analysis were obtained by slow evaporation of a THF solution of the purified complex. Anal. calcd for C₃₄H₃₄N₄O₂Pt·0.5H₂O: C, 55.58; H, 4.80; N, 7.63; found: C, 55.35; H, 4.40; N, 7.20; ¹H NMR (400 MHz, CDCl₃): δ 7.93-7.91 (m, 2H), 7.59 (dd, *J* = 7.6, 1.6 Hz, 2H), 7.44 (dd, *J* = 8.4, 1.2 Hz, 2H), 7.39-7.30 (m, 6H), 7.23-7.19 (m, 2H), 6.79 (ddd appearing as td, *J* = 8.0, 1.2 Hz, 2H), 4.05-3.98 (m, 2H), 3.84-3.76 (m, 2H), 2.19-2.01 (m, 2H), 1.56-1.45 (m, 2H), 1.18-1.02 (m, 4H), 0.57 (t, *J* = 7.4 Hz, 6H); ¹³C NMR (75 MHz, CDCl₃): δ 160.8, 157.8, 134.6, 132.2, 128.5, 128.2, 123.9, 123.8, 122.4, 121.2, 114.8, 112.8, 110.3, 48.1, 31.1, 20.0, 13.2; IR (KBr): 3061, 3030, 2964, 2933, 2874, 2862, 1585, 1489, 1473, 1294, 1113, 1038, 1020 cm⁻¹; HRMS *m/z* calcd for C₃₄H₃₅N₄O₂Pt [M+H⁺] 726.2408, found 726.2402.

1,5-Bis[(2-hydroxyphenyl)amino]-2,4-dinitrobenzene (2.21): A 500 mL flask was charged with 1,5-dichloro-2,4-dinitrobenzene (10.0 g, 42.2 mmol), 2-aminophenol (18.4 g, 169 mmol), EtOH (250 mL) and a magnetic stir bar. The flask was equipped with a H₂O-jacketed condenser and the mixture was heated under reflux for 48 h. The resulting red solution was allowed to cool to ambient temperature and the volume was reduced to approximately half its original volume under reduced pressure. The red slurry was then poured into H₂O (200 mL) and allowed to stand for 1 h. The red solids that had formed were collected by vacuum filtration, rinsed with H₂O, and dried under vacuum to give **2.21** (15.9 g, 99% yield). Although this material was routinely used without additional

purification, recrystallization from hot MeOH/H₂O affords orange-red crystals. ¹H NMR (400 MHz, DMSO-*d*₆): δ 9.64 (br s, 2H), 9.04 (s, 1H), 7.21 (dd, *J* = 7.6, 1.2 Hz, 2H), 7.03 (t, *J* = 6.8 Hz, 2H), 6.92 (d, *J* = 7.4 Hz, 2H), 6.76 (t, *J* = 7.0 Hz, 2H), 6.30 (s, 1H); ¹³C NMR (100 MHz DMSO-*d*₆): δ 150.8, 145.6, 128.3, 127.0, 125.0, 124.7, 124.6, 119.2, 116.3, 95.5; HRMS *m/z* calcd for C₁₈H₁₄N₄O₆ [*M*⁻] 382.0913, found 382.0912.

Benzobis(imidazole) 2.22: In an 500 mL flask, a suspension of 10% Pd/C (1.0 g, 0.94 mmol Pd) and NaO₂CH (22.6 g, 333 mmol) in formic acid (88%, 250 mL) was treated with dinitroarene **2.21** (10.6 g, 27.7 mmol) in several portions. The flask was then equipped with a H₂O-jacketed condenser and the mixture was heated under reflux for 48 h. Upon completion, the mixture was allowed to cool to ambient temperature, filtered through Celite and washed with 50 mL H₂O. The filtrate volume was then reduced under vacuum to approximately 50 mL and then slowly added to a stirred aqueous solution saturated with Na₂CO₃. The resulting precipitate was collected by vacuum filtration, rinsed with H₂O, and dried under vacuum to give benzobis(imidazole) **2.22** (8.1 g, 85% yield) as a tan powder. The material was routinely used without additional purification. ¹H NMR (400 MHz, DMSO-*d*₆): δ 10.2 (br s, 2H), 8.31 (s, 2H), 8.02 (s, 1H), 7.39 (d, *J* = 7.6 Hz, 2H), 7.30 (t, *J* = 7.6 Hz, 2H), 7.08 (d, *J* = 8.4 Hz, 2H), 6.95 (t, *J* = 7.2 Hz, 2H), 6.91 (s, 1H). ¹³C NMR (75 MHz DMSO-*d*₆): δ 152.2, 145.0, 140.1, 132.3, 129.6, 127.6, 123.2, 119.7, 117.1, 108.4, 90.9; HRMS *m/z* calcd for C₂₀H₁₄N₄O₂ [*M*⁻] 342.1117, found 342.1112.

Benzobis(imidazolium) dibromide 2.23: A Schlenk flask was charged with DMF (100 mL), benzobis(imidazole) **2.22** (11.8 g, 34.5 mmol), 1-bromobutane (22.2 mL, 207 mmol), and a magnetic stirbar. After sealing the flask, the resulting slurry was stirred at 110 °C for 48 h during which time the mixture became homogenous for a short period of time and then heterogeneous. Subsequently, the cooled mixture was poured into PhCH₃ (200 mL) and the solids were collected by vacuum filtration, rinsed with THF, and dried under vacuum. Recrystallization from MeOH/THF mixture (1:3 v/v) gave 19.8 g (93% yield) of the bis(azolium) salt as a tan powder. ¹H NMR (400 MHz, DMSO-*d*₆): δ 10.77 (br s, 2H) 10.52 (s, 2H), 9.46 (s, 1H), 7.72 (dd, *J* = 8.0, 1.2 Hz, 2H), 7.53-7.49 (m, 3H), 7.22 (d, *J* = 8.4 Hz, 2H), 7.09 (t, *J* = 8.2 Hz, 2H), 4.80 (t, *J* = 6.8 Hz, 4H), 2.08 (pent, *J* = 7.4 Hz, 4H), 1.46 (sext, *J* = 7.4 Hz, 4H), 0.97 (t, *J* = 7.2 Hz, 6H), ¹³C NMR (75 MHz DMSO-*d*₆): δ 152.2, 147.0, 132.5, 130.9, 130.0, 128.1, 120.0, 119.7, 117.5, 100.0, 98.9, 47.6, 30.2, 19.1, 13.5; HRMS *m/z* calcd for C₂₈H₃₁N₄O₂ [M-H⁺] 455.2447, found 455.2447.

General polymerization procedure: After dissolving bis(azolium) dibromide **2.23** (1.0 mmol, 1.0 equiv) in DMSO (5 mL), metal salt (1.0 mmol, 1.0 equiv) and NaOAc (2.0 mmol, 2.0 equiv if Ni(OAc)₂; 4.0 mmol, 4.0 equiv if PdCl₂ or PtCl₂) were then added to the reaction vessel. The resulting solution was then stirred at 80 °C for 24 – 48 h and monitored by ¹H NMR spectroscopy.⁶² Upon completion, the mixture was allowed to cool and added dropwise into H₂O (50 mL). The resulting precipitate was collected via vacuum filtration, rinsed with H₂O and dried under vacuum.

Polymer 2.24•Pd: ^1H NMR (400 MHz, DMSO- d_6): δ 8.15 (br, 2H), 7.40-6.80 (br, 8H), 4.40-5.00 (br, 4H), 2.15 (br, 4H), 1.45 (br 4H), 1.00 (br, 6H); IR (KBr): 3067, 2966, 2954, 2882, 1594, 1486, 1421, 1381, 1301 cm^{-1} .

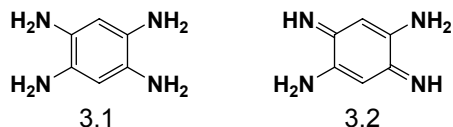
Polymer 2.24•Ni: ^1H NMR (400 MHz, DMSO- d_6): δ 8.02 (br 2H), 7.58-7.21 (br, 4H), 7.20-6.75 (br, 4H), 4.05-4.62 (br, 4H), 2.00 (br, 4H), 1.40 (br, 4H), 0.94 (br, 6H); IR (KBr): 3143, 3038, 2962, 2952, 2898, 1594, 1489, 1414, 1376, 1301 cm^{-1} .

Polymer 2.24•Pt: ^1H NMR (400 MHz, DMSO- d_6): δ 8.05 (br, 2H), 7.55-7.25 (br, 4H), 7.20-6.90 (br, 4H), 4.38-4.99 (br, 4H), 2.01 (br, 4H), 1.40 (br, 4H), 0.95 (br, 6H); IR (KBr): 3097, 3051, 2971, 2949, 2899, 2881, 1597, 1483, 1444, 1381, 1307 cm^{-1} .

Chapter 3: Highly Efficient Synthesis and Solid-State Characterization of 1,2,4,5-Tetrakis(alkyl- and arylamino)benzenes and Cyclization to their Respective Benzobis(imidazolium) Salts

3.1 Introduction

As a general class of highly electron-rich molecules, tetraaminobenzenes have seen a rich diversity of chemical applications. For example, 1,2,4,5-tetraaminobenzene⁶³ (**3.1**) and its oxidized derivative, 2,5-diamino-1,4-quinonediimine⁶⁴ (**3.2**), have found great utility in organic, organometallic, and macromolecular chemistry. They have been used as ditopic ligands in coordination chemistry,⁶⁵ as pH-dependent chromophores,⁶⁶ as difunctional monomers in the synthesis of main-chain organometallic⁶⁷ and supramolecular polymers,⁶⁸ and as π -complexation partners in supramolecular systems.⁶⁹



While **3.1**⁷⁰ is commercially available (as its tetrahydrochloride salt, i.e., **1.1**), access to its N,N',N'',N'''-tetra(alkyl and aryl) derivatives remains synthetically challenging due to the high propensity of these electron rich arenes to oxidize during isolation. For example, Braunstein obtained a variety of N,N',N'',N'''-tetraalkyl 2,5-diamino-1,4-benzoquinonediimines by reducing their respective 1,2,4,5-tetraamidobenzenes under aerobic conditions.^{65,66} Similarly, azophenines are generally obtained upon condensation of *o*-benzoquinone dioxime^{63,71} or N,N'-diphenylsulfonyl-

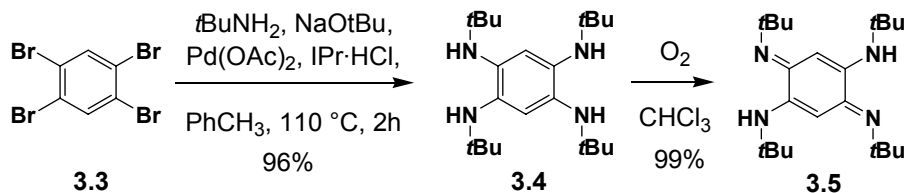
quinonediimine⁷² with various arylamines. More recently, in a breakthrough report by Harlan,⁷³ exhaustive Buchwald-Hartwig⁷⁴ Pd-catalyzed amination of 1,2,4,5-tetrabromobenzene with 2,6-dimethylaniline provided mixtures of the respective tetra(arylamino)benzene and azophenine in a promising 26% yield.⁷⁵ With these considerations in mind, we considered the possibility that large N-substituents (desired for bis(azolium) compounds) could serve a dual purpose to slow down (or even eliminate) undesired oxidative pathways and facilitate isolation of the targeted tetraamines.

3.2 Four-fold aryl amination

Inspired by Harlan's report,⁷³ we examined the Pd-catalyzed cross coupling of *tert*-butylamine with 1,2,4,5-tetrabromobenzene (**3.3**) under basic conditions as shown in Scheme 3.1. The reaction was performed in toluene (0.2 M) using 1,3-bis(2,6-diisopropylphenyl)imidazolyliidene·HCl^{26b} (IPr·HCl) / Pd(OAc)₂⁷⁶ (2:1 stoichiometry; 1 mol % Pd relative to **3.3**) as the catalyst precursor.⁷⁷ Surprisingly, after less than 1 h at 110 °C, a colorless solid precipitated from the reaction solution which was subsequently isolated in 96% yield via filtration under a cone of nitrogen.⁷⁸ The ¹H NMR spectrum of this compound exhibited a single, diagnostic signal at $\delta = 6.53$ ppm (solvent = CDCl₃) which was indicative of highly symmetric structure consistent with the desired 1,2,4,5-tetrakis(*tert*-butylamino)benzene (**3.4**). To confirm, a crystal suitable for X-ray crystallography was obtained by slow cooling of a hot saturated solution of **3.4** in toluene; an ORTEP diagram of the corresponding structure is shown in Figure 3.1 (left). Notably, the four nitrogen atoms were found to be co-planar with nearly equivalent N-C

(1.43-1.44 Å) and aryl C-C (1.39-1.41 Å) bond distances. In addition, the *tert*-butyl groups on the nitrogen atoms were situated above and below the plane of the arene ring with dihedral angles (C4-N1-C1-C2 and C8-N2-C2-N1) of 120-121°.

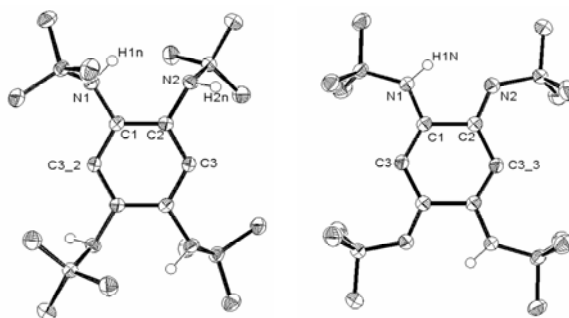
Scheme 3.1 Synthesis of 1,2,4,5-tetra(*tert*-butylamino)benzene (**3.4**) and its related 2,5-diamino-1,4-quinonediimine (**3.5**)



To compare **3.4** directly with its corresponding 2,5-diamino-1,4-quinonediimine, the tetramine was dissolved in CHCl₃ and stirred under an atmosphere of oxygen at room temperature.⁷⁹ The ¹H NMR spectrum (solvent = CDCl₃) of this compound exhibited a signal at $\delta = 5.53$ ppm which was consistent^{65h,66} with quinoid-derivative **3.5** (Scheme 3.1). Crystals of azophenine **3.5** suitable for X-ray analysis were also obtained which allowed for direct comparison of the related species. As shown in Figure 3.1 (right), the ORTEP diagram of **3.5** exhibited not only co-planar *tert*-butyl groups (with dihedral angles of 175-179°), but also varied N-C (N1-C1, 1.35 Å and N2-C2, 1.29 Å) and aryl C-C (1.51 Å, 1.37 Å, and 1.44 Å) bond lengths. This type of bonding pattern has been previously described^{65h,66} and is fully consistent with related azophenine solid-state structures.^{65h,66,73} To our knowledge, this is the first example of a crystalline 1,2,4,5-tetrakis(alkylamino)benzene and a direct comparison with its oxidized derivative. More importantly, the collective data suggested that the synthetic methodology detailed above

was successful in preparing and isolating bona fide N,N',N'',N'''-tetra(alkyl) 1,2,4,5-tetraminobenzenes.

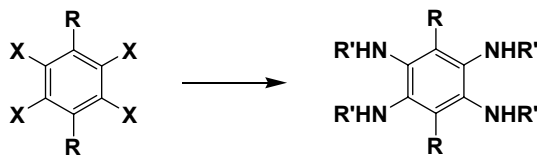
Figure 3.1 (left) ORTEP representation of the X-ray crystal structure of 1,2,4,5-tetra(*tert*-butylamino)benzene (**3.4**), showing non-hydrogen atoms as 50% thermal ellipsoids. (right) ORTEP representation of the X-ray crystal structure of N,N',N'',N'''-tetrakis(*tert*-butyl) 1,4-diamino-2,5-benzoquinone-diimine (**3.5**), showing non-hydrogen atoms as 50% thermal ellipsoids.



Selected bond lengths (Å) and degrees (°) for **3.4**: N1-C1, 1.429(2); N2-C2, 1.441(2); C1-C2, 1.411(2); C2-C3, 1.394(2); C1-C3_2, 1.394(2); N1-C1-C2, 121.1(1); N2-C2-C1, 119.6(1); C2-C1-N1-C4, 109.8(1); C1-C2-N2-C8, 99.8(2). Selected bond lengths (Å) and degrees (°) for **3.5**: N1-C1, 1.349(1); N2-C2, 1.294(1); C1-C2, 1.513(1); C1-C3, 1.367(1); C2-C3_3, 1.437(1); N1-C1-C2, 113.0(1); N2-C2-C1, 113.9(1); C2-C1-N1-C4, 175.1(1); C1-C2-N2-C8, 179.4(1).

Prompted by these results and using the protocol described above, a variety of other amines were probed for their ability to couple with **3.3**. As expected, the coupling of 1-adamantyl amine (AdNH₂) with **3.3** afforded similar results as *t*BuNH₂ (90% yield; Table 3.1, Entry 2). Aryl amines including aniline, relatively bulky mesitylamine,⁸⁰ and electron-rich *o*-anisidine were also found to successfully couple to **3.3** in excellent yields

(Entries 3 - 5). Unfortunately, primary (i.e., 1-butylamine), secondary (i.e., cyclohexylamine), or electron deficient aryl amines (nitro- and chloroanilines) either resulted in no reaction or afforded complex product mixtures. It is noteworthy that cross-coupling of 2,3,5,6-tetrabromo-*p*-xylene and 1,2,4,5-tetrachlorobenzene with *t*BuNH₂ afforded the corresponding tetraamines in 99 and 94% yields, respectively (Entries 6 and 7). The former result suggested that the bulky IPr-ligated Pd catalyst was not impeded by the presence of steric bulk *ortho* to both sites of amination and was a testament to the high activity of this catalyst system.

Table 3.1 Synthesis of various 1,2,4,5-tetra(N-substituted)benzenes^a

entry	tetrahalobenzene		amine	product	yield
	X	R			
1	Br	H	<i>t</i> BuNH ₂	3.4	96%
2	Br	H	AdNH ₂	3.6	90%
3	Br	H	PhNH ₂	3.7	76%
4	Br	H	MesNH ₂	3.8	94%
5	Br	H	2-MeOPhNH ₂	3.10	96%
6	Br	Me	<i>t</i> BuNH ₂	3.11	99%
7	Cl	H	<i>t</i> BuNH ₂	3.4	94%

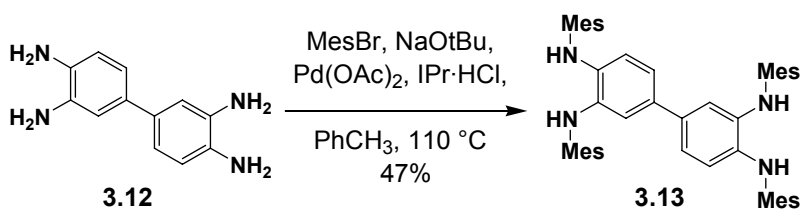
^aGeneral reaction conditions: IPr•HCl (0.04 equiv); Pd(OAc)₂ (0.02 equiv); NaOtBu (4.1 equiv); RNH₂ (4.1 equiv); solvent = toluene, temp = 110 °C. Isolated yields are indicated. *t*BuNH₂ = *tert*-butyl amine; AdNH₂ = 1-adamantyl amine; PhNH₂ = aniline; MesNH₂ = 2,4,6-trimethylaniline; 2-MeOPhNH₂ = *o*-anisidine.

After the 1,2,4,5-tetrakis(alkyl- and arylamino)-benzenes were synthesized, their relative susceptibilities toward oxidation were qualitatively investigated.⁸¹ The amines were independently dissolved in aerated CDCl₃ and examined by ¹H NMR spectroscopy periodically over time. In general, the 1,2,4,5-tetrakis(alkylamino)benzenes were found to oxidize slower ($\tau_{1/2}$ ~ days) than their N-aryl analogues ($\tau_{1/2}$ ~ hours). However, the electron-rich N-anisidyl derivative **3.10** was exceptional and was found to exhibit stability comparable to the N-alkyl derivatives (**3.4** and **3.6**). The most stable tetraamine

was the xylene derivative **3.11** which resisted oxidation even after dissolution in aerated solvents for several weeks. These results may be rationalized by examining individual sterics and electronic contributors which may kinetically and/or thermodynamically inhibit nitrogenyl formation.⁸² As expected, electronically rich and sterically hindered tetraamines show lower propensities to undergo oxidation.

Thus far we have demonstrated that various tetrakis(aryl and alkylamino)arenes can be prepared via aryl amination from their corresponding tetrahaloarene. However, in situations when the requisite polyhalogenated arenes are not readily available (e.g., 3,3',4,4'-tetrachlorobiphenyl⁸³), a complementary route to the respective tetrakis(amino)arenes would be desirable. As shown in Scheme 3.3, mesityl bromide was coupled to commercially available 3,3'-diaminobenzidine **3.12** using the catalyst system and conditions discussed above to afford the corresponding N,N',N'',N'''-tetramesityl 3,3'-diaminobenzidine (**3.13**) in 47% yield (Scheme 3.3).⁸⁴

Scheme 3.3 Synthesis of tetrakis(arylamino)arenes

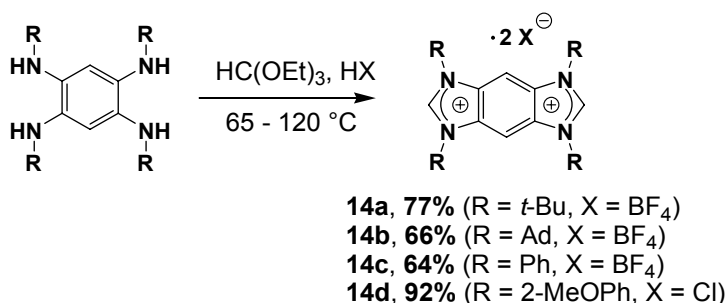


3.3 Formylative cyclization to produce benzobis(imidazolium) salts

With the tetraamines in hand we were poised to complete the synthesis of the desired N-aryl and bulky N-alkyl benzobis(imidazolium) salts (Scheme 3.4).⁸⁵ Using HCl

in HC(OEt)₃ at elevated temperatures was successful in cyclizing N-anisidyl substrate **3.10** in high (92%) yield. Although this substrate underwent clean cyclization within 2 h, other compounds were sluggish apparently due to solubility limitations of monocyclized intermediates. Gratifyingly, switching to HBF₄ in place of HCl sufficiently improved solubility such that each of the remaining substrates could be cyclized efficiently. Ultimately we found the N-mesityl tetraamine **3.8** was reluctant to undergo cyclization under a variety of conditions.

Scheme 3.4 Cyclization of tetraamines to give bis(azolium) salts



3.4 Conclusions

In summary, we have developed an efficient synthetic and isolation protocol for preparing 1,2,4,5-tetrakis(alkyl- and arylamino)benzenes, two elusive classes of electron rich arenes. Their structures were unambiguously proven using X-ray crystallography and compared with their oxidized derivatives. Immediate efforts will concentrate on expanding the substrate scope of this reaction and elucidating its unique substitution pattern. The tetraamines were successfully cyclized to give the desired bis(azolium) compounds in good to excellent yields. Currently we are also investigating applications

of the bis(azolium) salts for direct formation of non-chelating bis(carbene)s as well as their respective discrete bimetallic complexes.

3.5 Experimental Section

General Considerations: All reactions were conducted under an atmosphere of nitrogen using standard Schlenk techniques or in a nitrogen-filled glove-box. CHCl_3 was degassed by two freeze-pump-thaw cycles and stored over 4Å molecular sieves and K_2CO_3 . Hexanes were distilled from CaH_2 and degassed by two freeze-pump-thaw cycles. THF and toluene were freshly distilled from Na/benzophenone and degassed by two freeze-pump-thaw cycles. All reagents were purchased from Aldrich or Acros and were used without further purification. ^1H NMR spectra were recorded using a Varian Gemini (300 MHz or 400 MHz) spectrometer. Chemical shifts are reported in delta (δ) units, expressed in parts per million (ppm) downfield from tetramethylsilane using the residual protonated solvent as an internal standard (CDCl_3 , 7.24 ppm; C_6D_6 , 7.15 ppm). ^{13}C NMR spectra were recorded using a Varian Gemini (100 MHz) spectrometer. Chemical shifts are reported in delta (δ) units, expressed in parts per million (ppm) downfield from tetramethylsilane using the solvent as an internal standard (CDCl_3 , 77.0 ppm; C_6D_6 , 128 ppm). ^{13}C NMR spectra were routinely run with broadband decoupling. High-resolution mass spectra (HRMS) were obtained with a VG analytical ZAB2-E or a Karatos MS9 instrument and are reported as m/z (relative intensity).

1,2,4,5-Tetrakis-N-*tert*-butylaminobenzene (3.4). A catalyst for mediating aryl-amination coupling reactions was prepared by charging a 20 mL vial with 1,3-bis(2,6-

diisopropylphenyl)imidazolium chloride (0.127 g, 0.3 mmol), NaOtBu (0.03 g, 0.3 mmol), Pd(OAc)₂ (0.04 g, 0.17 mmol), toluene (5 mL), and a stir bar followed by stirring this mixture at 80 °C for 10 minutes. The catalyst solution was added to a 250 mL flask containing 1,2,4,5-tetrabromobenzene (2.22 g, 5.64 mmol) suspended in toluene (100 mL). *tert*-Butyl amine (1.73 g, 23.7 mmol) and NaOtBu (2.65 g, 27.6 mmol) were then added and the resulting mixture was sealed and stirred at 105 °C overnight. After cooling to ambient temperature, precipitated solids were collected by filtration under a cone of nitrogen, dissolved in degassed CHCl₃ (100 mL), and filtered to remove residual NaBr salts. Solvent was then removed under reduced pressure to afford 1.96 g (96% yield) of the desired product as a gray solid. Note: the product slowly oxidizes to the corresponding benzoquinonediiimine over several days in aerated solutions. As a solid, the product is bench stable for >months. ¹H NMR (CDCl₃): δ 6.53 (s, 2H), 3.73 (br, 4H), 1.22 (s, 36H); ¹³C NMR (CDCl₃): δ 131.7, 115.5, 52.0, 30.0. HRMS calcd. for C₂₂H₄₂N₄: 362.3409; Found, 362.3406.

N,N'-di(*tert*-butylamino)-1,4-di(*tert*-butylamino)-2,5-benzoquinone-diiimine (3.5).

Compound **3.4** was dissolved in CHCl₃ and stirred under a balloon of oxygen for 24 hours followed by removal of solvent to obtain a yellow powder. Alternatively, oxidation can be effected in less than 5 minutes by adding an excess of H₂O₂: ¹H NMR (CDCl₃) δ 5.53 (s, 2H), 1.35 (s, 36H); ¹³C NMR (CDCl₃) δ (ca 138), 90.8, 52.0, 29.8; HRMS calcd. for C₂₄H₄₁N₄: 361.3331, found: 361.3326.

1,2,4,5-Tetrakis-N-adamantylaminobenzene (3.6). The aryl amination was performed in a manner analogous to the synthesis of **3.4**. Upon completion, the cool reaction mixture was filtered in a drybox to afford a beige solid. The solids were rinsed with toluene and extracted with degassed CHCl_3 and the extract was concentrated under reduced pressure to afford 21.5 g (90% yield) of the desired product as a white powder. Note: the product slowly oxidizes to the corresponding benzoquinonediimine over several days in aerated solutions. As a solid, the product is bench stable for >months. ^1H NMR (CDCl_3): δ 6.59 (s, 2H), 2.06 (br, 12H), 1.81 (br, 24H), 1.66-1.58 (br, 24H); ^{13}C NMR (CDCl_3): δ 131.3, 117.8, 52.5, 43.7, 36.6, 29.8. HRMS calcd. for $\text{C}_{46}\text{H}_{66}\text{N}_4$: 674.5287; Found, 674.5286.

1,2,4,5-Tetrakis-N-phenylbenzene (3.7). The aryl amination was performed in a manner analogous to the synthesis of **3.4**. Upon completion, the cool reaction mixture was filtered in a drybox to afford a beige solid. The solids were rinsed with toluene and extracted with degassed CHCl_3 and the extract was concentrated under reduced pressure to afford 1.78 g (76 %) of the desired product as a light pink powder: ^1H NMR (CDCl_3): δ 7.24-7.19 (br m, 12H), 6.9-6.84 (br, 12H), 5.56 (s, 2H); ^{13}C NMR (CDCl_3): δ 144.5, 130.6, 129.3, 120.2, 116.6, 113.9; HRMS calcd. for $\text{C}_{30}\text{H}_{25}\text{N}_4$: 441.2074; found: 441.2074.

1,2,4,5-Tetrakis(2,4,6-trimethylphenylamino)benzene (3.8): The aryl amination was performed in a manner analogous to the synthesis of **3.4**. Upon completion, the cool reaction mixture was filtered in a drybox to afford a beige solid. The solids were rinsed

with toluene and extracted with degassed CHCl_3 and the extract was concentrated under reduced pressure to afford 2.71 g (94%) of the desired product as a white powder: ^1H NMR (CDCl_3): δ 6.75 (s, 8H), 5.40 (s, 2H), 4.86 (br s, 4H), 2.22 (s, 12H), 2.05 (s, 24 H); ^{13}C NMR (CDCl_3): δ 137.9, 132.6, 132.1, 129.4, 129.0, 105.3, 20.6, 18.2; HRMS m/z calcd for $\text{C}_{42}\text{H}_{49}\text{N}_4$: 609.3978, found: 609.3952.

Mesityl-derived azophenine (3.9): The tetraamine was stirred in CHCl_3 open air for 2 h. The mixture was concentrated to give an orange-red solid in quantitative yield. ^1H NMR (CDCl_3): δ 6.79 (s, 4H), 6.75 (s, 4H), 5.40 (s, 2H), 4.61 (s, 2H), 2.23 (s, 12H), 2.07 (s, 12H), 2.05 (s, 12H); ^{13}C NMR (CDCl_3): δ 137.9, 132.6, 132.1, 129.4, 129.0, 128.6, 88.9, 20.8, 20.6, 18.2, 18.0; HRMS m/z calcd for $\text{C}_{42}\text{H}_{49}\text{N}_4$: 609.3956, found: 609.3952.

1,2,4,5-Tetrakis(2-methoxyphenylamino)benzene (3.10): The aryl amination was performed in a manner analogous to the synthesis of **3.4**. Upon completion, the cool reaction mixture was filtered in a drybox to afford a beige solid. The solids were rinsed with toluene and extracted with degassed CHCl_3 and the extract was concentrated under reduced pressure to afford 6.92 g (96%) of the desired product as an off-white powder. Alternatively, the cooled reaction mixture was opened under a cone of nitrogen and HCl (2 mL) in MeOH (10 mL) was added quickly to produce a deep purple slurry. The mixture was poured into H_2O (25 mL) and the solids were collected via vacuum filtration, rinsed with H_2O and Et_2O , and dried under vacuum to provide the tetrahydrochloride salt as a light purple solid in nearly quantitative yield: ^1H NMR (CDCl_3): δ 7.33 (s, 2H), 7.06-7.04 (m, 4H), 6.86-6.76 (m, 12H), 6.02 (br s, 4H), 3.82 (s,

12 H); ^{13}C NMR (CDCl_3): δ 148.2, 134.4, 130.5, 121.0, 119.1, 114.4, 110.3, 114.2, 55.5; HRMS m/z calcd for $\text{C}_{34}\text{H}_{35}\text{N}_4\text{O}_4$: 563.2606, found 563.2653.

1,2,4,5-Tetrakis(*tert*-butylamino)-*para*-xylene (3.11). The aryl amination was performed according to the General Procedure. Upon completion, the cool reaction mixture was filtered over Celite under a cone of nitrogen with the aid of degassed toluene. The filtrate was concentrated under reduced pressure to afford 2.7g (99%) of the desired product as a brown solid. It should be noted that the product is bench stable in aerated solutions for >months: ^1H NMR (CDCl_3): δ 3.39 (br, 4H), 2.28 (s, 6H), 1.06 (s, 36H); ^{13}C NMR (CDCl_3): δ 138.1, 128.2, 55.3, 30.7, 18.6; HRMS m/z calcd. for $\text{C}_{24}\text{H}_{46}\text{N}_4$: 390.3722, found, 390.3719.

3,3',4,4'-Tetrakis(2,4,6-trimethylphenylamino)biphenyl (3.13). A catalyst for mediating aryl-amination coupling reactions was prepared by charging a 10 mL vial with 1,3-bis(2,6-diisopropylphenyl)imidazolium chloride (86 mg, 0.02 mmol), NaOtBu (3 mg, 0.03 mmol), $\text{Pd}(\text{OAc})_2$ (30 mg, 0.01 mmol), toluene (3 mL), and a stir bar followed by stirring this mixture at 23 °C for 10 minutes. 2-Bromomesitylene (410 mg, 2.05 mmol) was added to the catalyst solution. 3,3'-diaminobenzidine (110 mg, 0.5 mmol) and $\text{NaO-}t\text{Bu}$ (0.20 g, 2.05 mmol) were then added and the resulting mixture was sealed and stirred at 110 °C overnight. After cooling to ambient temperature, precipitated solids (NaBr) were removed by filtration under a cone of nitrogen. Solvent was removed under reduced pressure. Analysis of the crude product showed that the reaction was >98% complete. Crude product was triturated with hexanes and then dried under reduced pressure to

afford 160 mg (47 % yield) of the desired product as a grey solid: ^1H NMR (CDCl_3): δ 6.94 (s, 8H), 6.68-6.66 (m, 2H), 6.27-6.24 (m, 4H), 5.18 (br, 2H), 4.99 (br, 2H), 2.36 (br, 6H), 2.31 (s, 6H), 2.17 (s, 12H), 2.13 (s, 12H); ^{13}C NMR (CDCl_3): δ 137.11, 137.06, 136.7, 135.7, 135.6, 134.0, 133.9, 133.54, 133.48, 133.3, 133.2, 133.1, 129.30, 129.26, 117.8, 114.7, 112.4, 20.9, 20.8, 18.1, 18.0; HRMS m/z calcd for $\text{C}_{48}\text{H}_{55}\text{N}_4$: 687.4427, found: 647.4423.

Tetrakis(*tert*-butyl) benzobis(imidazolium) tetrafluoroborate (3.14a). A 10 mL flask was charged with triethylorthoformate (5 mL), compound **3.4** (300 mg, 0.45 mmol), and HBF_4 (0.5 mL, 48% aq.). The reaction mixture was heated to 65 °C for 24 hours. Upon completion, the product was collected by filtration, washed with hot acetonitrile (3 x 5 mL) to obtain 270 mg (70%) of the desired product as a light yellow powder: ^1H NMR ($\text{DMSO}-d_6$): δ 9.06 (s, 2H), 8.62 (s, 2H), 1.91 (s, 36H); ^{13}C ($\text{DMSO}-d_6$): δ 142.9, 128.9, 102.7, 62.0, 28.0, 9.1.

Tetraadamantyl benzobis(imidazolium) tetrafluoroborate (3.14b). In a manner analogous to **3.14a**, the product was obtained in 80% yield as a light yellow powder. Spectroscopic data was in agreement with our previous report: ^1H NMR (C_6D_6): δ 8.37 (s, 2H), 2.81 (s, 24H), 2.15 (s, 12H), 1.81-1.67 (br, 24H); ^{13}C NMR (C_6D_6): δ 227.6, 130.5, 98.5, 58.3, 43.6, 37.2, 30.5.

Tetraphenyl benzobis(imidazolium) tetrafluoroborate (3.14c): In a manner analogous to **3.14a**, with a reaction temperature of 130 °C and time of 16 hours 162 mg (51%) of

the desired product was obtained as a light yellow powder. Purification required rinsing with hot MeOH. Spectroscopic data was in agreement with our previous report. ^1H NMR (DMSO- d_6): δ 10.8 (s, 2H), 8.15(s, 2H) 7.9-7.8 (br, 20H); ^{13}C NMR (DMSO- d_6): δ 147.3, 132.9, 131.0, 130.6, 125.6, 99.2; HRMS calcd. for $\text{C}_{32}\text{H}_{24}\text{N}_4$: 464.2001, found: 464.2004.

Tetrakis(2-methoxyphenyl) benzobis(imidazolium) chloride (3.14d): From the tetraamine tetrahydrochloride: The tetraamine tetrahydrochloride (5.0 g, 7.06 mmol) was dissolved in $\text{HC}(\text{OEt})_3$ (60 mL) and conc. HCl (0.2 mL). The deep purple solution was stirred at 140 °C for 2 h during which time the homogenous reaction mixture became a light red slurry. The reaction mixture was allowed to cool and Et_2O (30 mL) was added to facilitate precipitation of the product. The solids were collected, rinsed with Et_2O and recrystallized from hot MeOH/ Et_2O to give 4.26 g (92%) of the bis(azolium) as a pink-brown solid: ^1H NMR (DMSO- d_6): δ 10.79 (s, 2H), 8.00 (dd, J = 7.8, 1.4 Hz, 2H), 7.98 (s, 2H), 7.73 (t, J = 8.0 Hz, 4H), 7.48 (d, J = 6.8 Hz, 4H), 7.28 (t, J = 7.2 Hz, 4H), 3.87 (s, 12H); ^{13}C NMR (DMSO- d_6): δ 153.7, 148.5, 133.0, 130.8, 128.4, 121.3, 120.6, 113.7, 100.4, 56.4; HRMS m/z calcd for $\text{C}_{36}\text{H}_{32}\text{N}_4\text{O}_4$: 584.2462, found: 584.2418.

Chapter 4: Synthesis of Benzobis(imidazolium) Salts via Tandem Cyclization-Oxidation of 2,5-Diamino-1,4-benzoquinonediimines

4.1 Introduction

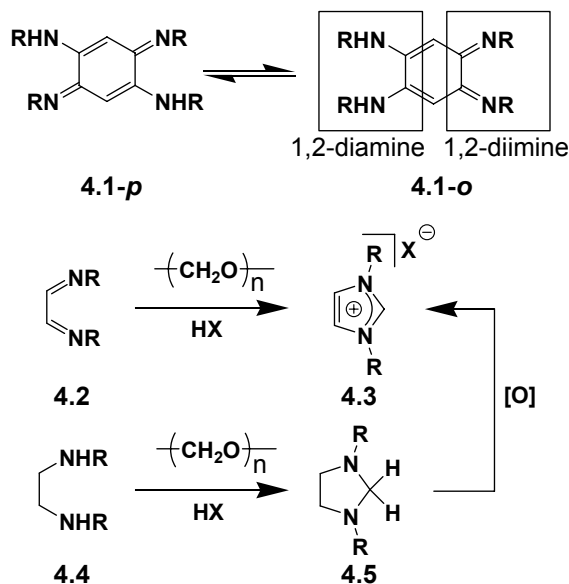
Azophenines⁶⁴ and related *N,N',N'',N'''*-tetraalkyl-2,5-diamino-1,4-benzoquinonediimines⁶⁵ are remarkable quinone derivatives which have found utility in coordination chemistry,⁶⁵ function as pH-dependent chromophores,⁶⁶ and are currently scrutinized for interesting π -electron delocalization characteristics.⁸⁶ Considering they are also robust, stable toward oxygen, and available *via* several synthetic methods,^{64,66,71} we desired an operationally-simple, “one-pot” procedure for transforming these versatile substrates to their respective benzobis(imidazolium) salts, a class of compounds that are finding increasing utility in organic, organometallic, and materials chemistry.⁴⁶

4.2 Tandem cyclization-oxidation of 2,5-diamino-1,4-benzoquinonediimines

As shown in Scheme 4.1, the *o*-quinoid tautomer (**1-*o***) of 2,5-diamino-1,4-benzoquinonediimine **4.1** displays 1,2-diamino and 1,2-diimino moieties which are independently known for undergoing dehydrative cyclizations. For example, treatment of 1,2-diimine **4.2** with formaldehyde affords imidazolium salt **4.3**⁸⁷ whereas the corresponding vicinal diamine **4.4** affords the cyclic *N,N'*-acetal **4.5**.⁸⁸ With these considerations in mind, we envisioned that analogous cyclization reactions with **4.1** should afford an annulated benzimidazolium/*N,N'*-acetal hybrid (e.g. **4.6**, Scheme 2). Oxidation of this intermediate using Thorn's recently reported⁸⁹ Pd-mediated process for

efficiently generating hydrogen gas from phenylene diamine-derived *N,N'*-acetals should then afford the respective benzobis(imidazolium) salts.⁹⁰

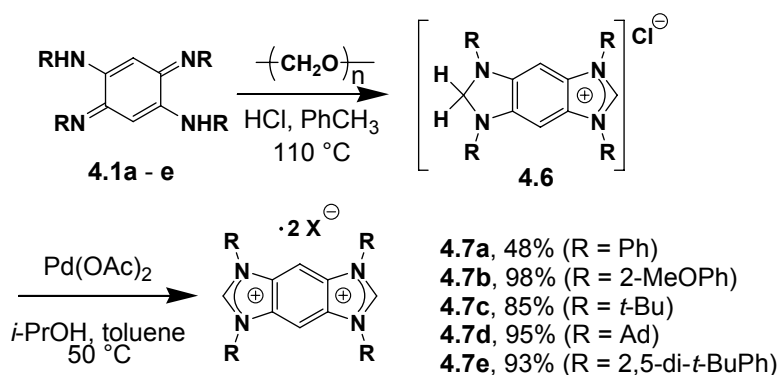
Scheme 4.1 (TOP) The o-tautomer of 2,5-diamino-1,4-benzoquinonediimine (**4.1-o**) exhibits 1,2-diamino and 1,2-diimino fragments which are (BOTTOM) independently known for undergoing dehydrative cyclizations with paraformaldehyde



To test this hypothesis, 2,5-diamino-1,4-quinonediimines **4.1a** – **e** were prepared *via* exhaustive Pd-catalyzed aryl amination of 1,2,4,5-tetrabromobenzene followed by spontaneous oxidation during an aerobic workup (see Chapter 3).⁹¹ Confirmation of the 2,5-diamino-1,4-quinonediimine structure was determined using ^1H NMR spectroscopy through identification of the diagnostic chemical shift of the vinylic proton of the quinoid ring ($\delta = 5.5$ ppm in CDCl_3) and single crystal X-ray analysis for **4.1b**. As shown in

Scheme 4.2, compounds **4.1** were each reacted with paraformaldehyde in PhCH₃ under acidic conditions at 110 °C.⁹² Within 2 – 6 h, the intense colors associated with these quinones derivatives had dissipated and the reaction mixtures developed yellow-brown solids suggesting hybrid intermediate **4.6** had formed. The reaction temperature was then reduced to 50 °C and, to facilitate dissolution of precipitated solids, *i*-PrOH (10% by volume) was added. Upon addition of catalytic amounts of Pd(OAc)₂ (1 mol %), slow and persistent generation of hydrogen gas was observed. Analysis of the crude reaction mixtures by ¹H NMR spectroscopy indicated the 2,5-diamino-1,4-benzoquinonediimines (diagnostic signals: tetraaminobenzene C-*H*, δ = 8 ppm and benzimidazolium C-*H*, δ = 10 - 11 ppm in DMSO-*d*₆), were cleanly converted to the desired benzobis(imidazolium) products **7** in good to excellent yields (48 – 98%).

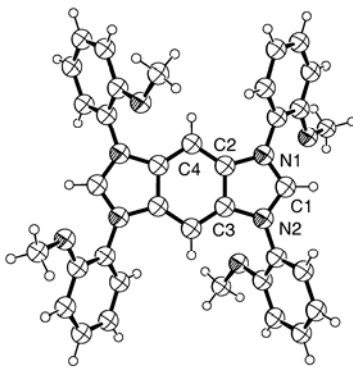
Scheme 4.2 Conversion of 2,5-diamino-1,4-quinonediimines to their respective benzobis(imidazolium) salts *via* tandem formylation/Wuest-Thorn oxidation



Although analysis of the products obtained above via ¹H NMR spectroscopy were strongly indicative of the desired benzobis(imidazolium) structure, they were further

characterized using X-ray analysis after quality crystals of benzobis(imidazolium) dichloride **4.7b** were obtained by slow cooling of a hot saturated DMSO solution. As shown in Figure 4.1, the N1-C2-N2 bond angle (110°) was typical of annulated imidazolium compounds as were the imidazole bond lengths.^{23,37} The *N*-anisidyl rings were rotated out-of-plane with respect to the benzobis(imidazolium) core (dihedral angles ranged between 35 and 60°) which indicated there was relatively minimal electronic overlap between the two moieties. Finally, C-C bond lengths typical of arene rings were observed (1.38 to 1.41 Å), which indicated the parent quinone core was successfully reduced.

Figure 4.1 ORTEP representation of benzobis(imidazolium) dichloride **4.7b** (counterions have been removed for clarity)



Selected bond lengths (Å) and angles (degs): N1-C1, 1.3352(19); N2-C1, 1.3398(19); N1-C2, 1.4007(18); N2-C3, 1.3986(18); C2-C3, 1.4062(19); C2-C4, 1.384(2); N1-C1-N2, 110.21(13); C1-N1-C2, 108.55(11); N1-C2-C3, 106.37(12); C4-C2-N1, 130.60(13); C6-C5-N1-C2, 126.27(15); C3-N2-C1-C2, 59.12(19).

4.3 Conclusions

In summary, we have developed an efficient one-pot synthetic protocol for preparing a variety of *N*-alkyl and *N*-aryl benzobis(imidazolium) salts from readily available 2,5-diamino-1,4-benzoquinonediimines. In particular, the *o*-quinoid tautomer of 2,5-diamino-1,4-benzoquinonediimines was cyclized using paraformaldehyde to obtain benzimidazolium/*N,N'*-acetal hybrids which were subsequently oxidized. Finally, a comparative solid-state study between an azophenine derivative and its corresponding benzobis(imidazolium) salt was also performed which ultimately aided in confirming the chemical structures of these compounds.

Chapter 5: Synthesis Study of Janus Bis(carbene)s and Their Transition Metal Complexes

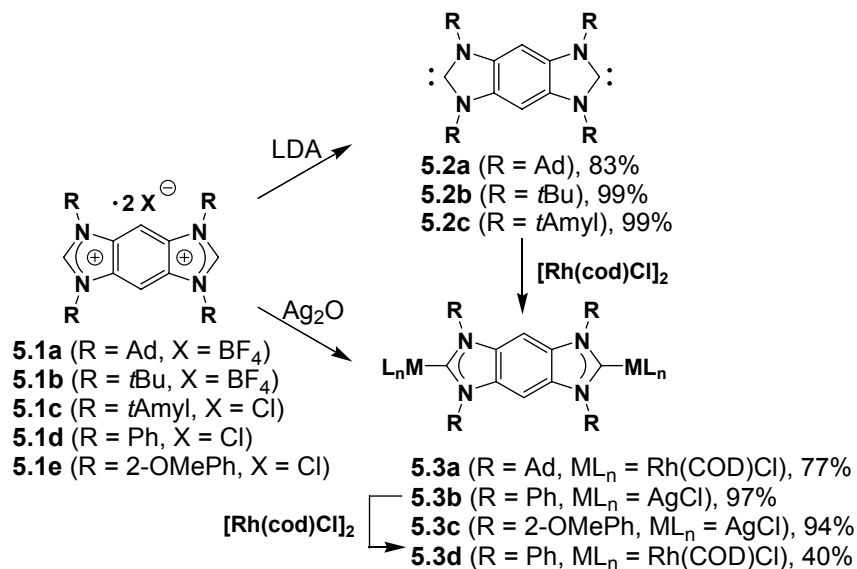
5.1 Introduction

The construction of new organic-inorganic hybrid materials with interesting structural features and technologically-useful functions is a vibrant area of research with considerable potential. The key to growth in this field is the development of new, tunable molecular scaffolds for bridging transition metals. Ideal linkers should be readily accessible, exhibit high affinities toward a broad range of transition metals, and possess modular features amenable for precisely manipulating their inherent physical and electronic characteristics. Stable N-heterocyclic carbenes (NHCs),² particularly imidazolyliidenes,⁹³ fall in this category. They have been found to form robust complexes with nearly every transition metal³ and the basic N-heterocyclic nucleus as well as its N-substituents can be acutely modified.⁹⁴ As such, an impressive amount of attention has been devoted toward optimizing and understanding the interaction of carbenes with various transition metals to form monometallic complexes.⁹⁵ However, comparatively less attention has been directed toward the development of discrete, multifunctional carbenes that are poised to bind multiple transition metals.^{27,28,29} Herein, we report the synthesis and characterization of benzobis(imidazolylidene)s, a new class of Janus⁹⁶ bis(carbene)s comprised of two linearly opposed imidazolyliidenes annulated to a common arene backbone, and demonstrate their utility in preparing new organometallic materials.

5.2 Synthesis and characterization of free bis(N-heterocyclic carbene)s

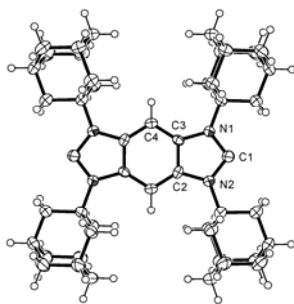
Requisite benzobis(imidazolium) salts possessing a range of *N*-substituents (**5.1**) were synthesized as described in Chapters 3 and 4. Independent treatment of **5.1a-c** with 2.2 equiv of lithium diisopropylamide (LDA) in THF at RT caused precipitation of products **5.2a** and **5.2b** which were subsequently isolated *via* filtration in yields of 83 and 99%, respectively (Scheme 5.1). While **5.2a** and **5.2b** were only slightly soluble in common organic solvents (THF, toluene, benzene, etc.), a highly soluble derivative featuring *N*-*t*-amyl groups (**5.2c**) was obtained in 99% yield after LiCl was precipitated with excess toluene and removed *via* filtration.

Scheme 5.1 Synthesis of benzobis(imidazolylidene)s and their related transition metal complexes



The ^{13}C NMR spectra of products **5.2a–c** in C_6D_6 each exhibited a single, diagnostic signal between $\delta = 227 - 231$ ppm which was indicative of the highly symmetric structures shown in Scheme 5.1 and consistent with other known annulated imidazolyliidenes.¹⁹ To confirm, a crystal of **5.2a** was obtained by vapor diffusion of pentane into a saturated toluene/THF solution (1:1 v/v) and analyzed using X-ray diffraction analysis. An ORTEP view of the molecular structure is shown in Figure 5.1 with selected bond lengths and angles in the caption. Notably, the N-C-N bond angle was found to be $104.8(2)^\circ$ which was similar to saturated imidazolyliidenes⁹⁷ and benzimidazolyliidenes.¹⁹ This promising result strongly suggested that each carbene “face” of these Janus ligands should display similar chemistries and affinities toward transition metals as their monofunctional analogues.

Figure 5.1 ORTEP view of **5.2a**

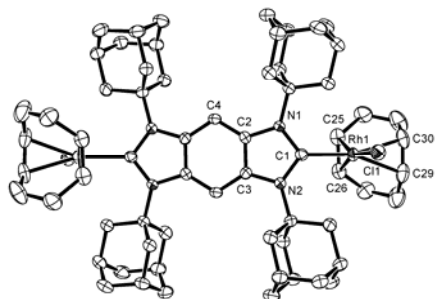


Selected bond lengths (Å) and angles ($^\circ$): C1-N1, 1.369(3); C1-N2, 1.368(3); N1-C3, 1.411(3); N2-C2, 1.408(3); N1-C1-N2, $104.8(2)^\circ$.

5.3 Synthesis and characterization of bimetallic complexes of bis(N-heterocyclic carbene)s

Addition of an equimolar amount of $[\text{Rh}(\text{cod})\text{Cl}]_2$ to a THF solution of **5.2a** at RT resulted in the precipitation of Rh complex **5.3a** as a yellow solid, which was isolated in 77% yield. Analysis of this complex by NMR spectroscopy confirmed the stoichiometry between the Rh centers and bis(carbene) nucleus was 2:1. A single ^{13}C resonance appeared at $\delta = 198$ ppm and two distinct sets of olefinic ^1H signals were observed at 3.0 (*cis* to the carbene) and 5.0 ppm (*trans*), which was suggestive of a square planar geometry for each of the metal centers.⁹⁸ The structure of **5.3a** was confirmed by X-ray diffraction analysis after a suitable crystal was obtained by slow cooling of a hot CHCl_3 solution (see Figure 5.2). Although key bond lengths were in accord with known NHC-Rh complexes,⁹⁸ a notable exception was the positions of Rh atoms which were displaced perpendicularly from the plane of the benzobis(imidazolyliene) by 0.75 Å. This unusual structural feature was attributed to the substantial steric bulk of the *N*-adamantyl groups balanced by the high affinity of imidazolylienes for Rh(I) (*vide infra*).

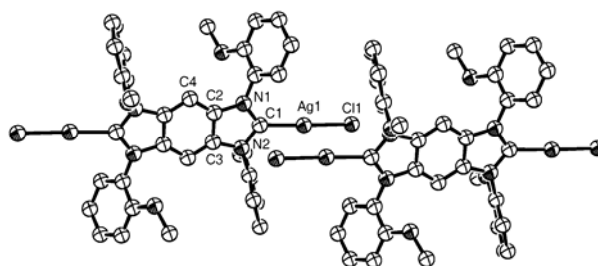
Figure 5.2 ORTEP view of **5.3a**



Selected bond lengths (Å) and angles (°): Rh1-C1, 2.073(3); Rh1-C25, 2.125(3); Rh1-C26, 2.131(3); Rh1-C29, 2.184(3); Rh1-C30, 2.197(3); C1-N1, 1.387(4); C1-N2, 1.406(4); N1-C1-N2, 105.7(2). Hydrogen atoms have been removed for clarity.

In cases where the free bis(carbene)s were not isolable (**5.1d-e**), an alternative method of forming metal complexes was desired. Direction shifted toward Lin's⁴¹ versatile Ag-mediated carbene transfer protocol for accessing organometallic complexes.⁴⁷ As shown in Scheme 5.1, bis(azolium) salts **5.1d** and **5.1e** were respectively treated with Ag₂O (1.0 equiv) in CH₂Cl₂ (23 °C) or CH₃CN (40 °C). Following filtration of inorganic salts which precipitated during the reaction, concentration of the resulting solutions afforded products **5.3b** and **5.3c** in excellent yields (97 and 94%, respectively). Crystals of **5.3c** were obtained from slow diffusion of hexanes into a saturated CH₂Cl₂ solution and analyzed using X-ray diffraction analysis. As shown in Figure 5.3, the structure was essentially linear along its main axis with a C1-Ag1-Cl1 bond angle of 176° and its *N*-aryl substituents were rotated out of the plane of the benzobis(imidazolyliene) with an average dihedral angle = 69°. Interestingly, in the solid-state the complexes arranged in infinite rows governed by intermolecular argentophilic interactions.

Figure 5.3 ORTEP view of **5.3c**



Selected bond lengths (Å) and angles (°): Ag1-Cl1, 2.072(11); Ag1-Cl2, 2.236(3); Cl1-N1, 1.352(12); Cl1-N2, 1.360(11); N1-C2, 1.409(11); N2-C3, 1.409(12); N1-C1-N2, 106.4(9). Ag-Ag, 3.3054(15). Hydrogen atoms have been removed for clarity.

Treatment of complex **5.3b** with an equimolar amount of $[\text{Rh}(\text{cod})\text{Cl}]_2$ in CH_2Cl_2 at 50 °C for 24 h afforded bimetallic Rh complex **5.3d** as an orange-brown powder in 40% yield. Although solution and solid-state structural analyses indicated **5.3d** was superficially similar to **5.3a**, a key difference was the Rh atoms were now coplanar with the benzobis(imidazolyliene). Considering the *N*-phenyl groups were rotated by an average of 63° relative to this same plane (minimizing any electronic contributions) and both complexes showed a similar *trans* effect (average Rh-olefin bond distances: **5.3a**: 2.20 Å vs. **5.3d**: 2.19 Å), the size of the *N*-substituents appeared to dominate structural features about the metals centers.

Finally, we focused on the synthesis of bis(azolium) **5.4**, a desymmetrized precursor that was envisioned to provide a Janus bis(carbene) with differential characteristics at each carbene “face.” The dissimilar environments of the 1,3-dimethyl- and 1,3-di-*t*-butylimidazolium fragments were manifested in the ^1H NMR spectrum ($\text{DMSO}-d_6$) of **5.4** which exhibited signals at $\delta = 9.9$ and 9.0 ppm, respectively. Deprotonation of **5.4** using 2.1 equiv of NaH (and catalytic KO^tBu) in toluene at 120 °C

resulted in selective dimerization to afford enetetraamine **5.5** which was subsequently isolated in 94% yield. Crystals suitable for X-ray analysis were obtained by slow cooling of a saturated toluene solution of **5.5** and an ORTEP view of the structure of this compound is shown in Figure 5.4. Key bond lengths and angles of the benzimidazolylidene fragments were in accord with **5.2b**, and the torsion angle about the enetetraamine was found to be 15.2°, consistent with the dimer of 1,3-dimethylbenzimidazolylidene.^{98a} The solution structure of **5.5** was confirmed by treatment with O₂ which rapidly and selectively oxidized the enetetraamine moiety to afford urea **5.6**.⁴⁴

Scheme 5.2 Selective dimerization and oxidation of a desymmetrized Janus bis(carbene) precursor

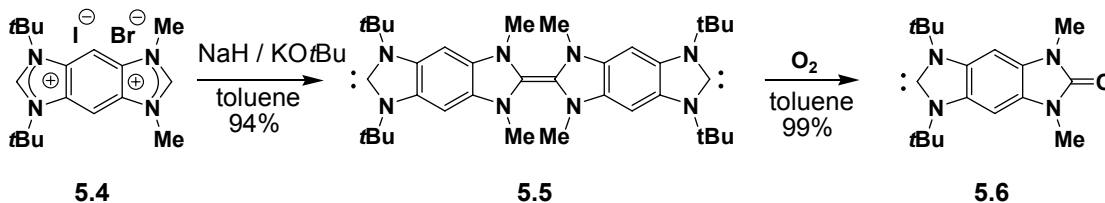
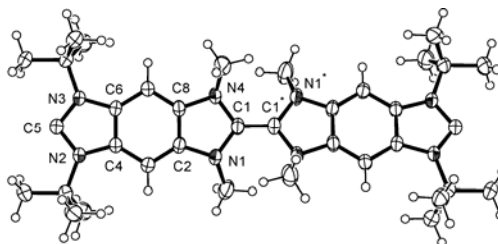


Figure 5.4. ORTEP view of **5.5**



Selected bond lengths (Å) and angles (°): C5-N3, 1.366(3); C5-N2, 1.371(3); N3-C6, 1.406(2); N2-C4, 1.404(3); C1-N1, 1.426(3); C1-N4, 1.424(3); N4-C8, 1.416(3); N1-C2, 1.408(2); C1-C1*, 1.349(4); C1-N4-C18, 117.79(18); N2-C5-N3, 104.00(17); N1-C1-N4, 108.48(16); N4-C1-C1*-N1*, 15.2.

5.4 Conclusions

In summary, we report the first Janus bis(carbene)s with facially opposed imidazolylikenes annulated to a common arene core. Solid-state analysis was performed for various intermediate and combine, the X-ray analyses suggest a sterically-governed binding arrangement. Synthetic routes employed to obtain these compounds were modular, high yielding, and permitted access to derivatives with *N*-alkyl or *N*-aryl substituents as well as a desymmetrized variant. Their promise as ligands was borne out through synthesis of new bimetallic complexes, and efforts toward heterobimetallic complexes are currently underway.

5.5 Experimental Section

General Considerations. All reactions were conducted under an atmosphere of dry nitrogen using standard Schlenk techniques or in a nitrogen filled glove-box. CH₂Cl₂ was distilled from CaH₂ under nitrogen and degassed by three freeze-pump-thaw cycles.

THF and toluene were distilled from Na/benzophenone under nitrogen and degassed by three freeze-pump-thaw cycles. $[\text{Rh}(\text{cod})\text{Cl}]_2$ and 1,3-bis(2,6-diisopropylphenyl)imidazolium chloride were purchased from Strem and used without further purification. All other reagents were purchased from Aldrich or Acros and were used without further purification. ^1H NMR spectra were recorded using a Varian Gemini (300 MHz or 400 MHz) spectrometer. Chemical shifts are reported in delta (δ) units, expressed in parts per million (ppm) downfield from tetramethylsilane using the residual protonated solvent as an internal standard (CDCl_3 , 7.24 ppm; C_6D_6 , 7.15 ppm, $\text{DMSO}-d_6$, 2.49 ppm). ^{13}C NMR spectra were recorded using a Varian Gemini (100 MHz) spectrometer. Chemical shifts are reported in delta (δ) units, expressed in parts per million (ppm) downfield from tetramethylsilane using the solvent as an internal standard (CDCl_3 , 77.0 ppm; C_6D_6 , 128.0 ppm, $\text{DMSO}-d_6$, 39.5 ppm). ^{13}C NMR spectra were routinely run with broadband decoupling. High-resolution mass spectra (HRMS) were obtained with a VG analytical ZAB2-E or a Karatos MS9 instrument and are reported as m/z (relative intensity).

Tetrakis-*N*-adamantylbenzobis(imidazolylidene) (5.2a). In a nitrogen-filled drybox, a 20 mL flask was charged with bis(azolium) salt **5.1a** (680 mg, 0.78 mmol), THF (10 mL), LDA (1.83 M in hexanes, 0.93 mL, 1.70 mmol), and a stir bar. The flask was sealed and the resulting slurry was stirred for 10 h at RT. Precipitated solids were collected by filtration, washed with THF (5 mL) and dried under reduced pressure to afford 450 mg (83%) of the desired product as a white solid. Crystals suitable for X-ray analysis were obtained by solvent diffusion of pentane into a saturated solution of **5.2a** in toluene/THF

(1:1 v/v). ^1H NMR (C_6D_6): δ 8.37 (s, 2H), 2.81 (s, 24H), 2.15 (s, 12H), 1.81-1.67 (br, 24H); ^{13}C NMR (C_6D_6): δ 227.6, 130.5, 98.5, 58.3, 43.6, 37.2, 30.5.

Tetrakis-*N*-*t*-butylbenzobis(imidazolylidene) (5.2b). In a nitrogen-filled drybox, a 20 mL flask was charged with bis(azolium) salt **5.1b** (1.27 g, 2.3 mmol), THF (10 mL), LDA (1.80 M in hexanes, 2.8 mL, 5.05 mmol), and a stir bar. The flask was sealed and the resulting slurry was stirred for 10 h at RT. Precipitated solids were collected by filtration, washed with THF (5 mL) and dried under vacuum to afford 870 mg (99%) of the desired product as a light gray solid. Crystals suitable for X-ray analysis were obtained by slow cooling of a hot, saturated toluene solution. ^1H NMR (C_6D_6): δ 7.79 (s, 2H), 1.78 (s, 36H); ^{13}C NMR (C_6D_6): δ 228.3, 130.9, 97.5, 57.2, 30.5; HRMS calcd. for $\text{C}_{24}\text{H}_{34}\text{N}_4$ [$\text{M}+\text{H}^+$]: 383.3175, found: 383.3177.

Tetrakis-*N*-*t*-amylbenzobis(imidazolylidene) (5.2c). In a nitrogen-filled drybox, a 10 mL flask was charged with bis(azolium) salt **5.1c** (50 mg, 0.098 mmol), LDA (0.41 M in THF, 0.48 mL, 0.195 mmol), and a stir bar. The resulting slurry was stirred for 15 minutes at RT, then toluene (1 mL) was added. The reaction mixture was filtered through Celite and the solvent was removed under reduced pressure to afford 22 mg (99%) of the desired product as a white solid. ^1H NMR (C_6D_6): δ 7.89 (s, 2H), 2.14 (q, $J = 7.2$ Hz, 8H), 1.85 (s, 24H), 0.76 (t, $J = 7.2$ Hz, 12H); ^{13}C NMR (C_6D_6): δ 230.2, 131.1, 96.9, 60.1, 33.7, 29.0, 8.5; HRMS calcd. for $\text{C}_{26}\text{H}_{46}\text{N}_4$ [$\text{M}+\text{H}^+$]: 438.3722, found: 438.3722.

Bimetallic Rhodium Complex 5.3a. In a nitrogen-filled drybox, a 10 mL flask was charged with bis(carbene) **5.2a** (70 mg, 0.1 mmol), [(COD)RhCl]₂ (50 mg, 0.1 mmol), THF (2 mL), and a stir bar. The resulting slurry became homogeneous after stirring for 5 min at RT. Product precipitation began within 30 min and the reaction was stirred for an additional 2 h. Precipitated solids were collected by filtration, washed with THF (3 mL), and dried under vacuum to afford 100 mg (77%) of the desired product as a yellow powder. Crystals suitable for X-ray analysis were obtained by slow evaporation of a saturated CHCl₃ solution. ¹H NMR (CDCl₃): δ 8.20 (s, 2H), 4.98 (s, 2H), 3.50-3.47 (m, 12H), 3.00-2.97 (m, 16H), 2.47-2.41 (m, 22H), 1.67-1.61 (m, 36H); ¹³C NMR (CDCl₃): δ 198 (d), 129.5, 109.7, 99.9, 92.5 (d, *J* = 6.9 Hz), 67.7 (d, *J* = 14.8 Hz), 62.2, 43.2, 36.6, 32.3, 30.4, 28.8.

Diargento Complex 5.3b. Bis(azolium) salt **5.1d** (535 mg, 1.0 mmol) was dissolved in CH₃CN (10 mL) and Ag₂O (243 mg, 1.05 mmol) was added. The resulting suspension was stirred at 40 °C for 2 h. The cooled reaction mixture was filtered through Celite and concentrated to give 726 mg (97%) of **5.3b** as a brown powder. ¹H and ¹³C NMR analysis revealed broad peaks indicative of aggregation/oligomerization. ¹H NMR (DMSO-*d*₆) δ 7.82-7.78 (m, 8H), 7.73-7.60 (m, 12H), 7.45 (s, 2H).

Diargento Complex 5.3c. Bis(azolium) salt **5.1e** (1.20 g, 1.82 mmol) was suspended in CH₂Cl₂ (100 mL). To the mixture was added Ag₂O (423 mg, 1.82 mmol) and the flask was protected from light using Al foil. After stirring for 2 h at room RT, a brown

suspension formed which was filtered over Celite and concentrated to a brown glassy solid (1.49 g, 94%). ^1H and ^{13}C NMR analysis revealed broad peaks indicative of aggregation/oligomerization. Crystals suitable for X-ray analysis were obtained by diffusion of hexanes into a solution of **3c** in CH_2Cl_2 .

Bimetallic Rhodium Complex 5.3d. From bis(azolium) salt **5.1d**· BF_4 : The bis(azolium) salt (100 mg, 0.157 mmol) was added to THF (3 mL) followed by NaHMDS (0.16 mL, 0.32 mmol, 2.0 M in THF). The slurry was stirred for 1 h, then $[(\text{COD})\text{RhCl}]_2$ (77 mg, 0.157 mmol) was added and the solution was heated to 50 °C in a sealed vial for 10 h. The cooled reaction mixture was diluted with hexanes (6 mL) and solids were collected by filtration, washed with toluene (5 mL) and hexanes (5 mL). Solvent was removed under reduced pressure. Residual inorganic salts were removed by treating the crude solid with chloroform and filtering through a 0.45 μm PTFE filter, followed by removal of solvent under reduced pressure to obtain the product as a tan solid (51 mg, 34%).

From diargento complex **5.3b**: The diargento complex **5.3b** (373 mg, 0.50 mmol) and $[(\text{COD})\text{RhCl}]_2$ (258 mg, 0.52 mmol) were partially dissolved in CH_2Cl_2 (12 mL) in a screw-cap vial under an atmosphere of dry nitrogen. The vial was sealed with a Teflon-coated cap and stirred at 50 °C for 20 h protected from light with Al foil. The cooled reaction mixture was then filtered through Celite and concentrated to give 191 mg (40%) of the desired product. Crystals suitable for X-ray analysis were obtained by slow diffusion of hexanes into a saturated CH_2Cl_2 solution. ^1H NMR (CDCl_3): δ 8.13 (br, 8H), 7.64-7.52 (br, 12H), 7.13 (s, 2H), 4.89 (br, 4H), 2.73 (br, 4H), 1.8-1.46 (br, 16H); ^{13}C

NMR (CDCl₃): δ 137.7, 132.7, 129.3, 128.9, 127.8, 127.4, 109.7, 99.3, 91.9, 68.5 (d, J = 13.9 Hz), 32.0, 28.2.

5,6-Bis(*t*-butylamino)-1-methylbenzimidazole. Under an atmosphere of nitrogen, a 10 mL vial was charged with 1,3-bis(2,6-diisopropylphenyl)imidazolium chloride (17 mg, 0.04 mmol), NaOtBu (2 mg, 0.02 mmol), Pd(OAc)₂ (5 mg, 0.02 mmol), toluene (5 mL), and a stir bar. The resulting mixture was stirred at 80 °C for 5 minutes. Then, 5,6-dichloro-1-methylbenzimidazole^[99] (101 mg, 0.50 mmol) was added, followed by *t*-butyl amine (146 mg, 2.0 mmol) and NaOtBu (101 mg, 1.05 mmol). The resulting mixture was sealed and stirred at 150 °C for 24 h. After cooling to RT, precipitated solids were removed by filtration and solvent was removed to obtain a brown solid which was used in the next step without additional purification. ¹H NMR (CDCl₃): δ 7.57 (s, 1H), 7.32 (s, 1H), 6.70 (s, 1H), 3.70 (s, 3H), 1.34 (s, 9H), 1.21 (s, 9H); ¹³C NMR (CDCl₃): δ 141.2, 140.0, 136.1, 131.9, 131.4, 115.6, 95.6, 52.8, 51.3, 38.5, 29.8, 29.7.

Desymmetrized Benzimidazolium Salt. Crude 5,6-bis(*t*-butylamino)-1-methylbenzimidazole was partially dissolved in HC(OEt)₃ and HBr (48%). The resulting slurry was stirred for 3 h at 65 °C. After cooling to RT, the solids were collected by vacuum filtration. The crude product was then dissolved in *i*PrOH and stirred with excess Na₂CO₃ for 2 h. Filtration through Celite followed by removal of solvent under reduced pressure provided the desired product as a golden solid in 65% yield from 5,6-dichloro-1-methylbenzimidazole. ¹H NMR (DMSO-*d*₆): δ 8.83 (s, 1H), 8.53 (s, 1H), 8.5

(s, 1H), 8.39 (s, 1H). 4.0 (s, 3H), 1.88 (s, 9H), 1.85 (s, 9H); ^{13}C NMR (DMSO- d_6): δ 148.8, 141.8, 139.1, 133.5, 127.5, 127.0, 105.4, 96.9, 60.72, 60.68, 31.4, 27.9, 27.8; HRMS calcd for $\text{C}_{17}\text{H}_{25}\text{N}_4$: 285.2079, found: 285.2079.

Desymmetrized Benzobisbis(imidazolium) Salt 5.4. The asymmetric benzimidazolium salt (3.00 g, 8.21 mmol) was dissolved in CH_3CN (100 mL) and MeI (5 mL, 78.0 mmol) was added. The solution was stirred in a sealed vessel at 60 °C for 3 h. The cooled reaction mixture was then concentrated under vacuum to obtain 4.17 g (99%) of **5.4** as a brown powder. ^1H NMR (DMSO- d_6): δ 9.96 (s, 2H), 9.05 (s, 2H), 8.85 (s, 2H), 4.24 (s, 6H), 1.93 (s, 18H); ^{13}C NMR (DMSO- d_6): δ 147.0, 142.4, 130.0, 129.4, 100.9, 61.8, 34.1, 27.7.

Enetetraamine 5.5. A 10 mL vial was charged with asymmetric salt **5.4** (100 mg 0.197 mmol), NaH (12 mg 0.48 mmol), a catalytic amount of KO t Bu (ca. 1 mg) and toluene (2 mL). The vial was then sealed and the reaction mixture was heated to 120 °C for 2 h. The cooled solution was then filtered through a 0.2 μm PTFE filter and solvent was removed under vacuum to obtain 55 mg (94%) of the desired product as a dark red powder. Crystals suitable for X-ray analysis were obtained by slowly cooling of a saturated toluene solution. ^1H NMR (C_6D_6): δ 6.84 (s, 2H), 2.84 (s, 6H), 1.82 (s, 18H); ^{13}C NMR (C_6D_6): δ 221.2, 138.7, 130.8, 125.9, 94.7, 57.0, 36.9, 30.7.

Urea 5.6. Enetetraamine **5.5** (0.05 g, 0.168 mmol) was dissolved in benzene and exposed to an atmosphere of oxygen for < 1 minute. After the color of the solution changed from red to brown, the solvent was removed under vacuum to obtain 51 mg (99%) of product as a brown powder. ^1H NMR (C_6D_6): δ 6.83 (s, 2H), 2.91 (s, 6H), 1.79 (s, 18H); ^{13}C NMR (C_6D_6): δ 223.0, 155.0, 130.6, 125.8, 92.7, 57.2, 20.5, 26.5; HRMS calcd. for $\text{C}_{18}\text{H}_{28}\text{N}_4\text{O}$ $[\text{M}+\text{H}]^+$: 315.2185; found, 315.2185.

Chapter 6: Ionic Liquids via Efficient, Solvent-Free Anion Metathesis

6.1 Introduction

The impact of ionic liquids (ILs) continues to spread unimpeded as their applications and utility transcend many areas of chemistry.¹⁰⁰ These neoteric solvents provide many desirable features for facilitating chemical reactions, including: 1) non-volatility, 2) commercial availability, 3) high polarity, 4) high thermal stability, 5) broad miscibility, and 6) facile recyclability. The particular combination of low vapor pressure, high stability, and reusability have earned ILs recognition as environmentally benign alternatives to traditional organic solvents.¹⁰¹ Recently, room-temperature ILs (RTILs) have found extraordinary utility in a number of synthetic applications,¹⁰⁰ and the anionic component is credited with strongly influencing their physical properties.¹⁰²

Obtaining RTILs with non-coordinating counteranions is typically accomplished from the corresponding halide salt. Common methods to exchange halides for non-coordinating anions are based on either metathesis (e.g., with a silver(I), alkali, or ammonium salt), or acid-base neutralization reactions.¹⁰⁰ The halide-containing byproduct salt resulting from these reactions is then removed by precipitation and filtration, or extraction.

Seeking alternatives to precipitation- or extraction-based halide removal, we considered capitalizing on the nucleophilic nature of the halide in such a way that would generate volatile reagents as the sole byproducts. Inspired by solution-based studies involving the nucleophilicity of halides in polar media,¹⁰³ we focused our attention on using stoichiometric amounts of organic halide salts in combination with alkyl sulfates,

sulfonates, phosphates, and phosphonates under solvent-free conditions. Herein, we report the scope and utility of a anion metathesis (AM) protocol that does not rely on extensive purification protocols, metal reagents, or organic solvents, and effectively offers a “cleaner,” general approach¹⁰⁴ to exchanging anions in ILs. Key data are summarized in Table 6.1.

6.2 Solvent-free anion metathesis

Initial experiments focused on using 1-butyl-3-methylimidazolium (BMIM) halides with Me₂SO₄ to generate the corresponding [BMIM][MeSO₄] and MeX (X = Cl, Br, I). Treatment of [BMIM]Cl with an equimolar amount of Me₂SO₄ at ambient temperature immediately resulted in rapid gas evolution, leaving a clear liquid product (entry 1). After stirring the mixture for ca 5 min, analysis of the remaining material by ¹H and ¹³C NMR spectroscopy revealed [BMIM][MeSO₄] as the sole product. The MeSO₄⁻ provided a useful and convenient handle for confirming the progress of halide removal (diagnostic signal at $\delta = 3.75$ ppm in CDCl₃). Importantly, no residual Me₂SO₄ was present ($\delta = 3.96$ ppm) which indicated the reaction had reached high conversion and was consistent with the high yield obtained (>99% yield). Similarly, treatment of [BMIM]Br with Me₂SO₄ also resulted in immediate gas evolution to provide [BMIM][MeSO₄] in quantitative yield (entry 2). In the case of [BMIM]I, MeI resulting from the AM reaction was removed under vacuum, and ultimately provided the desired product in high purity (as determined by ¹H and ¹³C NMR spectroscopy) and quantitative yield (entry 3).

Table 6.1 Halide-trapping anion metathesis of organic halide salts.

Entry	Trapping Agent ^a	Organic Halide Salt ^a	Product ^b	Temp (°C)	Time
1		[BMIM]Cl		RT	< 5 min
2		[BMIM]Br		RT	< 5 min
3		[BMIM]I		RT	< 5 min
4		[BPY]Cl		RT	< 5 min
5		[BPY]I		RT	< 5 min
6		[Hx ₃ PC ₁₄]Cl		RT	< 5 min
7		[Hx ₃ PC ₁₄]Br		RT	< 5 min
8		[BMIM]Br		50	< 5 min
9		[BMIM]I		RT	< 5 min
10		[BPY]Cl		120	< 5 min
11		[BPY]I		RT	< 5 min
12 ^c		[BPY]Cl		120	90 min

^aPurchased from commercial suppliers and stored in a desiccator until use. ^bProducts were analyzed by ¹H and ¹³C NMR, and compared with authentic samples from commercial sources where applicable. All reactions were gravimetrically determined to be quantitative. Complete removal of alkyl halides was facilitated under vacuum. ^cSee Experimental Section 6.4 for product characterization. BMIM = 1-butyl-3-methylimidazolium, BPY = 1-butylpyridinium, Hx₃PC₁₄ = trihexyl(tetradecyl)phosphonium.

Encouraged by these results, we shifted focus toward using Me₂SO₄ to effect AM in other classes of ILs. Treatment of 1-butylpyridinium (BPY) halides, [BPY]Cl and [BPY]I, with Me₂SO₄ afforded [BPY][MeSO₄] with equal success as the imidazolium-

based salts (entries 4 and 5, respectively). Phosphonium salts based on trihexyl(tetradecyl)phosphonium ($\text{Hx}_3\text{PC}_{14}$) cation were also investigated. Independently treating $[\text{Hx}_3\text{PC}_{14}]\text{Cl}$ and $[\text{Hx}_3\text{PC}_{14}]\text{Br}$ with a stoichiometric amount of Me_2SO_4 provided $[\text{Hx}_3\text{PC}_{14}][\text{MeSO}_4]$ in quantitative yields (entries 6 and 7, respectively).

Considering the tosylate (OTs) counterion has been incorporated into many ILs, we investigated solvent-free AM using MeOTs in lieu of Me_2SO_4 . Independently treating $[\text{BMIM}]\text{Br}$ and $[\text{BMIM}]\text{I}$ with MeOTs rapidly afforded $[\text{BMIM}][\text{OTs}]$ in quantitative yield and high purity (entries 8 and 9, respectively). As before, removal of MeI was facilitated under vacuum. Interestingly, $[\text{BPY}]\text{Cl}$ (melting point = 162 °C) required heating to 120 °C before a relatively rapid reaction would occur (entry 10). Optimal conditions involved heating $[\text{BPY}]\text{Cl}$ prior to addition of MeOTs, which provided the desired product rapidly (< 5 min) and in quantitative yield. A key difference in this reaction when compared to those described above is that neither the starting IL, nor the $[\text{BPY}][\text{OTs}]$ product are RTILs.¹⁰⁵ Use of $[\text{BPY}]\text{I}$, a RTIL, resulted in rapid reaction at room temperature (entry 11). Complete conversion with this substrate may be facilitated by partial solvation from MeI produced during the exchange.

Finally, attention was directed toward broadening the aforementioned methodology to access ILs containing other classes of non-nucleophilic, non-coordinating anions. Treatment of $[\text{BPY}]\text{Cl}$ with trimethylphosphate afforded corresponding dimethyl phosphate salt in 100% yield (entry 12). This reaction required higher temperature (120 °C) and an extended reaction time (90 min) to reach completion. This is believed to be related to the high melting points of the corresponding starting and product salts, in addition to the reduced electrophilicity of the phosphate. Importantly, de-alkylation of the

phosphate reagent was found to be highly selective, even in the presence of excess halide salt. Thus, this method offers a convenient means for obtaining mono-basic phosphonate and phosphate counterions. Notably, reactions involving diethyl phosphonates were met with limited success, identifying one boundary limit of this methodology.

6.3 Conclusions

In summary, we have developed an efficient “no workup” protocol for conducting concomitant halide-trapping/anion metathesis reactions in a range of widely used ILs. In particular, a variety of non-nucleophilic, non-coordinating anions were incorporated into ILs, including sulfates, sulfonates, phosphates, and phosphonates. The efficiency of the reaction was found to be dependent on a combination of factors, including the melting points of the starting and product salts, as well as the electrophilicity of the trapping reagent. Considering the practical and environmental benefits, the described methodology offers a new, general route for preparing non-coordinating, non-nucleophilic ILs and helps to minimize solvent dependency, metal waste byproducts, and purification protocols in accessing these important materials.

6.4 Experimental Section

General Considerations: NMR spectra were recorded using a Varian Unity Plus 300 or 400 spectrometer. Chemical shifts are reported in delta (δ) units, expressed in parts per million (ppm) downfield from tetramethylsilane using the residual protonated solvent as an internal standard (CDCl_3 , ^1H : 7.26 ppm; ^{13}C : 77.0 ppm). ^{13}C NMR spectra were routinely run with broadband decoupling. 1-Butyl-3-methylimidazolium ([BMIM])

halides were prepared via the reaction of 1-methylimidazole (1.0 equiv) and butyl halide (1.05 equiv) in a sealed vessel at 130 °C for 24 h, followed by removal of volatile components. 1-Butylpyridinium ([BPY]) halides were prepared in an analogous fashion from pyridine and the corresponding 1-haloalkane. All other reagents were purchased from commercial suppliers and used as received. All organic halide salts were stored in a desiccator prior to use. Iodide salts were protected from light using aluminum foil. Due to the hygroscopic nature of these salts, reactions were routinely protected with a drying tube containing Drierite, unless otherwise noted. All reactions were conducted in a ventilated fume hood. Note: For solvent-free reactions involving solid azolium halides and trialkyloxonium salts, gradual liquefaction occurs over time. For comparative analyses, [BMIM][MeSO₄], [BPY][MeSO₄], [BMIM][OTs], [BMIM]BF₄, [BMIM]PF₆, [BPY]BF₄, trihexyl(tetradecyl)phosphonium tetrafluoroborate ([Hx₃PC₁₄]BF₄), and 1,3-dimesitylimidazolium tetrafluoroborate ([IMes]BF₄) were purchased from commercial suppliers.

Table 6.2 Summary of anion metathesis reactions correlated with respective experimental procedures

Entry	Trapping Agent	Organic Halide Salt	Product
1	Me ₂ SO ₄	[BMIM]Cl	[BMIM][MeSO ₄]
2	Me ₂ SO ₄	[BMIM]Br	[BMIM][MeSO ₄]
3	Me ₂ SO ₄	[BMIM]I	[BMIM][MeSO ₄]
4	Me ₂ SO ₄	[BPY]Cl	[BPY][MeSO ₄]
5	Me ₂ SO ₄	[BPY]I	[BPY][MeSO ₄]
6	Me ₂ SO ₄	[Hx ₃ PC ₁₄]Cl	[Hx ₃ PC ₁₄][MeSO ₄]
7	Me ₂ SO ₄	[Hx ₃ PC ₁₄]Br	[Hx ₃ PC ₁₄][MeSO ₄]
8	MeOTs	[BMIM]Br	[BMIM][OTs]
9	MeOTs	[BMIM]I	[BMIM][OTs]
10	MeOTs	[BPY]Cl	[BPY][OTs]
11	MeOTs	[BPY]I	[BPY][OTs]
12	Me ₃ PO ₄	[BPY]Cl	[BPY][Me ₂ PO ₄]
13	Me ₃ O·BF ₄	[BMIM]Cl	[BMIM]BF ₄
14	Me ₃ O·BF ₄	[BMIM]Br	[BMIM]BF ₄
15	Me ₃ O·BF ₄	[BMIM]I	[BMIM]BF ₄
16	Et ₃ O·BF ₄	[BMIM]Br	[BMIM]BF ₄
17	Et ₃ O·PF ₆	[BMIM]Cl	[BMIM]PF ₆
18	Et ₃ O·BF ₄	[BPY]Cl	[BPY]BF ₄
19	Et ₃ O·BF ₄	[Hx ₃ PC ₁₄]Cl	[Hx ₃ PC ₁₄]BF ₄
20	Et ₃ O·BF ₄	[Hx ₃ PC ₁₄]Br	[Hx ₃ PC ₁₄]BF ₄
21	Et ₃ O·BF ₄	[IMes]Cl	[IMes]BF ₄
22	Et ₃ O·BF ₄	[BMIM]Br	[BMIM]BF ₄
23	Et ₃ O·BF ₄	[HPMIM]Br	[HPMIM]BF ₄

Entry 1. A flask was charged with a magnetic stirbar and 1-butyl-3-methylimidazolium chloride (521 mg, 2.98 mmol), and then sealed with a rubber septum. A drying tube containing Drierite was fitted with a needle and inserted through the septum. Dimethyl sulfate (0.28 mL, 2.98 mmol) was then injected via syringe through the septum. The

mixture was then vigorously stirred for 1 min, then placed under vacuum to provide 747 mg (100% yield) of the desired product.

Entry 2. A flask was charged with a magnetic stirbar and 1-butyl-3-methylimidazolium bromide (639 mg, 2.90 mmol), and then sealed with a rubber septum. A drying tube containing Drierite was fitted with a needle and inserted through the septum. Dimethyl sulfate (0.28 mL, 2.90 mmol) was then injected via syringe through the septum. The mixture was then vigorously stirred for 1 min, then placed under vacuum to provide 727 mg (100% yield) of the desired product.

Entry 3. A flask was charged with a magnetic stirbar and 1-butyl-3-methylimidazolium iodide (540.5 mg, 2.0158 mmol), and then sealed with a rubber septum. A drying tube containing Drierite was fitted with a needle and inserted through the septum. Dimethyl sulfate (0.19 mL, 2.02 mmol) was then injected via syringe through the septum. The mixture was then vigorously stirred for 1 min, then placed under vacuum to provide 509 mg (100% yield) of the desired product.

Entry 4. A flask was charged with a magnetic stirbar and 1-butylpyridinium chloride (603 mg, 3.51 mmol), and then sealed with a rubber septum. A drying tube containing Drierite was fitted with a needle and inserted through the septum. Dimethyl sulfate (0.33 mL, 3.51 mmol) was then injected via syringe through the septum. The mixture was then vigorously stirred for 1 min, then placed under vacuum to provide 868 mg (100% yield) of the desired product.

Entry 5. A flask was charged with a magnetic stirbar and 1-butylpyridinium iodide (528 mg, 2.01 mmol), and then sealed with a rubber septum. A drying tube containing Drierite was fitted with a needle and inserted through the septum. Dimethyl sulfate (0.19 mL, 2.01 mmol) was then injected via syringe through the septum. The mixture was then vigorously stirred for 1 min, then placed under vacuum to provide 496 mg (100% yield) of the desired product.

Entry 6. A flask was charged with a magnetic stirbar and trihexyl(tetradecyl)phosphonium chloride (141 mg, 0.27 mmol), and then sealed with a rubber septum. A drying tube containing Drierite was fitted with a needle and inserted through the septum. Dimethyl sulfate (0.03 mL, 0.27 mmol) was then injected via syringe through the septum. The mixture was then vigorously stirred for 1 min, then placed under vacuum to provide 162 mg (100% yield) of the desired product as a clear viscous liquid.

Entry 7. A flask was charged with a magnetic stirbar and trihexyl(tetradecyl)phosphonium bromide (152 mg, 0.27 mmol), and then sealed with a rubber septum. A drying tube containing Drierite was fitted with a needle and inserted through the septum. Dimethyl sulfate (0.03 mL, 0.27 mmol) was then injected via syringe through the septum. The mixture was then vigorously stirred for 1 min, then placed under vacuum to provide 162 mg (100% yield) of the desired product as a clear viscous liquid.

Entry 8. A flask was charged with a magnetic stirbar and 1-butyl-3-methylimidazolium bromide (534 mg, 2.43 mmol), methyl tosylate (452 mg, 2.43 mmol), and then sealed with a rubber septum. A drying tube containing Drierite was fitted with a needle and inserted through the septum. The mixture was then placed in an oil bath at 50 °C and vigorously stirred for 3 min, then placed under vacuum to provide 753 mg (100% yield) of the desired product.

Entry 9. A flask was charged with a magnetic stirbar and 1-butyl-3-methylimidazolium iodide (548 mg, 2.04 mmol), methyl tosylate (381 mg, 2.04 mmol), and then sealed with a rubber septum. A drying tube containing Drierite was fitted with a needle and inserted through the septum. The mixture was then vigorously stirred for 3 min, then placed under vacuum to provide 635 mg (100% yield) of the desired product.

Entry 10. A flask was charged with a magnetic stirbar and 1-butylpyridinium chloride (556 mg, 3.24 mmol), and then sealed with a rubber septum. A drying tube containing Drierite was fitted with a needle and inserted through the septum. The flask was then placed in an oil bath at 120 °C and methyl tosylate (608 mg, 3.27 mmol) was injected via syringe through the septum. The mixture was then vigorously stirred for 3 min, then placed under vacuum to provide 1.00 g (100% yield) of the desired product as a beige solid.

Entry 11. A flask was charged with a magnetic stirbar and 1-butylpyridinium iodide (699 mg, 2.66 mmol), methyl tosylate (495 mg, 2.66 mmol), and then sealed with a

rubber septum. A drying tube containing Drierite was fitted with a needle and inserted through the septum. The mixture was then vigorously stirred for 3 min, then placed under vacuum to provide 817 mg (100% yield) of the desired product as a beige solid.

Chapter 7: Phase-Tunable Fluorophores Based Upon Benzobis(imidazolium) Salts

7.1 Introduction

Conjugated organic salts are a versatile class of molecules that have found utility in a range of applications,^{100,106} including ion-conductive membranes for fuel cells, photovoltaics, ionic organic light-emitting diodes, and ionic liquid crystals (ILCs). A nascent area of fundamental research, that may significantly advance the aforementioned applications, focuses on enhancing the photoluminescent properties of liquid organic salts (i.e., fluorescent ionic liquids). Current efforts in this area have been centered on traditional imidazolium-based ionic liquids (ILs).^{106f-h,107,108} Unfortunately, due to their relatively small chromophores, such ILs typically display stifflingly low emission intensities in the visible region ($\Phi_f < 0.05$) which not only complicates analytical measurements but also limits their utilities.^{106f,g} Further exploration in this field has been thwarted by inherent barriers associated with imparting fluidic properties to rigid polycyclic aromatic systems. Herein, we report a general, modular route to fluorescent, conjugated organic salts with tunable phase characteristics including room-temperature fluidity and mesomorphic (i.e., liquid-crystalline (LC)) behavior at higher temperatures. As summarized in Figure 7.1, benzobis(imidazolium) (BBI) salts are poised for finely tuning the phase characteristics of fluorescent conjugated organic salts. They feature: (1) robust imidazolium components for dually providing phase control and high thermal stabilities, (2) fluorogenic heteroaromatic cores which should enable efficient luminescence, and (3) modular *N*-substituents to tailor LC phase properties. Overall,

BBIs should provide phase-tunability as well as increased emission relative to traditional imidazolium-based ILs.

7.2 Synthesis of benzobis(imidazolium) salts with low T_g s

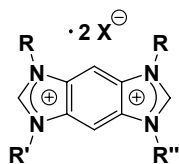
Initially, we investigated BBIs **7.1** and **7.2**, which possess *N*-alkyl and *N*-aryl groups, respectively (Figure 7.1). Not only was each salt found to display a high Φ_f , their disparate λ_{\max} values suggested a straightforward means to tune their electronic characteristics (Table 7.1) through *N*-substitution. Since **7.1** and **7.2** decomposed prior to melting, subsequent efforts shifted toward capitalizing on the structural features shown in Figure 7.1 to tune phase characteristics.

Systematic structural optimization was guided by knowledge of related ILs,^{106d} as well as solid-state analysis of select crystalline compounds. An advancement was made with BBI **7.3** which exhibited a relatively low glass transition temperature (T_g) of 89 °C due to its reduced molecular symmetry and non-coordinating counterions (c.f., **7.1** and **7.2**). Building from these results, BBI **7.4•MeSO₄** (T_g = 43 °C) was synthesized, which takes advantage of dissimilar imidazolium rings to reduce its molecular symmetry even further. Surveying other counterions associated with the same BBI core (c.f., **7.4•BF₄** and **7.4•I**) confirmed that MeSO₄ was ideal for lowering the T_g s of these salts.¹⁰⁹ By incorporating *N*-substituents that not only disrupted π - π interactions but also imparted π -facial asymmetry (**7.5** – **7.7**), a BBI with a T_g < 0 °C was ultimately synthesized. Notably, high T_d s were observed from each of the BBIs, typically exceeding 270 °C.

As mentioned above, desirable photoluminescence properties were a key objective of our study. The absorption, excitation, and emission properties of **7.3** – **7.7**

were initially investigated in MeOH. As summarized in Table 7.1, the absorption and emission spectra for **7.4** – **7.7** remained fairly consistent, which demonstrated an ability to selectively manipulate their physical properties without compromising control over electronic features. Importantly, each of the BBIs exhibited high Φ_{FS} (0.41–0.91), which should facilitate their application as functional, solution-based fluorophores.

Figure 7.1 Photoluminescent benzobis(imidazolium) salts



BBI	R	R'	R''	X	Yield (%) ^a
7.1	Bu	Bu	Bu	Br	93
7.2	Ph	Ph	Ph	Cl	48
3	Me	Ph	Ph	MeSO ₄	86
7.4•MeSO₄	Me	<i>i</i> -Bu	4-BuPh	MeSO ₄	89
7.4•BF₄	Me	<i>i</i> -Bu	4-BuPh	BF ₄	85
7.4•I	Me	<i>i</i> -Bu	4-BuPh	I	88
7.5	Me	<i>i</i> -Bu	3-MePh	MeSO ₄	90
7.6	Et	Me	3-MePh	MeSO ₄	91
7.7	Et	Me	4-OctPh	MeSO ₄	89
7.8a	C ₁₂ H ₂₅	C ₁₂ H ₂₅	C ₁₂ H ₂₅	BF ₄	99
7.8b	Me	4-OctPh	4-OctPh	BF ₄	78

^aIsolated overall yield from commercially available starting material.

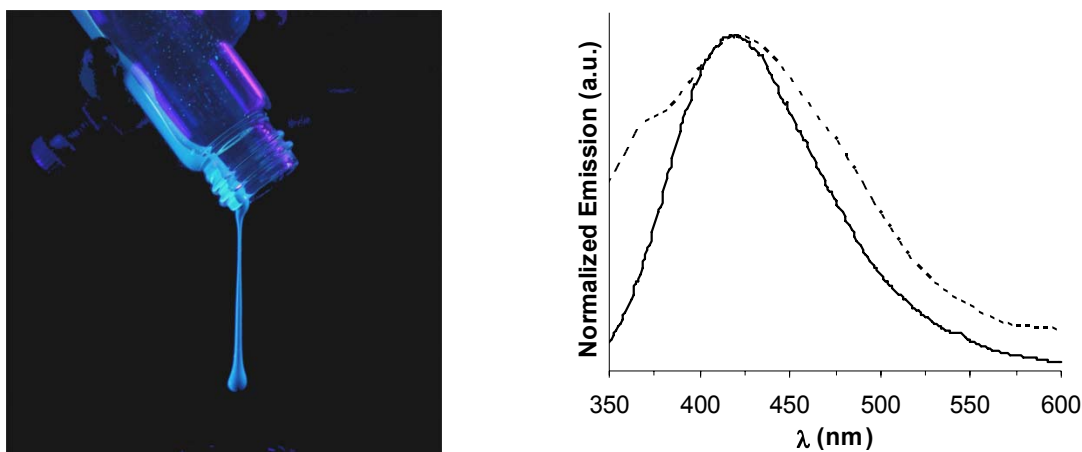
Table 7.1 Physical and photophysical properties of benzobis(imidazolium) salts

BBI	T _g (°C) ^a	T _d (°C) ^b	λ _{abs} (nm) ^c	Log (ε) ^c	λ _{em} (nm) ^c	Φ _f ^d
7.1	e	271	288	4.29	330	0.64
7.2	e	325	352	3.94	474	0.41
3	89	267	345	3.31	447	0.91
7.4•MeSO₄	43	273	287	4.04	410	0.53
7.4•BF₄	84	338	288	4.27	408	0.51
7.4•I	113	218	288	4.20	408	0.47
7.5	35	270	286	4.19	402	0.52
7.6	0.8	272	289	4.01	403	0.63
7.7	-0.3	274	289	4.13	408	0.57
7.8a	f	338	291	4.14	332	0.85
7.8b	f	341	348	4.03	451	0.72

^aGlass transition temperature (T_g) obtained from the second heating run using DSC under N₂, rate = 5 °C/min. ^bDecomposition temperature (T_d) was defined as the temperature at which 10% weight loss occurred as determined by TGA under N₂, rate = 10 °C/min. ^cIn MeOH under ambient conditions. ^dQuantum efficiencies (Φ_f) were determined relative to E-stilbene or anthracene. ^eNo transitions observed by DSC up to the T_d. ^fMesomorphic, see text.

Central to our primary objective, however, was the ability of the BBI chromophore to avoid self-quenching mechanisms and maintain intense emission in condensed phases. Photoluminescence was qualitatively observed from each of the glassy BBI fluorophores (i.e., **7.3** – **7.7**) at temperatures above and below their T_gs. For example, as depicted in Figure 2, bright blue emission obtained from a bulk sample of **7.4•MeSO₄** was found to persist at 200 °C, a temperature well above its T_g. Excitation of an annealed thin film of this material (obtained via melt-casting) produced a bright blue emission with a λ_{em} of 423 nm, consistent with the λ_{em} in solution (Figure 7.2). Collectively, these results indicated that BBI-based IL fluorophores maintained efficient luminescent properties in solution, solid-state, and as flowing liquids.

Figure 7.2 Left: Photoluminescence spectrum of **7.4•MeSO₄** in MeOH (solid line) and as a thin film (dotted line), each under ambient conditions. Right: Picture of **7.4•MeSO₄** heated at ca 80 °C under irradiation from a 365 nm lamp (5 W).



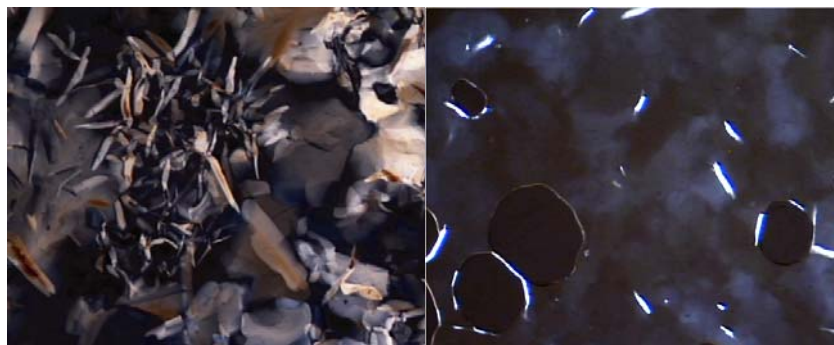
7.3 Synthesis of liquid crystalline benzobis(imidazolium) salts

Having obtained room-temperature fluorescent ILs, we focused next on fine-tuning phase control to obtain mesomorphic fluorophores based on BBIs. This was motivated largely by the observation that imparting LC behavior to neutral organic fluorophores can greatly improve their performance in electronic applications.¹¹⁰ Furthermore, the BBI architecture would introduce a unique structural class of ILCs featuring rigid, polycyclic cationic cores^{106i,j} similar to dye-based chromonic LCs but photoluminescent in nature.¹¹¹

Two BBI-based mesogens, **7.8a** and **7.8b** (see Figure 7.1), were synthesized and each was analyzed by differential scanning calorimetry (DSC), polarized light microscopy (PLM), and variable-temperature powder X-ray diffraction (VT-PXRD).

Investigation of the DSC cooling cycles of **7.8a** suggested a broad LC temperature range that began at 53 °C and extended to 194 °C, at which point the material became isotropic. Upon cooling from the isotropic melt, PLM of **7.8a** showed dendritic growth and domains characteristic of columnar LC phases (see Figure 7.3). Low-angle VT-PXRD, however, revealed reflections at intervals consistent with a smectic phase. DSC analysis of **7.8b** revealed a narrower and higher temperature LC range (188 – 238 °C). As shown in Figure 3, PLM of this mesogenic material revealed textures that were suggestive of a cubic mesophase, which was further confirmed by VT-PXRD.^{112,113}

Figure 7.3 PLM images (left: ILC **7.8a**, right: ILC **7.8b**) were obtained at 130 and 215 °C, respectively, on cooling from the isotropic melt. Mag = 100x



7.4 Conclusions

In conclusion, unprecedented phase-tunable fluorophores based upon a series of highly photoluminescent BBI salts have been synthesized. A key structural feature of these fluorophores is that they incorporate imidazolium moieties, whereupon annulation

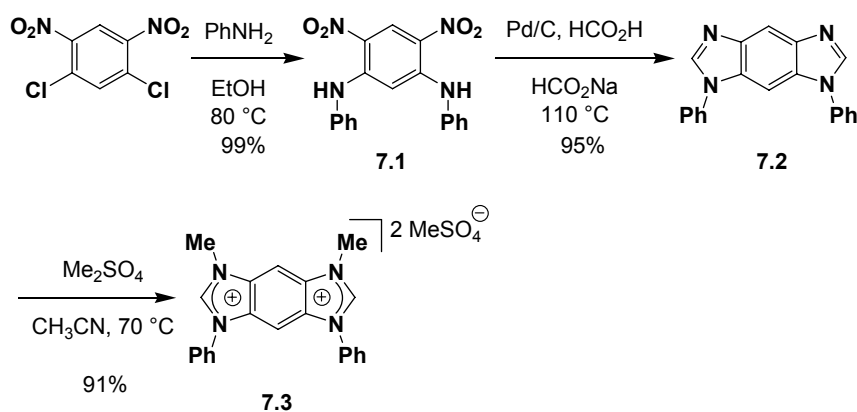
leads to desirable luminescent properties. Through judicious choice of *N*-substituents and counterions, BBI salts with T_{ds} as high as 338 °C were obtained for materials that were fluidic below 0 °C. This feature also enabled access to two BBI-based mesogens, thus introducing a new platform for fluorescent ILC design. Collectively, these organic salts produced constant blue emission from solution to cooled glassy states to free flowing liquids. Considering their high thermal stability, amphiphilic properties, and structural modularity, BBI salts effectively form a new class of emissive chromophores with promise as processable fluorophores, sensory materials, and models for fundamental photophysical investigations.

7.5 Experimental Section

General Considerations: ^1H and ^{13}C NMR spectra were recorded using a Varian Unity Plus 300 or 400 spectrometer. Chemical shifts (δ) are expressed in ppm downfield from tetramethylsilane using the residual protio solvent as an internal standard (CDCl_3 , ^1H : 7.26 ppm and ^{13}C : 77.0 ppm; $\text{DMSO}-d_6$, ^1H : 2.49 ppm and ^{13}C : 39.5 ppm). Coupling constants are expressed in hertz (Hz). HRMS (ESI, CI) were obtained with a VG analytical ZAB2-E instrument. UV-vis spectra were recorded using a Perkin Elmer Instruments Lambda 35 spectrometer. Emission spectra were recorded using a QuantaMaster Photon Technology International fluorometer. Differential scanning calorimetry (DSC) data was recorded using a TA Instruments DSC-Q100. Thermogravimetric analysis (TGA) was performed using a TA Instruments TGA-Q500 under nitrogen atmosphere. The decomposition temperature (T_d) was defined as the temperature at which 10% weight loss occurred. Samples were dried under vacuum for \geq

8 h immediately prior to DSC and TGA experiments. Polarized light microscopy studies were performed with a Leica DMRXP polarizing light microscope equipped with an Optronics digital camera assembly. Powder X-ray diffraction spectra were obtained with an Inel CPS 120 diffraction system using monochromated Cu K α X-ray radiation. Unless otherwise noted, reactions were conducted under ambient atmosphere. All starting materials and solvents were of reagent quality and used as received from commercial suppliers.

Scheme 7.1 Synthesis of benzobis(imidazolium) salt **7.3**



4,6-Dinitro-N,N'-diphenyl-benzene-1,3-diamine (7.1). A flask was charged with a magnetic stirbar, EtOH (25 mL), and aniline (7.5 mL, 82.3 mmol). After 1,5-dichloro-2,4-dinitrobenzene (4.87 g, 20.6 mmol) was added to the reaction mixture, the flask was fitted with a H₂O-jacketed condenser. The mixture was then stirred in an oil bath at 80 °C for 36 h during which time a thick orange slurry developed. The mixture was then allowed to cool and poured into H₂O (100 mL). Precipitated solids were collected via vacuum filtration, rinsed with H₂O, and dried under vacuum to give 7.15 g (99% yield) of

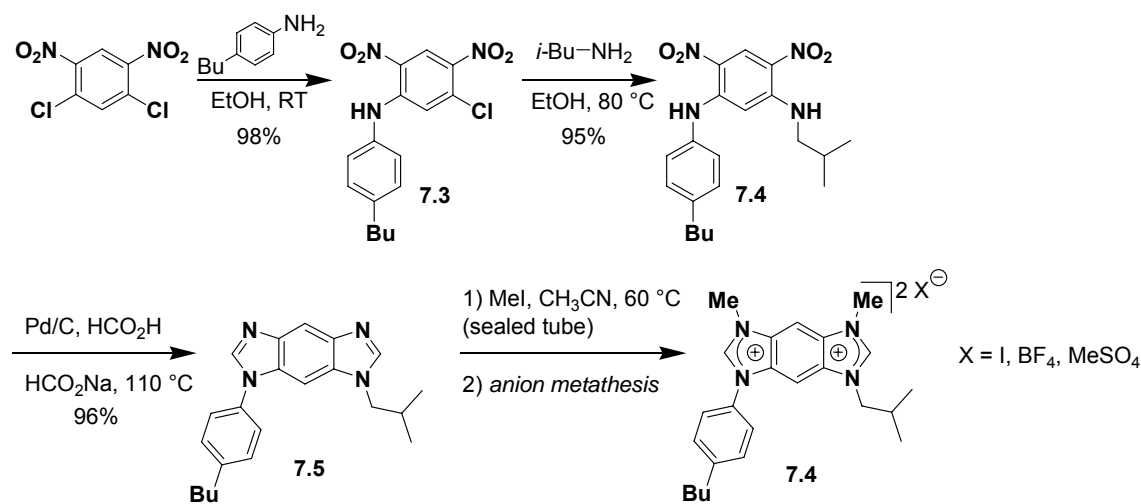
the desired product as an orange-red powder. ^1H NMR (300 MHz, CDCl_3): δ 9.74 (br s, 2H), 9.32 (s, 1H), 7.37-7.32 (m, 4H), 7.23-7.14 (m, 6H), 6.53 (s, 1H); ^{13}C NMR (75 MHz, CDCl_3): δ 146.8, 137.1, 129.6, 129.3, 126.6, 125.3, 124.7, 95.2; HRMS m/z calcd for $\text{C}_{18}\text{H}_{15}\text{N}_4\text{O}_4$ $[\text{M}+\text{H}^+]$ 351.1093, found 351.1090.

1,7-Diphenylbenzobis(imidazole) (7.2). A flask was charged with a magnetic stirbar and HCO_2H (100 mL, 88%). NaHCO_3 (15.3 g, 183 mmol) was added portionwise with vigorous stirring. To the mixture was added Pd/C (1.94 g, 5 wt % Pd, 0.91 mmol Pd) and dinitroarene **7.1** (3.20 g, 9.13 mmol). After the flask was fitted with a H_2O -jacketed condenser, the reaction mixture was stirred in an oil bath at 110 $^\circ\text{C}$ for 48 h. The mixture was then allowed to cool and filtered through Celite with the aid of 50 mL H_2O . After the filtrate volume was reduced to approximately 50 mL under reduced pressure, the resulting mixture was added to a vigorously stirred solution of saturated aqueous K_2CO_3 . Precipitated solids were collected via vacuum filtration, rinsed with H_2O and dried under vacuum to provide 2.70 g (95% yield) of the desired product as a beige powder. ^1H NMR (400 MHz, CDCl_3): δ 8.34 (s, 1H), 8.16 (s, 2H), 7.60-7.51 (m, 9H), 7.48-7.44 (m, 2H); ^{13}C NMR (100 MHz, CDCl_3): δ 143.3, 141.3, 136.4, 132.1, 130.1, 127.9, 123.9, 110.6, 90.1; HRMS m/z calcd for $\text{C}_{20}\text{H}_{15}\text{N}_4$ $[\text{M}+\text{H}^+]$ 311.1297, found 311.1293.

1,7-Dimethyl-3,5-diphenylbenzobis(imidazolium) bis(methyl sulfate) (7.3). Diphenylbenzobis(imidazole) **7.2** (660 mg, 2.13 mmol) was dissolved in CH_3CN (4 mL). After dimethyl sulfate (0.41 mL, 4.37 mmol) was added to the solution, the resulting mixture was stirred at 70 $^\circ\text{C}$ for 4 h. The mixture was then concentrated under vacuum.

After rinsing the residual solids several times with excess EtOAc, they were dried under vacuum to give 1.10 g (91% yield) of the desired benzobis(imidazolium) salt as a beige powder. Crystals suitable for X-ray analysis were obtained by slow evaporation of a MeOH/Et₂O solution. ¹H NMR (400 MHz, DMSO-*d*₆): δ 10.37 (s, 2H), 9.07 (s, 1H), 8.04 (s, 1H), 7.88-7.85 (m, 4H), 7.77-7.68 (m, 6H), 4.28 (s, 6H), 3.35 (s, 6H); ¹³C NMR (100 MHz, DMSO-*d*₆): δ 147.1, 133.0, 131.2, 130.7, 130.6, 130.1, 125.3, 99.6, 98.0, 52.9, 32.1; HRMS *m/z* calcd for C₂₂H₁₉N₄ [M-H⁺] 339.1610, found 339.1606; T_d = 267 °C; T_g = 89 °C.

Scheme 7.2 Synthesis of benzobis(imidazolium) salts **7.4**



N-(5-Chloro-2,4-dinitrophenyl)-4-butylaniline (7.3). 1,5-Dichloro-2,4-dinitrobenzene (100.0 g, 422 mmol) was suspended in EtOH (1.3 L) and 4-butylaniline (81.8 mL, 844 mmol) was added. After the resulting orange-red slurry was stirred for 24 h, it was poured into excess H₂O (200 mL). Precipitated solids were collected via vacuum

filtration, rinsed with H₂O, and dried under vacuum to provide 145.2 g (98% yield) of the desired product as a red powder. ¹H NMR (400 MHz, CDCl₃): δ 9.80 (br s, 1H), 9.08 (s, 1H), 7.32 (d, *J* = 8.2 Hz, 2H), 7.19 (d, *J* = 8.2 Hz, 2H), 7.14 (s, 1H), 2.68 (t, *J* = 7.8 Hz, 2H), 1.68-1.61 (m, 2H), 1.44-1.35 (m, 2H), 0.96 (t, *J* = 7.4 Hz, 3H); ¹³C NMR (100 MHz, CDCl₃): δ 145.9, 143.2, 135.8, 135.6, 133.6, 130.3, 129.3, 126.7, 125.4, 117.9, 35.2, 33.4, 22.3, 13.9; HRMS *m/z* calcd for C₁₆H₁₇N₃O₄Cl [M+H⁺] 350.0908, found 350.0906.

1-(4-Butylphenyl)amino-5-(2-methylpropyl)amino-2,4-dinitrobenzene (7.4).

Chloroarene **7.3** (1.35 g, 3.86 mmol) was treated with *iso*-butylamine (0.76 mL, 7.72 mmol) in EtOH (4 mL) at 80 °C for 24 h. The mixture was then allowed to cool and poured into H₂O (50 mL). Precipitated solids were collected via vacuum filtration, rinsed with H₂O, and dried under vacuum to provide 1.42 g (95% yield) of the desired product as an orange powder. ¹H NMR (400 MHz, CDCl₃): δ 9.73 (br s, 1H), 9.29 (s, 1H), 8.36 (br t, 1H), 7.28 (d, *J* = 8.4 Hz, 2H), 7.21 (d, *J* = 8.4 Hz, 2H), 6.04 (s, 1H), 2.88-2.86 (m, 2H), 2.67 (t, *J* = 7.8 Hz, 2H), 1.93-1.83 (m, 1H), 1.67-1.59 (m, 2H), 1.42-1.33 (m, 2H), 0.95 (t, *J* = 7.2 Hz, 3H), 0.94 (d, *J* = 6.8 Hz, 6H); ¹³C NMR (100 MHz, CDCl₃): δ 148.5, 147.6, 142.0, 134.9, 129.8, 129.5, 125.3, 124.9, 124.2, 92.6, 50.6, 35.1, 33.5, 27.5, 22.2, 20.2, 13.9; HRMS *m/z* calcd for C₂₀H₂₇N₄O₄ [M+H⁺] 387.2032, found 387.2030.

1-(4-Butylphenyl)-7-(2-methylpropyl)benzobis(imidazole) (7.5). This compound was prepared analogously to **7.2** from dinitroarene **7.4** (5.00 g, 12.93 mmol). The crude material was recrystallized from Et₂O and hexanes to provide 4.31 g (96% yield) of the desired product as a tan solid. ¹H NMR (400 MHz, CDCl₃): δ 8.24 (s, 1H), 8.08 (s, 1H),

7.89 (s, 1H), 7.44 (d, $J = 8.2$ Hz, 2H), 7.40 (d, $J = 8.2$ Hz, 2H), 7.33 (s, 1H), 3.94 (d, $J = 7.2$ Hz, 2H), 2.72 (t, $J = 7.6$ Hz, 2H), 2.27-2.17 (m, 1H), 1.72-1.64 (m, 2H), 1.45-1.37 (m, 2H), 0.96 (t, $J = 7.4$ Hz, 3H), 0.92 (d, $J = 6.8$ Hz, 6H); ^{13}C NMR (100 MHz, CDCl_3): δ 144.3, 143.1, 142.9, 141.2, 141.0, 134.2, 132.5, 131.9, 130.0, 123.9, 110.3, 89.3, 52.6, 35.2, 33.5, 28.5, 22.3, 20.1, 13.9; HRMS m/z calcd for $\text{C}_{22}\text{H}_{27}\text{N}_4$ $[\text{M}+\text{H}^+]$ 347.2236, found 347.2232.

1-(4-Butylphenyl)-7-(2-methylpropyl)-3,5-dimethylbenzobis(imidazolium) diiodide (7.4•I). A vial was charged with benzobis(imidazole) **7.5** (3.21 g, 9.26 mmol), CH_3CN (6 mL), and MeI (2.0 mL, 32.1 mmol). The vial was sealed with a Teflon-lined cap and the mixture was stirred in an oil bath at 60 °C for 8 h. The mixture was then allowed to cool, transferred to a round-bottom flask, and concentrated to provide 5.69 g (97% yield) of the desired product as a beige powder. ^1H NMR (400 MHz, $\text{DMSO}-d_6$): δ 10.36 (s, 1H), 10.07 (s, 1H), 9.03 (s, 1H), 8.61 (s, 1H), 7.81 (d, $J = 8.4$ Hz, 2H), 7.63 (d, $J = 8.4$ Hz, 2H), 4.48 (d, $J = 7.6$ Hz, 2H), 4.26 (s, 3H), 4.24 (s, 3H), 2.76 (t, $J = 7.8$ Hz, 2H), 2.33-2.23 (m, 1H), 1.70-1.62 (m, 2H), 1.43-1.34 (m, 2H), 0.94 (t, $J = 7.4$ Hz, 3H), 0.93 (d, $J = 6.8$ Hz, 6H); ^{13}C NMR (100 MHz, $\text{DMSO}-d_6$): δ 146.7, 146.4, 145.2, 130.9, 130.68, 130.66, 130.0, 125.2, 99.2, 98.5, 53.3, 34.4, 34.3, 32.8, 28.1, 21.8, 19.3, 13.8; HRMS m/z calcd for $\text{C}_{24}\text{H}_{31}\text{N}_4$ $[\text{M}-\text{H}^+]$ 375.2549, found 375.2543; $T_d = 218$ °C; $T_g = 113$ °C.

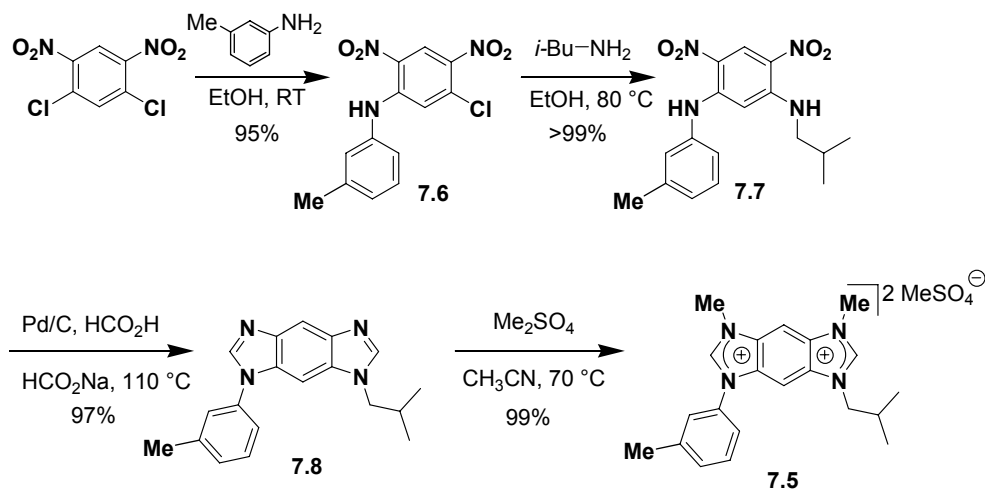
1-(4-Butylphenyl)-7-(2-methylpropyl)-3,5-dimethylbenzobis(imidazolium) bis(tetrafluoroborate) (7.4•BF₄). Bis(imidazolium) diiodide **7.4•I** (1.23 g, 1.95 mmol) was dissolved in dry CH_2Cl_2 (8 mL) under an atmosphere of dry N_2 and triethyloxonium

tetrafluoroborate (741 mg, 3.90 mmol) was added. The reaction was monitored by ^1H NMR spectroscopy and upon completion (≤ 10 min) the mixture was concentrated to provide 1.02 g (95% yield) of the desired product as a beige powder. ^1H NMR (300 MHz, DMSO- d_6): δ 10.31 (s, 1H), 9.99 (s, 1H), 8.94 (s, 1H), 8.64 (s, 1H), 7.80 (d, $J = 8.4$ Hz, 2H), 7.66 (d, $J = 8.4$ Hz, 2H), 4.49 (d, $J = 7.5$ Hz, 2H), 4.27 (s, 3H), 4.24 (s, 3H), 2.80 (t, $J = 7.6$ Hz, 2H), 2.34-2.25 (m, 1H), 1.75-1.65 (m, 2H), 1.48-1.36 (m, 2H), 0.98 (t, $J = 7.2$ Hz, 3H), 0.96 (d, $J = 6.6$ Hz, 6H); ^{13}C NMR (75 MHz, DMSO- d_6): δ 146.8, 146.6, 145.4, 131.1, 131.0, 130.8, 130.3, 130.2, 125.2, 99.0, 98.6, 53.3, 34.5, 34.0, 32.9, 28.2, 21.9, 19.3, 13.8; HRMS m/z calcd for $\text{C}_{24}\text{H}_{31}\text{N}_4$ $[\text{M}-\text{H}^+]$ 375.2549, found 375.2543; $T_d = 338$ °C; $T_g = 84$ °C.

1-(4-Butylphenyl)-7-(2-methylpropyl)-3,5-dimethylbenzobis(imidazolium)

bis(methyl sulfate) (7.4•MeSO₄). Bis(imidazolium) diiodide **7.4•I** (833 mg, 1.32 mmol) was dissolved in CH_2Cl_2 (2 mL) and dimethyl sulfate (0.25 mL, 2.64 mmol) was added. The reaction was monitored ^1H NMR spectroscopy. Upon completion (approximately 3 h), the mixture was concentrated to provide 788 mg (100% yield) of the desired product as a beige powder. ^1H NMR (400 MHz, DMSO- d_6): δ 10.29 (s, 1H), 9.99 (s, 1H), 8.95 (s, 1H), 8.61 (s, 1H), 7.76 (d, $J = 8.4$ Hz, 2H), 7.62 (d, $J = 8.4$ Hz, 2H), 4.45 (d, $J = 7.6$ Hz, 2H), 4.24 (s, 3H), 4.21 (s, 3H), 3.35 (s, 6H), 2.76 (t, $J = 7.8$ Hz, 2H), 2.31-2.20 (m, 1H), 1.70-1.62 (m, 2H), 1.43-1.34 (m, 2H), 0.95 (t, $J = 8.2$ Hz, 3H), 0.91 (d, $J = 6.8$ Hz, 6H); ^{13}C NMR (100 MHz, DMSO- d_6): δ 146.8, 146.6, 145.3, 131.0, 130.8, 130.7, 130.3, 130.1, 125.2, 99.1, 98.6, 53.3, 52.8, 34.5, 34.0, 32.9, 28.1, 21.9, 19.3, 13.8; HRMS m/z calcd for $\text{C}_{24}\text{H}_{31}\text{N}_4$ $[\text{M}-\text{H}^+]$ 375.2549, found 375.2543; $T_d = 273$ °C; $T_g = 43$ °C.

Scheme 7.3 Synthesis of benzobis(imidazolium) salt **7.5**



N-(5-chloro-2,4-dinitrophenyl)-3-methylaniline (7.6). This compound was prepared analogously to **7.3** from 1,5-dichloro-2,4-dinitrobenzene (2.04 g, 8.61 mmol) and *m*-toluidine (1.88 mL, 17.2 mmol) in EtOH (10 mL) to provide 2.51 g (95% yield) of the desired product as an orange powder. ¹H NMR (400 MHz, CDCl₃): δ 9.81 (br s, 1H), 9.07 (s, 1H), 7.42-7.38 (m, 1H), 7.23-7.21 (m 1H), 7.16 (s, 1H), 7.11-7.10 (m, 2H), 2.43 (s, 3H); ¹³C NMR (100 MHz, CDCl₃): δ 145.7, 140.7, 136.1, 135.8, 135.6, 130.1, 129.4, 128.9, 126.6, 126.1, 122.4, 118.0, 21.4; HRMS *m/z* calcd for C₁₃H₁₁N₃O₄Cl [M+H⁺] 308.0438, found 308.0442.

1-(3-Methylphenyl)amino-5-(2-methylpropyl)amino-2,4-dinitrobenzene (7.7). This compound was prepared analogously to **7.4** from chloroarene **7.6** (11.0 g, 35.8 mmol) and *iso*-butylamine (7.1 mL, 71.5 mmol) in EtOH (70 mL) at 80 °C to provide 12.3 g (>99% yield) of the desired product as an orange powder. ¹H NMR (400 MHz, CDCl₃): δ 9.76

(br s, 1H), 9.29 (s, 1H), 8.37 (br t, 1H), 7.37-7.33 (m, 1H), 7.15-7.11 (m, 3H), 6.13 (s, 1H), 2.90-2.87 (m, 2H), 2.40 (s, 3H), 1.95-1.84 (m, 1H), 0.95 (d, $J = 6.8$ Hz, 6H); ^{13}C NMR (75 MHz, CDCl_3): δ 148.6, 147.3, 140.1, 137.4, 129.6, 129.5, 127.6, 125.8, 125.0, 124.3, 122.1, 92.7, 50.7, 27.6, 21.3, 20.2; HRMS m/z calcd for $\text{C}_{17}\text{H}_{21}\text{N}_4\text{O}_4$ $[\text{M}+\text{H}^+]$ 345.1563, found 345.1561.

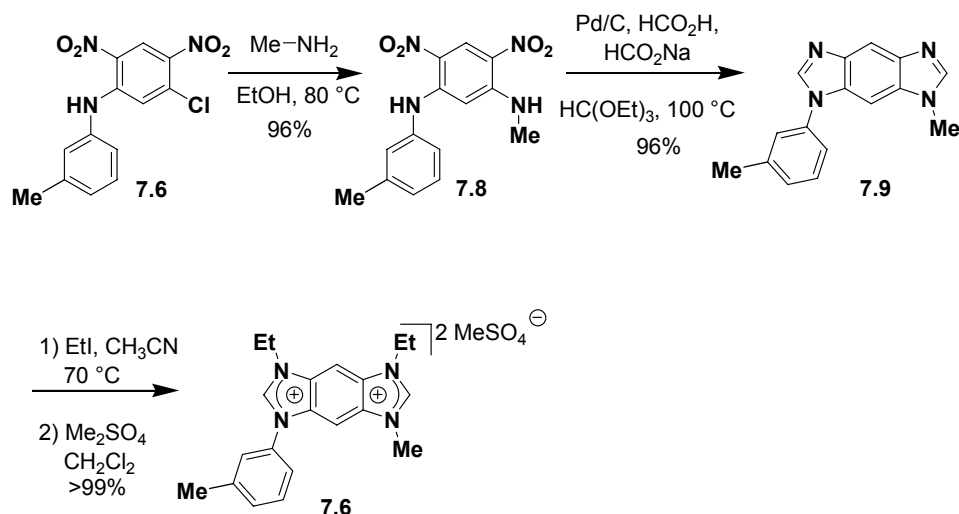
1-(3-Methylphenyl)-7-(2-methylpropyl)benzobis(imidazole) (7.8). This compound was prepared analogously to **7.2** from dinitroarene **7.7** (12.7 g, 34.8 mmol). The crude material was recrystallized from Et_2O and hexanes to provide 10.27 g (97% yield) of the desired product as a tan solid. ^1H NMR (400 MHz, CDCl_3): δ 8.25 (s, 1H), 8.12 (s, 1H), 7.93 (s, 1H), 7.50 (t, $J = 8.0$ Hz, 1H), 7.38-7.35 (m, 2H), 7.35 (s, 1H), 7.32-7.30 (m, 1H), 3.96 (d, $J = 7.2$ Hz, 2H), 2.49 (s, 3H), 2.28-2.18 (m, 1H), 0.94 (d, $J = 6.4$ Hz, 6H); ^{13}C NMR (100 MHz, CDCl_3): δ 144.4, 143.0, 141.3, 141.0, 140.3, 136.6, 132.5, 131.7, 129.8, 128.6, 124.7, 121.0, 110.3, 89.3, 52.6, 28.6, 21.4, 20.1; HRMS m/z calcd for $\text{C}_{19}\text{H}_{21}\text{N}_4$ $[\text{M}-\text{H}^+]$ 305.1764, found 305.1761.

1-(3-Methylphenyl)-7-(2-methylpropyl)-3,5-dimethylbenzobis(imidazolium)

bis(methyl sulfate) (7.5). This compound was prepared analogously to **7.3** from benzobis(imidazole) **7.7** (758 mg, 2.49 mmol) to provide 1.37 g (99% yield) of the desired product as a brown foam. ^1H NMR (400 MHz, $\text{DMSO}-d_6$): δ 10.31 (s, 1H), 10.00 (s, 1H), 8.96 (s, 1H), 8.60 (s, 1H), 7.72-7.66 (m, 3H), 7.59-7.57 (m, 1H), 4.45 (d, $J = 7.2$ Hz, 2H), 4.25 (s, 3H), 4.21 (s, 3H), 3.34 (s, 6H), 2.29-2.22 (m, 1H), 0.92 (d, $J = 6.4$ Hz, 6H); ^{13}C NMR (75 MHz, $\text{DMSO}-d_6$): δ 146.8, 146.7, 140.4, 133.0, 131.3, 131.00, 130.96,

130.8, 130.4, 130.1, 125.8, 122.5, 99.1, 98.6, 53.3, 52.8, 34.0, 28.2, 21.0, 19.3; HRMS m/z calcd for $C_{21}H_{25}N_4$ $[M-H]^+$ 333.2078, found 333.2074; $T_d = 270\text{ }^\circ\text{C}$; $T_g = 35\text{ }^\circ\text{C}$.

Scheme 7.4 Synthesis of benzobis(imidazolium) salt **7.6**



1-Methylamino-5-(3-methylphenyl)amino-2,4-dinitrobenzene (7.8). Chloroarene **7.6** (2.00 g, 6.50 mmol), methylamine (40 wt% in H_2O , 2.02 g, 26.0 mmol), and EtOH (15 mL) were combined in a vial, which was later sealed with a Teflon-lined screw-cap. The mixture was vigorously stirred at $70\text{ }^\circ\text{C}$ for 24 h. After pouring the cooled reaction mixture into H_2O (50 mL), precipitated solids were collected by vacuum filtration, rinsed with H_2O , and dried under vacuum to provide 1.89 g (96% yield) of the desired product as a yellow powder. 1H NMR (300 MHz, $CDCl_3$): δ 9.80 (br s, 1H), 9.29 (s, 1H), 8.25 (br s, 1H), 7.38-7.33 (m, 1H), 7.15-7.13 (m, 3H), 6.14 (s, 1H), 2.84 (d, $J = 5.1\text{ Hz}$, 3H), 2.41 (s, 3H); ^{13}C NMR (75 MHz, $CDCl_3$): δ 149.3, 147.5, 140.1, 137.4, 129.7, 129.4, 127.7,

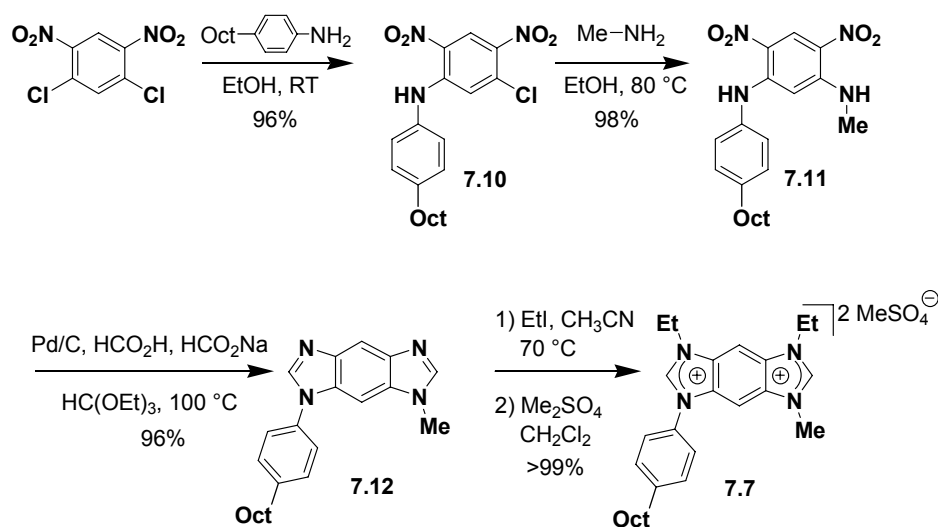
125.8, 122.1, 92.4, 29.8, 21.3; HRMS m/z calcd for $C_{14}H_{15}N_4O_4$ $[M+H^+]$ 303.1084, found 303.1088.

1-Methyl-7-(3-methylphenyl)benzobis(imidazole) (7.9). Dinitroarene **7.8** (1.78 g, 5.89 mmol) was suspended in $HC(OEt)_3$ (45 mL) in a 100 mL high-pressure, Schlenk flask. To the suspension was added HCO_2H (5 mL, 88%), HCO_2Na (8.03 g, 118 mmol), and Pd/C (2.50 g, 5 wt%, 1.18 mmol Pd). The Schlenk flask was sealed and the mixture was stirred at 100 °C for 36 h. After cooling to ambient temperature, the Schlenk flask was carefully opened to slowly release pressure. The mixture was then filtered through a pad of Celite. The filtrate was treated with 5% aqueous HCl (100 mL) and stirred for 10 min. The solution was then made alkaline using 10% aqueous NaOH and allowed to stand for approximately 1 h. The resulting solids were collected via vacuum filtration, rinsed with H_2O , and dried under vacuum to give 1.48 g (96% yield) of the desired product as a beige powder. 1H NMR (400 MHz, $CDCl_3$): δ 8.23 (s, 1H), 8.13 (s, 1H), 7.92 (s, 1H), 7.52-7.48 (m, 1H), 7.40-7.37 (m, 2H), 7.38 (s, 1H), 7.32-7.30 (m, 1H), 3.85 (s, 3H), 2.50 (s, 3H); ^{13}C NMR (75 MHz, $CDCl_3$): δ 144.5, 143.0, 141.1, 140.4, 136.6, 133.1, 131.9, 129.9, 128.7, 124.8, 121.2, 110.4, 89.0, 31.2, 21.4; HRMS m/z calcd for $C_{16}H_{15}N_4$ $[M+H^+]$ 263.1297, found 263.1299.

1,7-Diethyl-3-methyl-5-(3-methylphenyl)benzobis(imidazolium) bis(methylsulfate) (7.6). A vial was charged with benzobis(imidazole) **7.9** (131 mg, 0.50 mmol), CH_3CN (5 mL), and EtI (0.12 mL, 1.50 mmol). The vial was sealed with a Teflon-lined cap and the mixture was stirred in an oil bath at 70 °C for 8 h. The mixture was then allowed to cool

and concentrated under vacuum. To the resulting brown foam was added CH_2Cl_2 (4 mL) and Me_2SO_4 (95 μL , 1.00 mmol). The solution was stirred for 6 h and then concentrated under vacuum. The thick tan oil was rinsed with Et_2O and dried under vacuum to provide 287 mg (100% yield) of the desired product. X-ray quality crystals were obtained by slow evaporation of a $\text{CH}_2\text{Cl}_2/\text{EtOAc}/\text{Et}_2\text{O}$ solution. ^1H NMR (400 MHz, $\text{DMSO}-d_6$): δ 10.35 (s, 1H), 9.96 (s, 1H), 9.02 (s, 1H), 8.50 (s, 1H), 7.71-7.68 (m, 3H), 7.58-7.57 (m, 1H), 4.68 (quart, $J = 7.2$ Hz, 2H), 4.63 (quart, $J = 7.2$ Hz, 2H), 4.14 (s, 3H), 3.34 (s, 6H), 2.49 (s, 3H), 1.68 (t, $J = 7.2$ Hz, 3H), 1.61 (t, $J = 7.2$ Hz, 3H); ^{13}C NMR (75 MHz, $\text{DMSO}-d_6$): δ 146.3, 145.8, 140.4, 133.0, 131.30, 131.25, 130.3, 130.04, 129.98, 129.9, 125.8, 122.5, 98.92, 98.86, 52.8, 43.1, 42.6, 34.0, 20.9, 14.1, 13.8; HRMS m/z calcd for $\text{C}_{20}\text{H}_{23}\text{N}_4$ $[\text{M}-\text{H}^+]$ 319.1925, found 319.1917; $T_d = 272$ $^\circ\text{C}$; $T_g = 0.8$ $^\circ\text{C}$.

Scheme 7.5 Synthesis of benzobis(imidazolium) salt **7.7**



N-(5-chloro-2,4-dinitrophenyl)-4-octylaniline (7.10). This compound was prepared analogously to **7.3** from 1,5-dichloro-2,4-dinitrobenzene (1.52 g, 6.40 mmol) and 4-octylaniline (2.85 mL, 12.8 mmol) to provide 2.49 g (96% yield) of the desired product as an orange powder. ^1H NMR (300 MHz, CDCl_3): δ 9.81 (br s, 1H), 9.07 (s, 1H), 7.32 (d, $J = 8.1$ Hz, 2H), 7.19 (d, $J = 8.1$ Hz, 2H), 7.14 (s, 1H), 2.67 (t, $J = 7.8$ Hz, 2H), 1.68-1.63 (m, 2H), 1.34-1.28 (m, 10H), 0.89 (t, $J = 6.6$ Hz, 3H); ^{13}C NMR (75 MHz, CDCl_3): δ 145.9, 143.3, 135.5, 133.6, 130.3, 129.8, 129.3, 126.7, 125.4, 117.9, 35.5, 31.8, 31.3, 29.4, 29.3, 29.2, 22.6, 14.1; HRMS m/z calcd for $\text{C}_{20}\text{H}_{25}\text{N}_3\text{O}_4\text{Cl}$ $[\text{M}+\text{H}^+]$ 406.1534, found 406.1529.

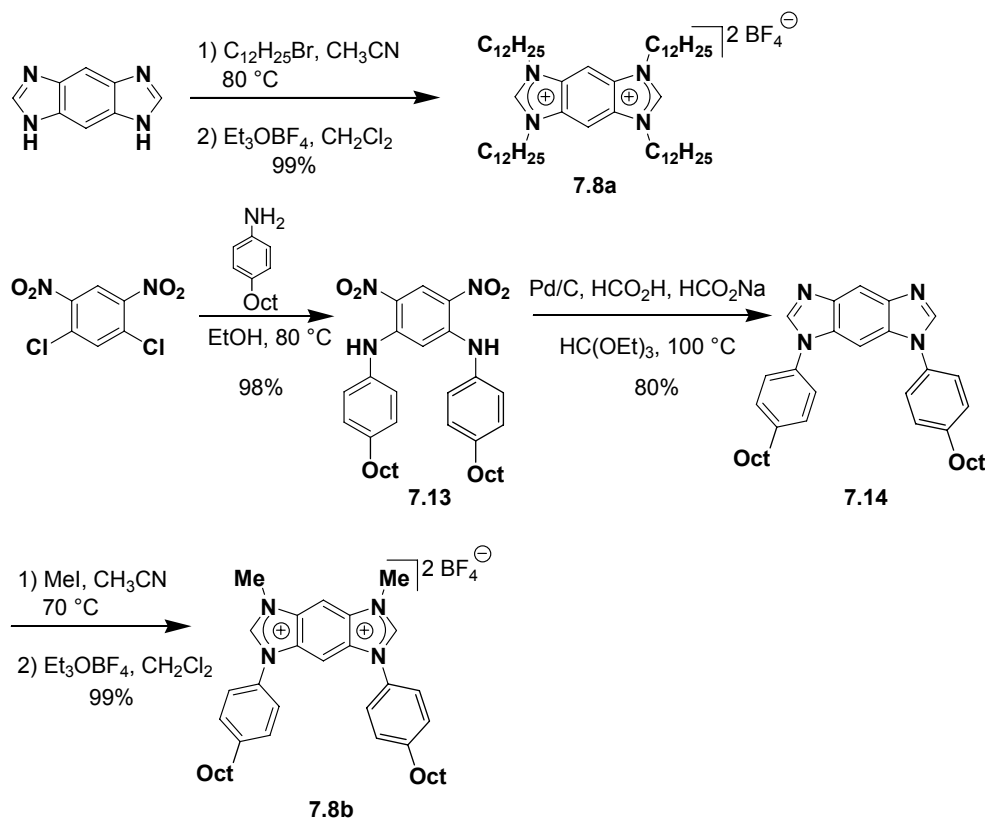
1-(4-Butylphenyl)-5-methylamino-2,4-dinitrobenzene (7.11). This compound was prepared analogously to **7.8** from chloroarene **7.10** (1.05 g, 2.59 mmol) and methylamine (40 wt% in H_2O , 804 mg, 10.4 mmol) to provide 1.02 g (98% yield) of the desired product as an orange powder. ^1H NMR (300 MHz, CDCl_3): δ 9.79 (br s, 1H), 9.29 (s, 1H), 8.24 (br s, 1H), 7.28 (d, $J = 8.8$ Hz, 2H), 7.23 (d, $J = 8.8$ Hz, 2H), 6.08 (s, 1H), 2.82 (d, $J = 4.8$ Hz, 3H), 2.65 (t, $J = 7.7$ Hz, 2H), 1.67-1.62 (m, 2H), 1.33-1.28 (m, 10H), 0.88 (t, $J = 6.5$ Hz, 3H); ^{13}C NMR (75 MHz, CDCl_3): δ 149.3, 147.7, 142.0, 134.9, 129.8, 129.4, 125.2, 124.9, 124.3, 92.2, 35.5, 31.8, 31.3, 29.7, 29.4, 29.2, 22.6, 14.1; HRMS m/z calcd for $\text{C}_{21}\text{H}_{29}\text{N}_4\text{O}_4$ $[\text{M}+\text{H}^+]$ 401.2186, found 401.2183.

1-(4-Butylphenyl)-7-methylbenzobis(imidazole) (7.12). This compound was prepared analogously to **7.9** from dinitroarene **7.11** (801 mg, 2.00 mmol) to provide 694 mg (96% yield) of the desired product as a tan solid. ^1H NMR (400 MHz, CDCl_3): δ 8.26 (s, 1H),

8.12 (s, 1H), 7.90 (s, 1H), 7.47 (d, $J = 8.4$ Hz, 2H), 7.41 (d, $J = 8.4$ Hz, 2H), 7.37 (s, 1H), 3.84 (s, 3H), 2.72 (t, $J = 7.8$ Hz, 2H), 1.74-1.66 (m, 2H), 1.40-1.26 (m, 10H), 0.89 (t, $J = 7.0$ Hz, 3H); ^{13}C NMR (100 MHz, CDCl_3): δ 144.5, 143.1, 141.2, 141.1, 134.3, 133.1, 132.1, 130.0, 124.1, 113.0, 110.4, 89.0, 35.6, 31.9, 31.5, 31.2, 29.4, 29.3, 29.2, 22.7, 14.1; HRMS m/z calcd for $\text{C}_{23}\text{H}_{29}\text{N}_4$ $[\text{M}+\text{H}^+]$ 361.2392, found 361.2390.

1-(4-Butylphenyl)-3,5-diethyl-7-methylbenzobis(imidazolium) bis(methyl sulfate) (7.7). A vial was charged with benzobis(imidazole) **7.12** (180 mg, 0.50 mmol), CH_3CN (5 mL), and EtI (0.12 mL, 1.50 mmol). The vial was sealed with a Teflon-lined cap and the mixture was stirred in an oil bath at 70 °C for 8 h. The mixture was then allowed to cool and concentrated under vacuum. To the resulting brown foam was added CH_2Cl_2 (4 mL) and Me_2SO_4 (95 μL , 1.00 mmol). The solution was stirred for 6 h, then concentrated under vacuum. The thick tan oil was rinsed with Et_2O and dried under vacuum to provide 320 mg (>99% yield) of the desired product. ^1H NMR (400 MHz, $\text{DMSO}-d_6$): δ 10.33 (s, 1H), 9.96 (s, 1H), 9.02 (s, 1H), 8.51 (s, 1H), 7.80 (d, $J = 8.4$ Hz, 2H), 7.62 (d, $J = 8.4$ Hz, 2H), 4.68 (quart, $J = 7.2$ Hz, 2H), 4.64 (quart, $J = 7.2$ Hz, 2H), 4.14 (s, 3H), 3.34 (s, 6H), 2.75 (t, $J = 7.6$ Hz, 2H), 1.68 (t, $J = 7.2$ Hz, 3H), 1.65 (br, 2H), 1.61 (t, $J = 7.2$ Hz, 3H), 1.33-1.27 (m, 10H), 0.86 (t, $J = 6.8$ Hz); ^{13}C NMR (75 MHz, $\text{DMSO}-d_6$): δ 146.3, 145.8, 145.4, 138.0, 131.2, 130.8, 130.2, 130.1, 130.0, 129.9, 125.2, 98.8, 52.8, 43.0, 42.6, 34.8, 33.9, 31.3, 30.9, 28.8, 28.71, 28.69, 22.1, 14.03, 13.97, 13.8; HRMS m/z calcd for $\text{C}_{27}\text{H}_{37}\text{N}_4$ $[\text{M}-\text{H}^+]$ 417.3015, found 417.3013; $T_d = 274$ °C; $T_g = -0.3$ °C.

Scheme 7.6 Synthesis of mesomorphic benzobis(imidazolium) salts **7.8a** and **7.8b**



1,3,5,7-Tetradodecylbenzobis(imidazolium) bis(tetrafluoroborate) (7.8a).

Benzobis(imidazole) (208 mg, 1.32 mmol) was suspended in CH₃CN (15 mL), and 1-bromododecane (1.6 mL, 6.58 mmol). NaHCO₃ (1.11 g, 13.15 mmol) was added and the mixture was stirred in an oil bath at 80 °C for 72 h. The cooled solution was then filtered through Celite and concentrated under vacuum. The waxy residue was triturated with hexanes and the resulting tan powder was collected via vacuum filtration. The resulting 1,3,5,7-tetradodecylbenzobis(imidazolium) dibromide was then subjected to anion metathesis analogously to **4•BF₄** using triethyloxonium tetrafluoroborate to obtain 1.32 g (99% yield) of the desired product. ¹H NMR (300 MHz, CDCl₃): δ 9.28 (s, 2H), 8.52 (s,

2H), 4.61 (br t, 8H), 1.97 (br, 8H), 1.34-1.24 (m, 72H), 0.87 (t, $J = 6.6$ Hz, 12H); ^{13}C NMR (75 MHz, CDCl_3): δ 144.2, 130.6, 99.5, 48.1, 31.9, 29.7, 29.63, 29.56, 29.5, 29.3, 29.0, 26.4, 22.7, 14.1; HRMS m/z calcd for $\text{C}_{56}\text{H}_{105}\text{N}_4$ $[\text{M}+\text{H}]$ 833.8339, found 833.8336.

4,6-Dinitro-N,N'-bis(4-octylphenyl)-benzene-1,3-diamine (7.13). This compound was prepared analogously to **7.1** from 1,5-dichloro-2,4-dinitrobenzene (1.53 g, 6.48 mmol) and 4-octylaniline (5.32 g, 25.9 mmol) in EtOH (20 mL) to obtain 3.65 g (98% yield) of the desired product as an orange-red powder. ^1H NMR (300 MHz, CDCl_3): δ 9.68 (br s, 2H), 9.31 (s, 1H), 7.13 (d, $J = 8.2$ Hz, 4H), 7.04 (d, $J = 8.2$ Hz, 4H), 6.47 (s, 1H), 2.57 (t, $J = 7.7$ Hz, 4H), 1.61-1.53 (m, 4H), 1.33-1.29 (m, 20H), 0.90 (t, $J = 6.6$ Hz, 6H); ^{13}C NMR (75 MHz, CDCl_3): δ 147.0, 141.6, 134.7, 129.4, 129.3, 125.2, 124.7, 95.1, 35.5, 31.9, 31.6, 29.5, 29.33, 29.28, 22.7, 14.1; HRMS m/z calcd for $\text{C}_{34}\text{H}_{47}\text{N}_4\text{O}_4$ $[\text{M}+\text{H}^+]$ 575.3597, found 575.3602.

1,7-Bis(4-octylphenyl)benzobis(imidazole) (7.14). This compound was prepared analogously to **7.9** from dinitroarene **7.13** (1.30 g, 2.26 mmol) to provide 972 mg (80% yield) of the desired product as a tan powder. ^1H NMR (400 MHz, CDCl_3): δ 8.32 (s, 1H), 8.13 (s, 2H), 7.53 (s, 1H), 7.41 (br d, 4H), 7.37 (br d, 4H), 2.69 (t, $J = 6.4$ Hz, 4H), 1.67 (br, 4H), 1.28 (br, 20H), 0.89 (br, 6H); ^{13}C NMR (75 MHz, CDCl_3): δ 143.4, 143.0, 141.4, 134.1, 132.3, 129.9, 123.9, 110.6, 90.2, 35.5, 31.8, 31.4, 29.4, 29.3, 29.2, 22.6, 14.1; HRMS m/z calcd for $\text{C}_{36}\text{H}_{47}\text{N}_4$ $[\text{M}+\text{H}^+]$ 535.3801, found 535.3798.

1,7-Dimethyl-3,5-bis(4-octylphenyl)benzobis(imidazolium) bis(tetrafluoroborate) (**7.8b**). The corresponding diiodide salt was obtained analogously to **7.4•I** from benzobis(imidazole) **7.14** (348 mg, 0.65 mmol), and was subjected to anion metathesis analogously to **7.4•BF₄** using triethyloxonium tetrafluoroborate to provide 476 mg (99% yield) of the desired product. ¹H NMR (400 MHz, CDCl₃): δ 9.10 (s, 2H), 8.74 (s, 1H), 7.57 (s, 1H), 7.54 (d, *J* = 8.4 Hz, 4H), 7.29 (d, *J* = 8.4 Hz, 4H), 4.19 (s, 6H), 2.58 (t, *J* = 7.6 Hz, 4H), 1.60-1.53 (m, 4H), 1.29-1.21 (m, 20H), 0.87 (t, *J* = 6.8 Hz, 6H); ¹³C NMR (100 MHz, CDCl₃): δ 146.2, 145.3, 131.8, 131.3, 130.5, 130.2, 125.4, 99.9, 97.7, 35.6, 34.4, 31.8, 31.2, 29.5, 29.4, 29.2, 22.6, 14.1; HRMS *m/z* calcd for C₃₈H₅₁N₄ [M-H⁺] 563.4114, found 563.4111.

Figure 7.4 Top: Crystal packing diagram of **7.3**. Bottom: Crystal packing diagram of **7.6**. Counterions, hydrogen atoms, and solvent molecules have been removed for clarity. Molecules of **7.3** arranged such that the chromophores were stacked (intermolecular distance ~ 4.0 Å) with the methyl groups pointing inward. No π - π interactions were observed in from **7.6**.

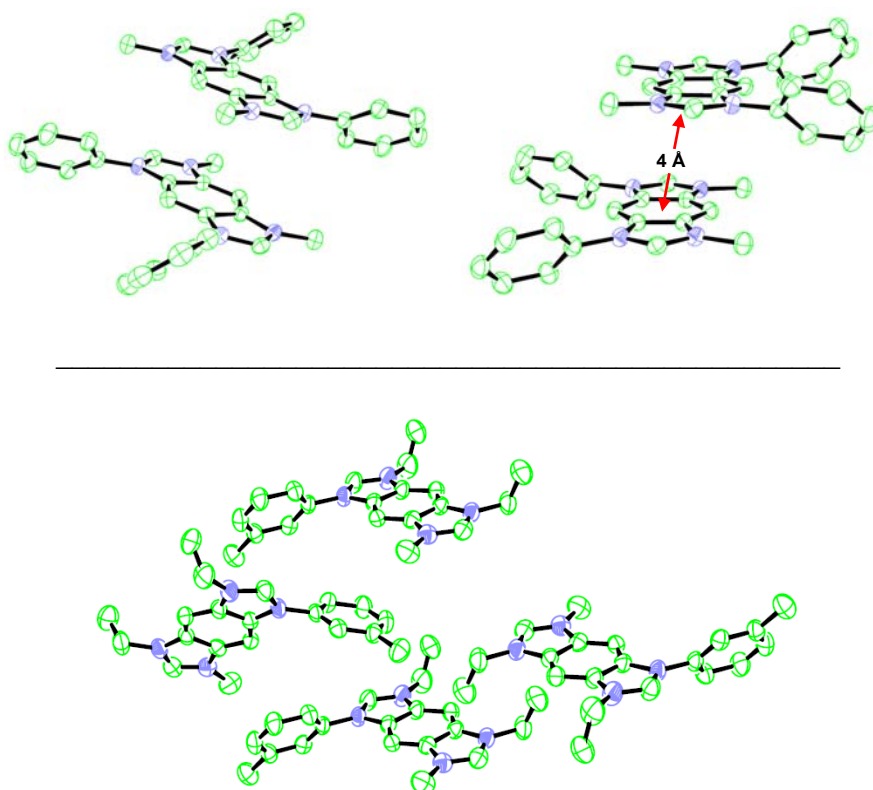
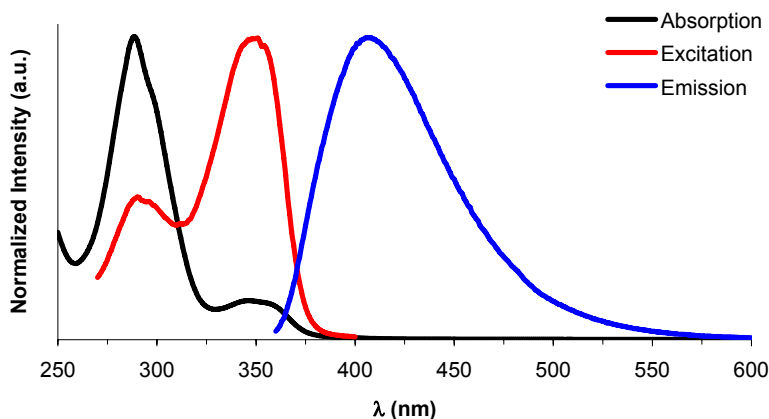


Figure 7.5 UV-Vis (black), excitation (red, 415 nm emission), and emission (blue, 350 nm excitation) spectra for **7.4**•BF₄ in MeOH under ambient conditions. BBIs **7.4** – **7.7** gave similar spectra.



Determination of quantum efficiencies. Solutions of BBIs **7.1** – **7.8** were prepared in MeOH and passed through a 0.2 μm PTFE filter. Concentrations were adjusted such that the absorbance at the excitation wavelength was between 0.01 and 0.10 AU. The fluorescence spectrum was then collected for each sample. Plots of integrated fluorescence intensity versus absorbance were prepared (see below) for each compound, and a linear regression was performed using Microsoft Excel. Y-intercepts were set to zero. The procedure was repeated for *E*-stilbene and anthracene, in hexane and cyclohexane solvent, respectively. The literature quantum efficiencies for the standards (Φ_{std}),¹¹⁴ gradients from the plots (Grad_{BBI} = gradient of BBI fluorophore, Grad_{std} = gradient of standard fluorophore), and refractive index for each solvent (n_{MeOH} = refractive index of MeOH, n_{std} = refractive index of the solvent used for the standard)

were used in the following equation to determine the quantum efficiency of the BBI fluorophore (Φ_{BBI}):

$$\Phi_{\text{BBI}} = \Phi_{\text{std}}(\text{Grad}_{\text{BBI}}/\text{Grad}_{\text{std}})(\eta_{\text{MeOH}}/\eta_{\text{std}})^2$$

Figure 7.6 Integrated fluorescence intensity versus absorbance for solutions of **7.8b** in MeOH (black), **7.4•MeSO₄** in MeOH (red), anthracene in cyclohexane (green), and *E*-stilbene in hexane (blue). Linear regressions were performed with y-intercepts set to zero.

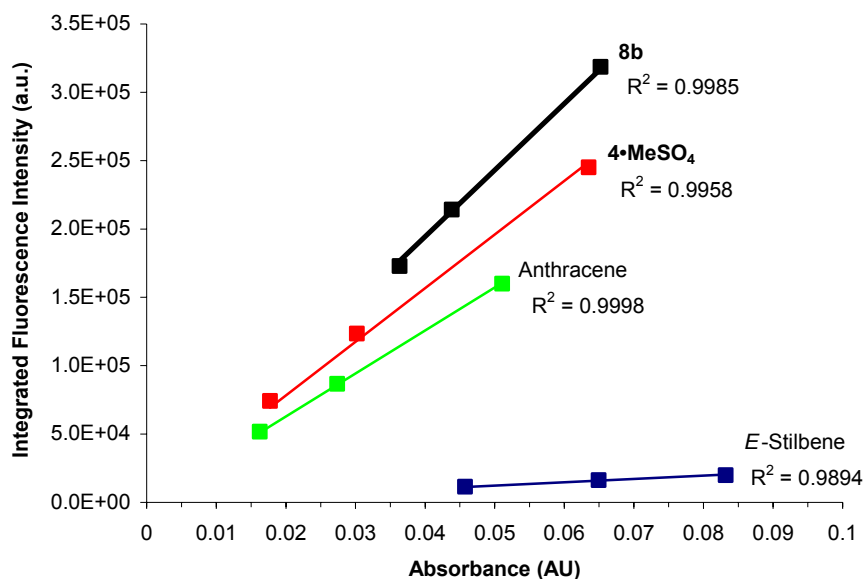


Figure 7.7 VT-PXRD data for **7.8a** (left) and **7.8b** (right) at 130 °C and 205 °C, respectively

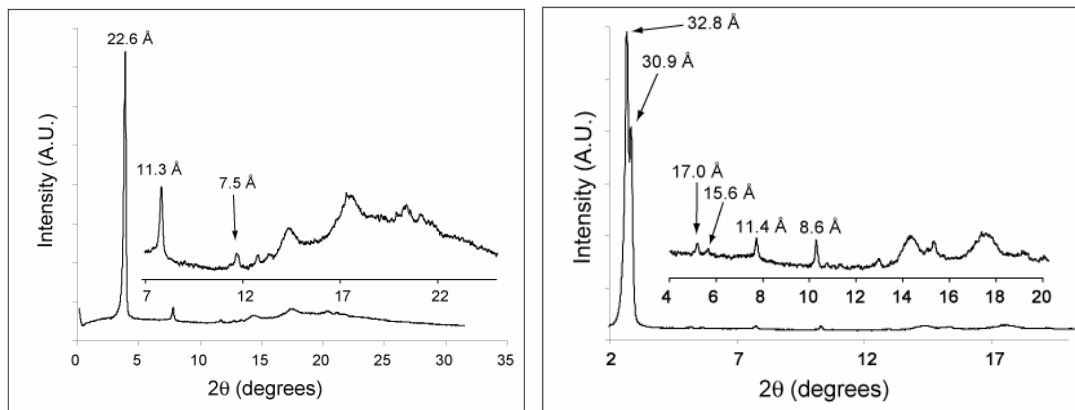
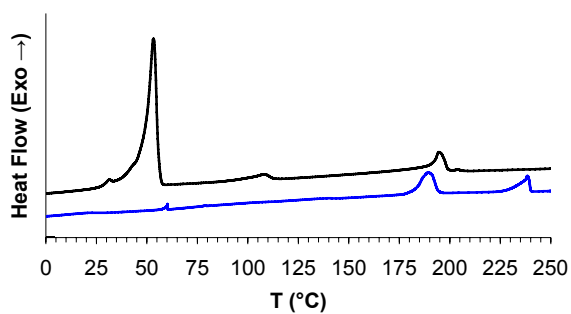


Figure 7.8 DSC scans of **7.8a** (black) and **7.8b** (blue). Data collected from the third cooling cycle at a rate of 5 °C/min.



Chapter 8: Fluorescent Benzobis(imidazolium) Salts: Synthesis and Photophysical Analyses

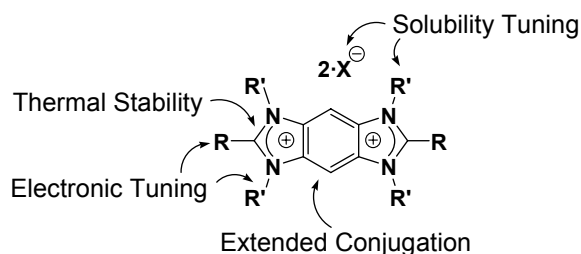
8.1 Introduction

The discovery and development of novel organic emissive materials is essential for advancement in a multitude of areas of chemical research.¹¹⁵ Fluorescent organic salts are an emerging sub-class of emissive materials that are receiving considerable attention due to their unique attributes. They not only exhibit tunable electronic and physical characteristics, including solution-based and solid-state fluorescence, but also offer other advantages ascribed specifically to their charged nature. For example, the incorporation of ionic moieties in emissive salts have been credited with imparting high thermal stabilities, phase tunabilities, water-solubility, chemoselective sensing *via* electrostatic interactions, and strengthened solid-state intermolecular interactions. These features have already inspired research in a number of areas including fundamental photophysical investigations,^{106,116} sensory materials,^{117,118,119} novel materials for display applications,^{106b,c} multi-photon excitation (MPE),¹²⁰ and nanoscopic fluorescent ionic liquids.¹⁰⁷ Overall, these materials encompass a tremendous breadth of structural diversity, each targeting a specific application or area of study.

To complement these systems, we sought a single, modular platform from which task-specific fluorophores could be obtained rapidly and efficiently. Benzobis(imidazolium) (BBI) salts are one class of such compounds that feature a number of attributes poised for achieving this goal (see Figure 8.1). The BBI architecture features two imidazolium moieties annulated to a common arene linker. An important

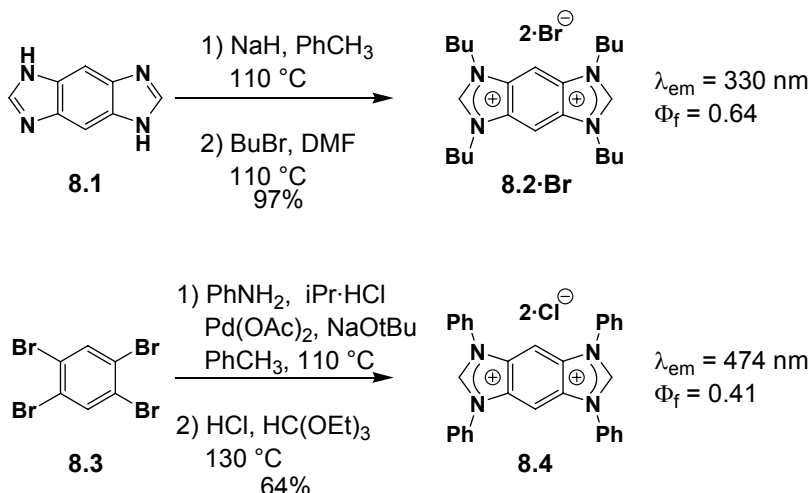
consequence of this arrangement is that the charged moieties are embodied within the system's chromophore, which distinguishes these materials from common types of fluorescent organic salts. In addition, BBIs feature four N-substituents, two C1-substituents, and two counterions which can be independently varied. As such, the physical, electronic, and chemical properties exhibited by these materials may be finely tuned. Combined, these features may synergistically open new opportunities for fluorescent organic salts that not only display versatile photoluminescence characteristics, but also may be used in a broad array of applications.

Figure 8.1 Key features of fluorescent benzobis(imidazolium) salts



As described in previous chapters, our preliminary interest in annulated bis(imidazolium) salts was as precursors to facially-opposed bis(*N*-heterocyclic carbene)s. As such, syntheses were designed to provide predominantly symmetric, and exclusively C1-unsubstituted systems (i.e., $R = H$, Figure 8.1). Initial efforts focused on two primary variants exemplified in Scheme 8.1: one featuring four *N*-alkyl groups (e.g. **8.2•Br**) and the other containing four *N*-aryl groups (e.g., **8.4**).

Scheme 8.1 Synthesis and photoluminescence properties of tetrabutyl BBI salt **8.2•Br** and tetraphenyl BBI salt **8.4**



During our initial studies, we observed that systems such as **8.2•Br** and **8.4** were highly photoluminescent with λ_{em} of 330 and 474 nm, respectively. In addition, high photoluminescence efficiencies (Φ_f) were observed from each BBI, with Φ_f = 0.64 and 0.41 for **8.2•Br** and **8.4**, respectively. This inspired the design and synthesis of new subclasses of phase-tunable (i.e., ionic liquid and ionic liquid crystal) BBI salts, as described in Chapter 7. These materials also displayed high Φ_fs, and their emission maxima (λ_{em}) suggested an ability to tune the electronic properties of BBIs *via* judicious control of the *N*-substituents. To further investigate the photophysics and applications of fluorescent BBI salts, a systematic series of these materials were prepared and studied. Syntheses and analyses were aimed at understanding the electronic delocalization throughout the BBI chromophores and methods for controlling their emission properties.

8.2 Syntheses of benzobis(imidazolium) salts

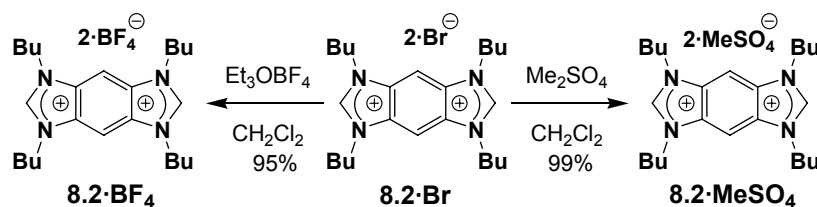
To develop comprehensive structure-property relationships based on BBI salts, focus was placed on controlling four areas of structural modulation: 1) counterions, 2) regioisomers, 3) *N*-aryl electronics, and 4) C1-aryl electronics. Photophysical studies and applications of BBI salts are described in subsequent sections. General syntheses utilized one of four strategies, summarized in Schemes 8.2 – 8.5 below. Tetra-*N*-butyl (**8.2•Br**) and tetra-*N*-phenyl (**8.4**) BBIs were prepared as previously described (see Chapters 1, 3, and 4). Overall, syntheses of the BBIs in this Chapter required a maximum of four steps, were chromatography-free, and afforded products in yields ranging from 40 – 97% from commercial starting materials.

A unique feature of organic salts is that in principle both their cation and anion constituents may be independently tuned. While the anion has been shown to play a key role in controlling physical properties,^{100,102,106} photophysical anion-dependencies have not been studied in detail.¹²¹ This is likely due to the fact that for emissive organic salts, focus is placed primarily on cationic chromophores. Alternatively, ion-pairing interactions may greatly influence the photophysical characteristics of an organic salt under specific conditions. For example, red-edge effects from charged compounds, have been attributed to different orientations of associated species.^{106,116} Accordingly, one might expect that the counterion would influence a fluorescent salt's response to red-edge excitation.

To facilitate a comparative study involving counterion effects on photophysical properties of BBIs, compounds with simple, highly symmetric dicationic cores and either Br, BF₄ or MeSO₄ counterions were investigated. Capitalizing on the nucleophilic nature

of halides, **8.2·Br** was treated with either $\text{Et}_3\text{O}\cdot\text{BF}_4$ or Me_2SO_4 to produce anion metathesis products **8.2·BF₄** and **8.2·MeSO₄**, respectively, as shown in Scheme 8.2. Subsequent removal of residual, volatile byproducts afforded each of the desired BBIs in excellent isolated yields ($\geq 95\%$). As will be discussed below, the counterions had little effect on the λ_{em} , provided excitation was performed at the λ_{abs} ; however, analysis of these compounds ultimately revealed counterion-dependent REEs in dilute solutions.

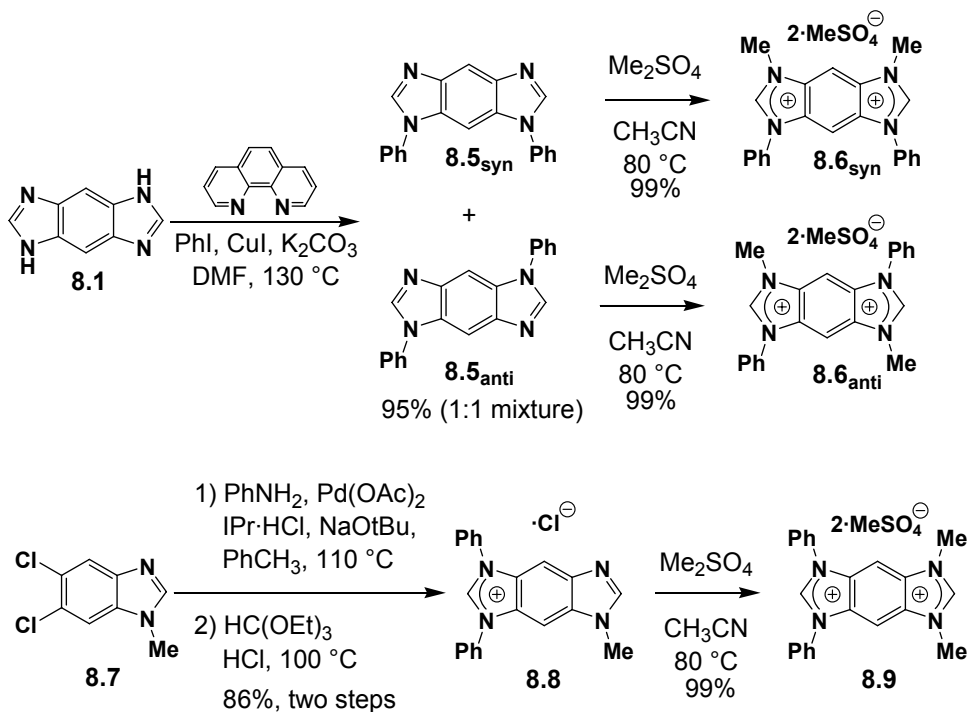
Scheme 8.2 Synthesis of BBI salts **8.2** via anion metathesis



Incorporation of distinct functional groups around the BBI core was expected to provide additional degree of control over the λ_{em} of the resulting BBIs. Prior to engaging in the synthesis of compounds bearing substituents with different electronic properties, however, we investigated the effects of site-specific *N*-arylation. Hence, BBI regioisomers bearing two *N*-phenyl and two *N*-methyl groups in various substitution patterns were synthesized as shown in Scheme 8.3. Benzobis(imidazole) **8.1** underwent Cu-catalyzed cross coupling with PhI to provide a 1:1 mixture of 1,7-diphenyl- (**8.5_{syn}**) and 1,5-diphenylbenzobis(imidazole)s (**8.5_{anti}**) in 95% combined yield.¹²² Separation of the two isomers was accomplished *via* recrystallization from hot DMSO. Subsequent

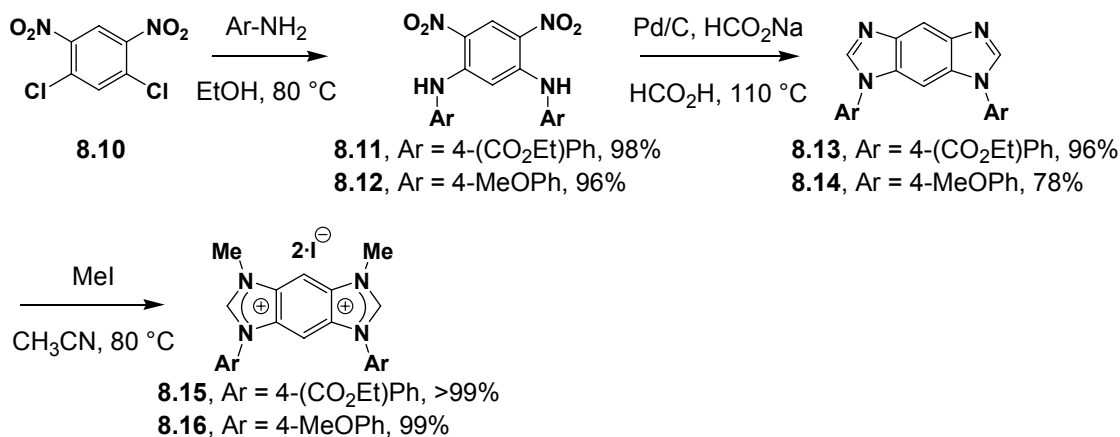
alkylation with MeI afforded BBIs **8.6_{syn}** and **8.6_{anti}**, respectively. As shown in Scheme 8.3, the other possible regioisomer (**8.9**) was obtained from 5,6-dichloro-1-methylbenzimidazole (**8.7**).¹²³ Aryl amination with PhNH₂, followed by formylative cyclization of the resulting diamine with HC(OEt)₃, afforded benzimidazolium chloride **8.8** in 86% yield. Treatment of **8.8** with 2.0 equiv of Me₂SO₄ not only resulted in *N*-methylation but also effectively removed the Cl⁻ anion (as gaseous CH₃Cl), affording the desired bis(methyl sulfate) salt (**8.9**) in 85% overall yield from **8.7**. As will be discussed below, BBI **8.6_{syn}** displayed longer λ_{em} than **8.6_{anti}** and **8.9**. Hence, further structural modulation focused on 1,7-diaryl BBIs.

Scheme 8.3 Synthesis of regioisomeric diphenyl-dimethylbenzobis(imidazolium) salts



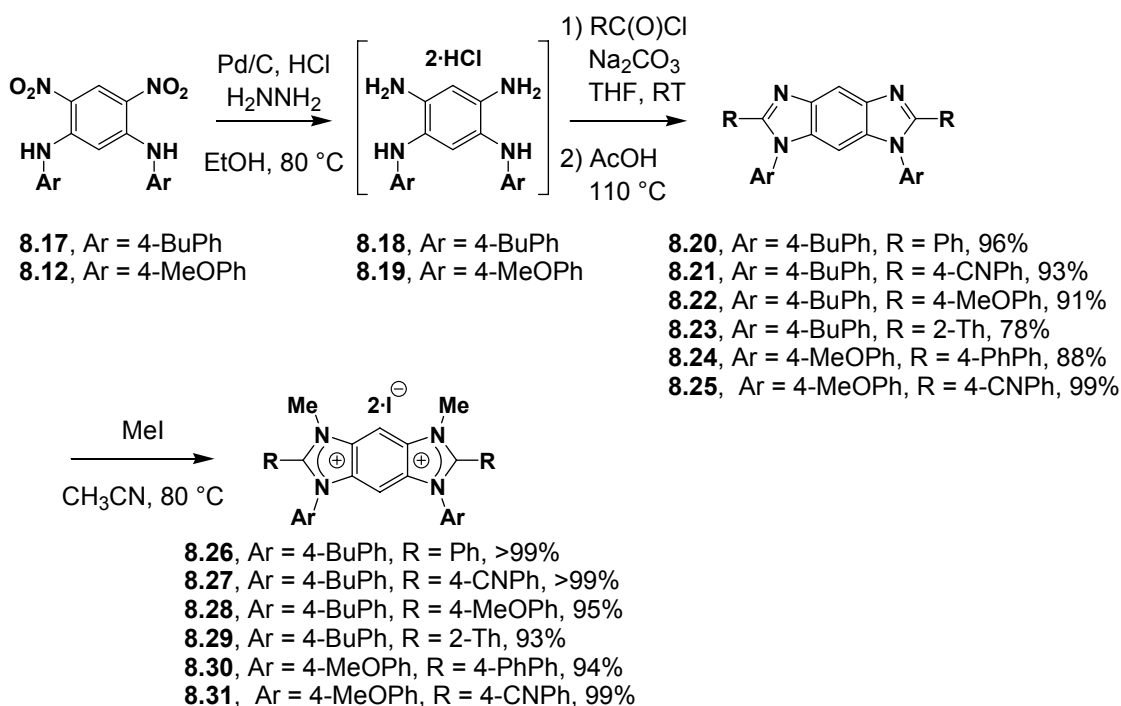
As stated previously, the photophysics of BBI salts were found to be dependent on the nature of the *N*-substituent (c.f., **8.2•Br** and **8.4** in Scheme 8.1). Thus, BBIs bearing electron-donating and withdrawing *N*-aryl groups (Scheme 8.4) were synthesized to further explore the effects of differential *N*-aryl electronic factors. This was accomplished from 2,4-dinitro-1,5-dichlorobenzene (**8.10**), which underwent S_NAr reactions with benzocaine and *p*-anisidine to provide dinitroarenes **8.11** and **8.12**, respectively. Reduction followed by *in situ* formylative cyclization afforded the corresponding benzobis(imidazole)s **8.13** and **8.14**. Finally, alkylation with MeI afforded the BBI salts **8.15** and **8.16** in 95 and 74% overall yield, respectively from **8.10**. As will be discussed below, incorporation of electron-rich *N*-arenes bathochromically shifted the λ_{em} of these compounds by as much as 61 nm. In contrast, electron-poor *N*-arenes resulted in significant hypsochromic shifts in the λ_{em} .

Scheme 8.4 Synthesis of BBI salts with electronically modified *N*-aryl substituents



As stated previously, the ability to independently-substitute the *N*- and C1-positions of the BBI structure provides an additional handle for precisely tuning their photophysical properties. To obtain systems comprising both *N*- and C1-aryl substituents, we employed dinitroarenes **8.12** (Scheme 8.4) and **8.17** (Scheme 8.5), which were each obtained from S_NAr reaction of **8.10** with the appropriate aryl amine. While the 4-MeOPh groups of **8.12** ultimately provided longer wavelength λ_{em} , the 4-BuPh groups of **8.17** lead to increased solubilities

Scheme 8.5 Synthesis of BBI salts bearing *N*- and C1-aryl substituents



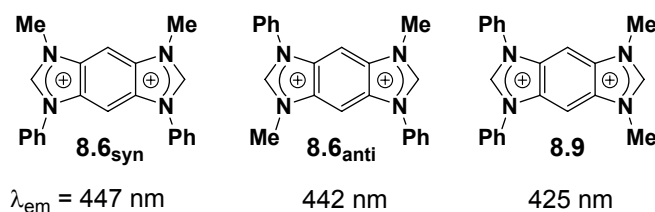
To complete the syntheses, the nitro groups of **8.12** and **8.17** were first reduced using Pd/C and hydrazine under acidic conditions to afford the corresponding tetraaminobenzenes **8.18** and **8.19**, as their hydrochloride salts. Reaction of these tetraamines with various aroyl chlorides afforded diamide intermediates (structures not shown), which underwent dehydrocyclization in AcOH to give benzobis(imidazole)s **8.20** – **8.25**.¹²⁴ The aroyl chlorides chosen for study were commercially-available and encompassed both electron-withdrawing (e.g., R = 4-CNPh) and donating functional groups (e.g., R = 4-MeOPh, 2-thienyl, 4-biphenyl). Subsequent alkylation of bis(imidazole)s **8.20** – **8.25** with MeI provided a series of highly functionalized BBI salts (**8.26** – **8.31**) in overall yields of 72 – 93% based on **8.10**. As discussed below, the different electron-donating and withdrawing capabilities of the C1-substituents lead to λ_{em} tunability over a broad range of wavelengths. Ultimately, we observed that optimal combinations of N- and C1-aryl groups were able to bathochromically shift λ_{em} by up to 227 nm, relative to BBI **8.2•Br**; specific details are discussed in the following section.

8.3 Photophysical analyses

With a systematic series of BBI salts in hand, attention turned toward studying the electronic and physical characteristics of these materials; a summary of key results is shown in Table 8.1. Collectively, these BBI salts displayed good Φ_f s and molar absorptivities as well as a broad range of λ_{em} . The following sections discuss a combination of structural, substituent, and solvent effects on the photophysical properties of BBI fluorophores, as well as their utility in specific applications.

As stated previously, the emission properties of the BBI salts are strongly influenced by the nature of the *N*-substituents. In particular, comparing **8.2•Br** versus **8.4** revealed a relatively large $\Delta\lambda_{\text{em}}$ (124 nm). Hence, we aimed to better understand the impact of systematically placing *N*-aryl groups at different positions on the BBI core. Comparison of the emission spectra of diphenyl BBIs **8.6_{syn}**, **8.6_{anti}**, and **8.9** (see Figure 8.2) indicated that the longest wavelength λ_{em} were obtained when *N*-phenyl groups were placed on opposite imidazolium rings; however, the two possible regioisomers displayed nearly identical absorption and emission characteristics. Specifically, BBIs **8.6_{syn}** and **8.6_{anti}** exhibited identical $\lambda_{\text{abs}} = 345$ nm with slightly different $\lambda_{\text{em}} = 447$ and 442 nm, respectively. In contrast, BBI **8.9**, which bears two *N*-phenyl substituents on the same imidazolium ring, showed hypsochromically shifted λ_{em} at 403 nm. Considering BBI **8.6_{syn}** displayed the longest λ_{em} values, and was straightforward to synthesize, subsequent efforts focused on derivatizing this compound to further tune λ_{em} values (see below).¹²⁵

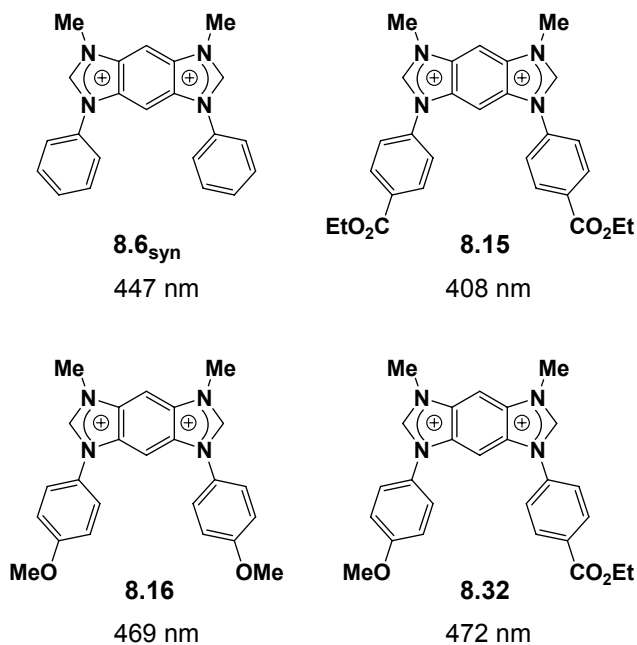
Figure 8.2 BBI salts used to evaluate the electronic impacts of *N*-aryl versus *N*-alkyl substitution



8.4 Effects of incorporating functional *N*-aryl groups

To compare the effects of electronic tuning the *N*-aryl substituents, we compared BBIs **8.6_{syn}**, **8.15**, and **8.16** (see Figure 8.3). Whereas BBI **8.6_{syn}** showed a λ_{em} at 447 nm, incorporation of electron-withdrawing groups on the *N*-aryl substituents (**8.15**) resulted in a hypsochromically shifted λ_{em} at 408 nm. In contrast, BBI **8.16**, which has electron-donating groups on the *N*-aryl substituents, showed a λ_{em} at 469 nm. Thus, from this series of BBIs it is apparent that increased electron density at the *N*-substituent is advantageous for increasing λ_{em} values.

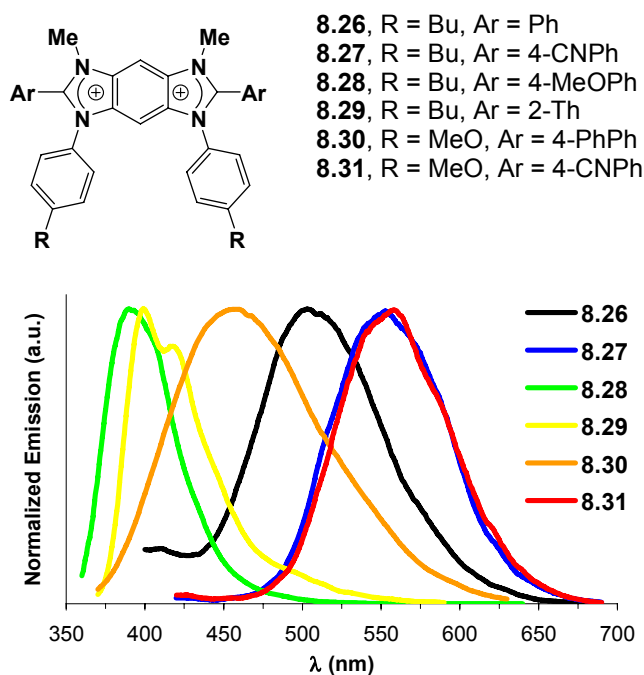
Figure 8.3 BBI salts used to evaluate *N*-aryl electronic effects on λ_{em} . Values shown are $\lambda_{e,m}$ (excitation at the λ_{abs}) in MeOH under ambient conditions



To better study the electronic communication within the BBI chromophore and ability to further tune λ_{em} , we prepared an *N*-to-*N'* “donor-acceptor” BBI (**8.32**) featuring *N*-(4-MeOPh) and *N'*-(4-CO₂EtPh) groups. Stepwise treatment of 1,5-dichloro-2,4-dinitrobenzene (**8.10**) with benzocaine (to afford intermediate **8.33**) followed by *p*-anisidine provided dinitroarene **8.34** in 93% yield over the two steps. Following reductive cyclization, the intermediate benzobis(imidazole) **8.35** was alkylated with MeI to provide BBI **8.32** (see Figure 8.3) in 78% overall yield from **8.10**. Analysis of the emission spectra of this compound revealed a λ_{em} at 472 nm, representing a slight bathochromic shift relative to **8.16**. Overall, comparison of the BBIs in Figure 8.3 emphasize the ability to tune the emission characteristics through variation of *N*-aryl electronics, and establish a means to increase λ_{em} , primarily *via* incorporation of electron-rich *N*-arenes.

Next, we turned our attention toward evaluating the feasibility of tuning fluorescence properties through C1-substitution. Analysis of BBIs **8.26** – **8.31** (see Figure 8.4) revealed a strong dependence of the λ_{em} on the nature of the C1-substituent. Since C1-substituted BBI fluorophores were essentially unexplored, we initially investigated the effects of placement of phenyl groups at these positions. Thus, we compared BBI **8.6_{syn}**, which is unsubstituted at C1, with C1-Ph substituted BBI **8.26**. The λ_{em} of the latter appeared at a considerably longer wavelength (507 nm) than the former (447 nm). Having revealed a strong dependence of the λ_{em} on the C1-substituent, we considered electronic variation at this position as an additional parameter for tuning emission properties.

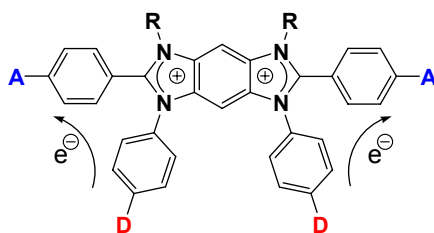
Figure 8.4 Photoluminescence spectra of C1-aryl BBI salts in MeOH, excited at the absorption maximum, under ambient conditions. Concentration ca 5 μ M, signal intensities have been normalized.



Installation of electron-donating C1-aryl groups such as 4-MeOPh (**8.28**), 2-thienyl (**8.29**), or 4-biphenyl (**8.30**) resulted in hypsochromic shifts in the λ_{em} relative to BBI **8.26**. The magnitudes of these shifts were consistent with the relative electron-donating abilities of the respective C1-arenes (i.e., 4-MeOPh > 2-thienyl > 4-biphenyl). In other words, increased electron density at C1 was consistently accompanied by a decrease in λ_{em} . Interestingly, the increased electron density at C1 in BBIs **8.29** and **8.30** was significant enough to cause the λ_{em} of these BBIs to appear at lower wavelengths than even C1-unsubstituted BBI **8.6_{syn}**.

Electron-withdrawing C1-substituents, on the other hand, increased λ_{em} relative to BBI **8.26**. For example, installation of 4-CNPh groups at C1 (**8.27**) resulted in a λ_{em} at 551 nm, which is bathochromically shifted by 44 nm relative to **8.26**. Overall, it appeared that electronic influences from the N- and C1-substituents were complementary in that *increased* electron density at the N-positions, and *decreased* electron density at C1 each resulted in longer λ_{em} . Considering these two factors, we envisioned it should be possible to take advantage of a donor-acceptor functionalized BBI featuring electron-donating N-aryl groups in combination with electron-withdrawing C1-aryl groups. Such a system was expected to display electronic communication as depicted in Figure 8.5.

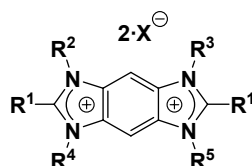
Figure 8.5 Proposed diagram of the major electronic communication pathways throughout the BBI chromophore. D = Electron-donor, A = Electron-acceptor



To investigate, we synthesized BBI **8.31** which features 4-MeOPh groups at the 1- and 7-positions, and 4-CNPh groups at C1. The λ_{em} of BBI **8.31** appeared at 561 nm, which is the longest λ_{em} of all the BBIs described herein. The discernable increase in the λ_{em} relative to BBI **8.27** (see Table 8.1) confirmed a synergistic electronic impact resulting from judicious control of both the N- and C1-substituents. Notably, both BBI

8.27 and **8.31** undergo efficient excitation in the visible region, as the absorption cutoff of each appeared at approximately 450 nm.

Table 8.1 Photophysical properties of benzobis(imidazolium) salts



BBI	R ¹	R ²	R ³	R ⁴	R ⁵	X	λ_{abs} (nm) ^a	λ_{em} (nm) ^{a,b}	Yield (%) ^c
8.2•Br	H	Bu	Bu	Bu	Bu	Br	288 (4.29)	330 (0.64)	97
8.2•BF₄	H	Bu	Bu	Bu	Bu	BF ₄	290 (4.25)	329 (0.55)	92
8.2•MeSO₄	H	Bu	Bu	Bu	Bu	MeSO ₄	289 (4.26)	331 (0.63)	92
8.4	H	Ph	Ph	Ph	Ph	Cl	352 (3.94)	474 (0.41)	64
8.6_{syn}	H	Me	Me	Ph	Ph	MeSO ₄	345 (3.31)	447 (0.91)	86
8.6_{anti}	H	Ph	Me	Me	Ph	MeSO ₄	345 (4.05)	442 (0.38)	40
8.9	H	Ph	Me	Ph	Me	MeSO ₄	330 (3.92)	425 (0.31)	83 ^d
8.15	H	Me	Me	4-MeOPh	4-MeOPh	I	343 (3.93)	469 (0.05)	74
8.16	H	Me	Me	4-(CO ₂ Et)Ph	4-(CO ₂ Et)Ph	I	360 (4.13)	408 (0.02)	95
8.32	H	Me	Me	4-MeOPh	4-(CO ₂ Et)Ph	I	362 (3.60)	472 (0.01)	78
8.26	Ph	Me	Me	4-BuPh	4-BuPh	I	322 (4.54)	507 (0.14)	94
8.27	4-CNPh	Me	Me	4-BuPh	4-BuPh	I	388 (4.94)	551 (0.43)	93
8.28	4-MeOPh	Me	Me	4-BuPh	4-BuPh	I	332 (4.51)	393 (0.55)	89
8.29	2-Th	Me	Me	4-BuPh	4-BuPh	I	349 (4.00)	400 (0.18)	72
8.3	4-PhPh	Me	Me	4-MeOPh	4-MeOPh	I	331 (4.61)	461 (0.05)	82
8.31	4-CNPh	Me	Me	4-MeOPh	4-MeOPh	I	389 (4.91)	561 (0.06)	97

^aData taken in MeOH under ambient conditions; log(ϵ) given in parentheses. ^bQuantum efficiencies (Φ_f) are given in parentheses and were determined relative to *E*-stilbene, anthracene, or 9,10-bis(phenylethynyl)anthracene. ^cIsolated overall yield from commercial material. ^dIsolated overall yield from 5,6-dichloro-1-methylbenzimidazole (**8.7**).

8.5 Solvent effects on absorption and emission properties

Many classes of molecules exhibit solvent-dependent photophysical properties.^{126,127,128} Most commonly, the λ_{abs} and λ_{em} respond to changes in solvent dielectric in a manner consistent with changes in the polarity of the chromophore as it

transitions from the ground to excited state. Other factors such as solvent reorganization energies, solvent donor and acceptor abilities, and chemical reactions taking place in the excited state can each alter the Stokes shift, and thus the λ_{em} , as the solvent is varied.^{129,130} Regardless of the origins, it is important to note that solvent-dependency can offer an excellent handle for tuning the photophysical characteristics of a solute.¹³¹

To probe the effects of different solvents on the photophysical properties of BBI salts, the absorption and emission spectra of BBI **8.27** (see Figure 8.6) were analyzed in CH₃CN, (MeO)₃PO, DMF, and DMSO; limited solubilities precluded analysis in less polar solvents (i.e., PhCH₃, THF, CH₂Cl₂, dioxane, etc.) As shown in Table 8.2, the λ_{abs} of **8.27** remained fairly constant upon increasing solvent polarity. The λ_{em} of this compound, however, was found to be strongly dependent on the nature of the solvent, displaying positive solvatofluorochromism with λ_{em} ranging from 437 – 557 nm.¹³²

Figure 8.6 BBI salts used to evaluate photophysical solvents effects as a function of structure

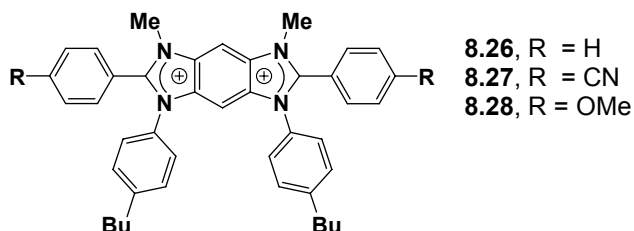


Table 8.2 Solvent effects on the photophysical properties of various BBI salts

BBI	Absorption and Emission Maxima (nm)			
	CH ₃ CN	(MeO) ₃ PO	DMF	DMSO
8.27	312 / 437	313 / 439	315 / 551	315 / 557
8.27 •BF ₄	312 / 446	313 / 436	315 / 550	316 / 561
8.26	310 / 420	310 / 412	312 / 412	314 / 438
8.28	331 / 392	331 / 390	332 / 394	333 / 395
8.21	350 / 436	336 / 438	358 / 439	354 / 442

^aData taken under ambient conditions. Concentration ca 5 μ M. Solvent donor numbers and dielectric constants are: CH₃CN = 14.1, 38.0; (MeO)₃PO = 23.0, 20.6; DMF = 26.6, 38.3; DMSO = 29.8, 45.0.¹³³

One possible explanation for the large, solvent-induced shifts in the λ_{em} may be significant structural reorganizations of the BBI solute that are unique to the excited state. The Stokes shifts exhibited by BBI **8.27** were also consistent with large structural changes in the excited state (see Table 8.3). For BBI **8.27**, the Stokes shifts increased with solvent DN, ranging from 9118 to 13597 cm⁻¹. These values are in the range of unusually large Stokes shifts (5000 – 15000 cm⁻¹), commonly ascribed to structural reorganization of the fluorophore or excited state reactions.¹³⁴ Furthermore, consistent with the trend in λ_{em} (see below), the magnitudes of the Stokes shifts decreased with increasing electron density of the BBI core. For example, BBI **8.27** exhibited Stokes shifts ranging from 9168 – 13793 cm⁻¹, whereas the increased electron density from the 4-MeOPh groups of **8.28** manifested in Stokes shifts ranging from 4570 – 4740 cm⁻¹.

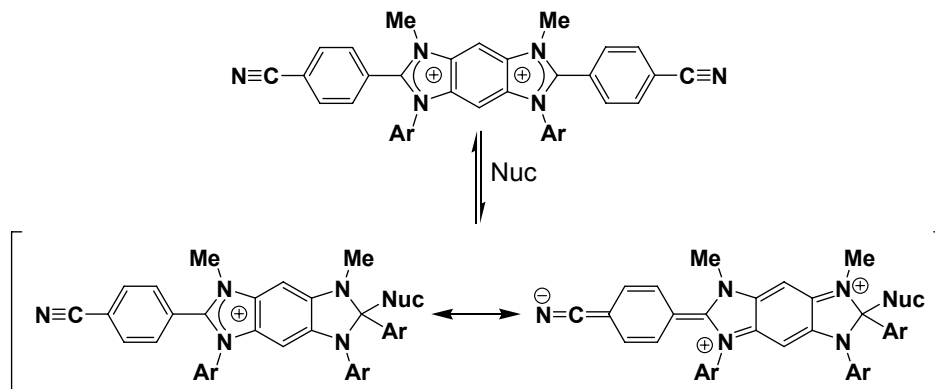
Table 8.3 Stokes shifts of various BBIs in different solvents

BBI	Stokes Shift (cm ⁻¹)			
	CH ₃ CN	(MeO) ₃ PO	DMF	DMSO
27	9168	9170	13597	13793
26	8449	7986	7779	9016
28	4701	4570	4740	4714

^aStokes shifts, in various solvents, given in cm⁻¹ by $10^7(1/\lambda_{\text{em}} - 1/\lambda_{\text{abs}})$. Solvents are listed in order of increasing donor number (DN).

As described in Scheme 8.6, one plausible reorganization may involve nucleophilic attack at one of the electrophilic C1-positions. Such an event would result in a strongly dipolar system capable of extended delocalization, features commonly manifested in large positive solvatochromism.^{126,127} The most likely nucleophilic species (Nuc) are either an iodide counterion or a solvent molecule. To exclude the former from consideration, we prepared **8.27•BF₄** from **8.27**, using the anion metathesis method previously described in Chapter 6. As shown in Table 8.2, nearly identical spectroscopic signals were observed in each of the aforementioned solvents suggesting that excited state structural changes were independent of the anion.

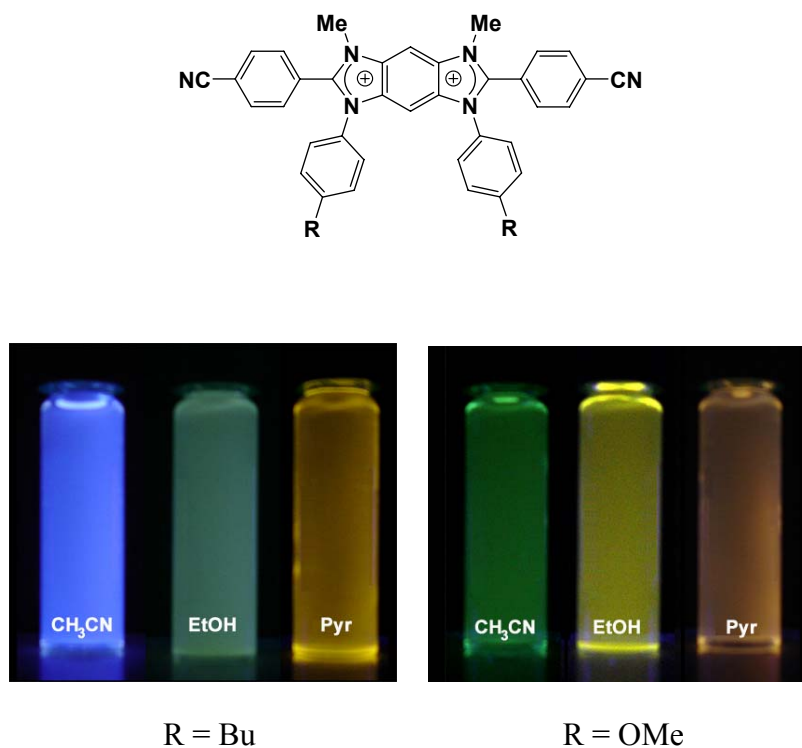
Scheme 8.6 Proposed excited state reaction giving rise to large Stokes shifts and positive solvatofluorochromism



We next considered the solvent as a possible nucleophile in the mechanism described in Scheme 8.6 above. An interesting relationship was realized after comparing the solvatofluorochromic shifts with solvent donor numbers (DN) and dielectric constants (κ).¹³³ The λ_{em} for BBI **8.27** correlated better with increasing solvent DN than with κ . For example, CH_3CN and DMF have nearly identical κ (38.0 and 38.3, respectively), but different DN (14.1 and 26.6, respectively). The λ_{em} of **8.27** appeared at 409 nm in CH_3CN , but was shifted to 555 nm in DMF. This strong dependence on solvent DN,¹³³ further supported the proposed excited state reaction described in Scheme 8.6. To further investigate the existence of a nucleophile-electrophile interaction as the cause of the solvatofluorochromism, we compared the λ_{em} solvent-dependency of less electrophilic BBIs **8.26** and **8.28**, as well as neutral benzobis(imidazole) **8.21** (see Table 8.2). BBI **8.26** showed only very small changes in λ_{em} upon increasing solvent DN as did electron-rich BBI **8.28** and benzobis(imidazole) **8.21**. Collectively, comparing chromophores of

different electrophilicities suggested that the dicationic nature of BBI **8.27**, in combination with the electron-withdrawing C1-substituents, were responsible for the large solvatochromic shifts. Encouraged by the sensitivity of the observed solvatofluorochromism to the nature of the BBI core, we compared various solutions of BBIs **8.27** and **8.31**. As can be seen in Figure 8.7, marked differences were visually observed upon irradiation of the two dicyano BBIs.

Figure 8.7 Solutions of BBIs **8.28** (left) and **8.33** (right) irradiated with a 365 nm (5 W) lamp. Solvents in each series from left to right: CH₃CN, EtOH, pyridine.

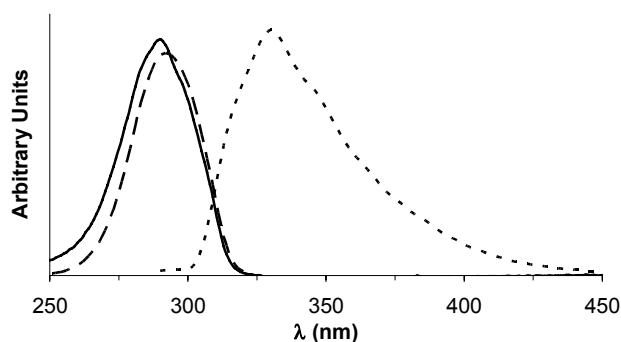


8.6 Red-edge effects

A red-edge effect (REE) refers to shifting of the λ_{em} to longer wavelengths in response to an increase in the excitation wavelength, along the red-edge of the absorption band.^{116,135} Multiple polar organic fluorophores have been found to display a REE, and this phenomenon has found application in a number of areas.^{106,116} Particularly interesting to our studies were recent reports of REEs from imidazolium-based ionic liquids.¹⁰⁶ The specific cause of the REE in imidazolium species is not entirely understood, but it has been speculated that its origins involve different ground state orientations of associated species.^{106,136} Considering the BBI structure comprises two imidazolium moieties, we envisioned a REE may be observable from these materials. In addition, differential ion-pairing interactions of BBIs **8.2•Br**, **8.2•BF₄**, and **8.2•MeSO₄** may manifest in counterion-dependent REEs.

Since REEs of BBI-type fluorophores were unexplored, we began our investigations with a simple BBI structure (**8.2**) that would also be amenable to probing counterion effects. To determine if a REE was observable from BBI solutions, and explore any resulting counterion dependency, MeOH solutions (ca. 1 μM) of BBIs **8.2•Br**, **8.2•BF₄**, and **8.2•MeSO₄** were each excited at various wavelengths along the red-edge of their excitation spectra. As shown in Table 8.1, the absorption and emission spectra (excitation at the λ_{abs}) for **8.2** in MeOH were independent of the counterion; a representative set of spectra for **8.2•MeSO₄** is shown in Figure 8.8.

Figure 8.8 Electronic absorption (solid line), excitation (dashed line, emission intensity monitored at 330 nm), and emission (dotted line, excitation at 290 nm) spectra of **8.2•MeSO₄** in MeOH under ambient conditions. For aesthetic purposes, signal intensities have been adjusted.



Both **8.2•Br** and **8.2•BF₄** gave nearly identical spectra upon red-edge excitation; the resulting spectra for **8.2•Br** are depicted in Figure 8.9. Excitation at 330 nm resulted in a shoulder protruding at ca. 410 nm, which becomes the only apparent peak at $\lambda_{\text{ex}} \geq 340$ nm. Notably, a mixture of **8.2•Br** and **8.2•BF₄** (1:1 molar ratio) also gave the same response. In contrast, red-edge excitation of **8.2•MeSO₄** gave bimodal emission spectra that continued to shift bathochromically when excited at 330, 340, and 350 nm (see Figure 8.10). The difference in fine structure and overall response to REE between **8.2•MeSO₄** and **8.2•Br/BF₄** strongly suggested that the counterion plays a decisive role in dictating the photophysical properties under these conditions. These results demonstrate, for the first time, REEs in extended, highly photoluminescent imidazolium-

based chromophores and support the contention that REE may be influenced by cation-anion interactions.

Figure 8.9 Emission spectra of **8.2•Br** in MeOH under ambient conditions excited at 330 (solid line), 340 (dashed line) and 350 nm (dotted line). Concentration = 1 μ M.

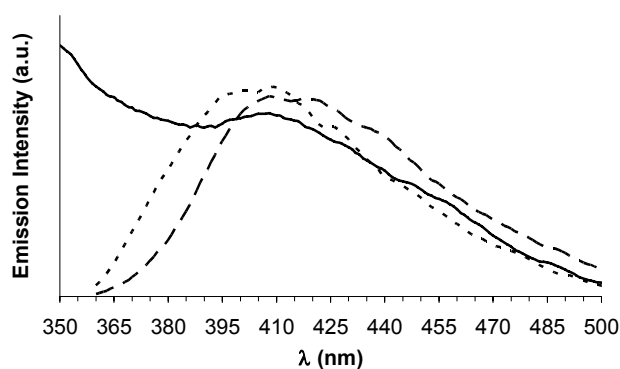
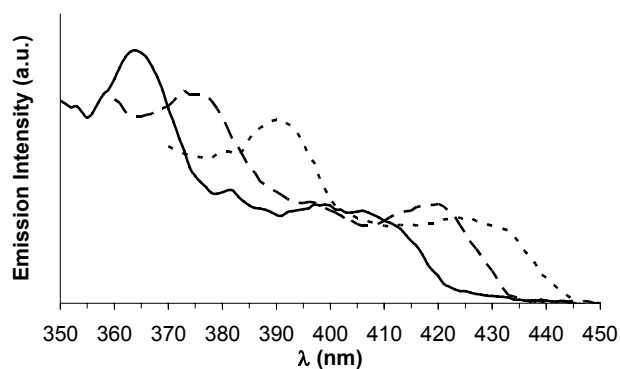


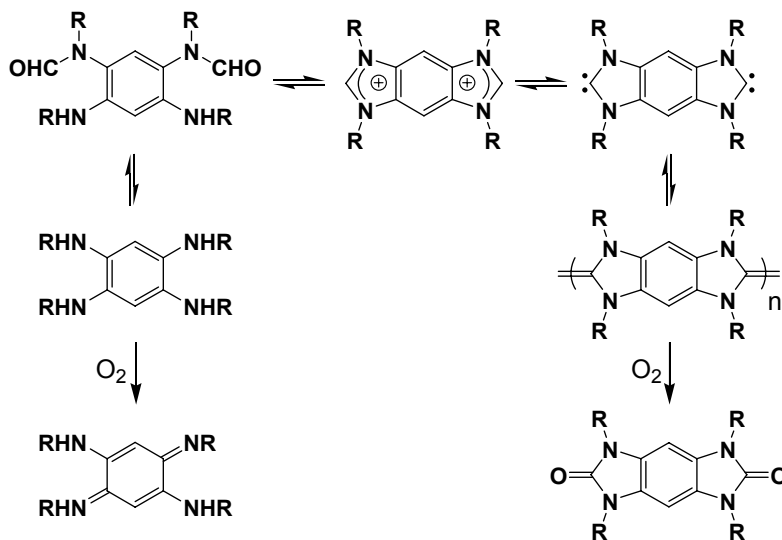
Figure 8.10 Emission spectra of **8.2•MeSO₄** (1 μ M) in MeOH under ambient conditions excited at 330 (solid line), 340 (dashed line) and 350 nm (dotted line).



8.7 pH stability of benzobis(imidazolium) salts

It has been previously demonstrated that BBI salts can be deprotonated¹³⁷ under strongly basic conditions to generate bis(*N*-heterocyclic carbene)s.⁴⁶ When the *N*-substituents were small, such as 1°-alkyl groups (e.g., **8.2•Br**), carbene dimerization occurred resulting in the formation of poly(enetetraamine)s as depicted in Scheme 8.7. Enetetraamines are well-known to be extremely oxygen sensitive and rapidly convert to ureas upon exposure to air.⁴⁴ Alternatively, one may envision hydrolysis of the BBI to generate a diamide, which upon further hydrolysis and oxidation would result in a diamino-benzoquinonediimine. These reactivities to strong base prompted us to explore the pH stability of a simple BBI chromophore (**8.2•Br**) in aqueous solutions; key data are summarized in Table 8.4.

Scheme 8.7 Possible reaction pathways of BBI salts under basic aqueous conditions



In neutral H₂O, BBI **8.2•Br** showed absorption and emission characteristics nearly identical to those observed in MeOH solvent. After 30 min in H₂O (pH 7), emission intensity of BBI **8.2•Br** was at 93% of its initial value (see Table 8.4). After 2 h, 85% of the emission intensity persisted. To investigate the emission properties of **8.2•Br** under more basic conditions, a fresh sample was dissolved in aqueous media buffered to pH 9. Under these conditions, the emission intensity remained essentially unchanged from that at pH 7, and did not diminish significantly even after 2 h. At pH 11, the photoluminescence disappeared almost instantly, and was not returned upon acidification to pH 7. Thus, the upper limit of tolerable pH levels appeared to be approximate 9. Furthermore, the irreversibility of the fluorescence loss suggested that the BBI chromophore was in fact destroyed *via* hydrolysis or oxidation, as described in Scheme 8.7.

Table 8.4. Total emission intensity observed from BBI **8.2•Br** at various pH values and durations^a

pH	I_x/I_7 at time n			I_n/I_0 at pH X	
	0 min	30 min	120 min	30 min	120 min
1	0.09	0.09	0.10	0.94	0.93
3	0.87	0.92	1.00	0.98	0.98
5	0.87	0.89	1.04	0.95	1.02
7	1.00	1.00	1.00	0.93	0.85
9	0.86	0.91	0.98	0.98	0.97
11	0.01	0.01	0.01	0.98	1.03

^aEmission data collected under ambient conditions. Excitation at 290 nm. I_x = total integrated emission intensity at pH = X, and time indicated. I_7 = total integrated emission intensity at pH = 7, and time indicated. I_0 = total integrated emission intensity at time 0 for the pH indicated.

To elucidate the degradation pathway of BBI **8.2•Br** under basic aqueous conditions, we performed NMR-scale experiments in D₂O/NaOH (pH = 11). Analysis of the products after 2 h at room temperature revealed complete loss of the C1-proton signals (δ = 9.57 in D₂O). Mass-spectral analysis confirmed hydrolysis products consistent with the bis(formamide) shown in Scheme 8.7.

Next, we explored the stability of **8.2•Br** under acidic aqueous conditions. At pH levels of 5 and 3, the emission intensities remained essentially unchanged after 2 h, and were similar to the emission intensity observed at pH 7. Upon further acidification (pH 1), however, photoluminescence was lost immediately and was not regained upon neutralization to pH 7. Overall, despite reactive imidazolium moieties, BBI **8.2•Br** showed excellent stability in aqueous solutions ranging in pH from 3 – 9. Outside of these limits, degradation was observed consistent with the formation of a diamino-benzoquinonediimine/bis(urea), depending on pH.

8.8 Conclusions

In summary, a new series of ionic fluorophores based upon benzobis(imidazolium) salts has been developed. A variety of characteristics and applications of this new class of fluorophores have been studied, including emission wavelength tunability, pH stability, solvatochromism and solvatofluorochromism, and red-edge excitation. The scope of potential applications of these materials was facilitated by a modular synthetic design. Each of the fluorophores described herein was synthesized in at most four steps without the need for chromatographic purification.

Installation of functional groups at various sites on the BBI core allowed for emission wavelength tunability. Ultimately it was found that longer λ_{em} were obtained when electron-rich N-substituents and electron-deficient C1-substituents were in place. Furthermore, evidence for N-to-C1 electronic communication was observed. Overall, the emission wavelengths were tunable over a broad range, extending from the ultraviolet (330 nm) into the visible region (up to 561 nm), and Φ_{fs} were generally good, reaching a maximum of 0.91.

Fundamental studies regarding the solution photophysics were carried out with focus on solvatochromism, solvatofluorochromism, and red-edge excitation. The λ_{em} solvent-dependency was found to be strongly influenced by the nature of the BBI core as well as solvent, and independent of the nature of the counterions. Collectively, the response to changes in solvent DN, and the magnitude of the Stokes shifts suggested a nucleophilic attack from solvent molecules as the cause of the solvatofluorochromism. REE was observed from solutions of BBIs with varying counterions. The REE was found to be counterion dependent, even in dilute MeOH solutions. Importantly, these results not only demonstrated for the first time REE of extended imidazolium-based fluorophores, but also unveiled the influence of cation-anion pairing in addition to solvate interactions.

8.9 Experimental Section

General Considerations. ^1H and ^{13}C NMR spectra were recorded using a Varian Unity Plus 300 or 400 spectrometer. Chemical shifts (δ) are expressed in ppm downfield

from tetramethylsilane using the residual protio solvent as an internal standard (CDCl_3 , ^1H : 7.26 ppm and ^{13}C : 77.0 ppm; $\text{DMSO}-d_6$, ^1H : 2.49 ppm and ^{13}C : 39.5 ppm). Coupling constants are expressed in hertz (Hz). HRMS (ESI, CI) were obtained with a VG analytical ZAB2-E instrument. UV-vis spectra were recorded using a Perkin Elmer Instruments Lambda 35 spectrometer. Emission spectra were recorded using a QuantaMaster Photon Technology International fluorometer. Unless otherwise noted, all reactions were performed under ambient atmosphere. All starting materials and solvents were of reagent quality and used as received from commercial suppliers.

1,3,5,7-Tetrabutylbenzobis(imidazolium) bis(tetrafluoroborate) ($8.2\cdot\text{BF}_4$): After suspending BBI $8.2\cdot\text{Br}$ (992 mg, 1.82 mmol) in dry CH_2Cl_2 , $\text{Et}_3\text{O}\cdot\text{BF}_4$ (692 mg, 3.64 mmol) was added in a single portion. The reaction progress was monitored by ^1H NMR spectroscopy and upon completion (ca 10 min), the solution was concentrated to provide 969 mg (95% yield) of the desired product as a white powder. ^1H NMR (400 MHz, $\text{DMSO}-d_6$): δ 10.10 (s, 2H), 8.97 (s, 2H), 4.59 (t, $J = 7.2$ Hz, 8H), 2.00-1.93 (m, 8H), 1.42-1.33 (m, 8H), 0.94 (t, $J = 7.2$ Hz, 12H); ^{13}C NMR (75 MHz, $\text{DMSO}-d_6$): δ 145.5, 130.2, 98.8, 47.1, 30.2, 19.1, 13.4. HRMS m/z calcd for BF_4 87.0029, found 87.0026.

1,3,5,7-Tetrabutylbenzobis(imidazolium) bis(methyl sulfate) ($8.2\cdot\text{MeSO}_4$): After suspending BBI $8.2\cdot\text{Br}$ (488 mg, 0.90 mmol) in dry CH_2Cl_2 , Me_2SO_4 (0.17 mL, 1.80 mmol) was added in a single portion. The reaction progress was monitored by ^1H NMR spectroscopy and upon completion (ca 4 h), the solution was concentrated to provide 542 mg (99% yield) of the desired product as a beige powder. ^1H NMR (400 MHz, CDCl_3): δ

9.94 (s, 2H), 8.84 (s, 2H), 4.72, (t, $J = 7.0$ Hz, 8H), 3.76 (s, 6H), 1.96-1.89 (m, 8H), 1.42-1.32 (m, 8H), 0.93 (t, $J = 7.2$ Hz, 12H); ^{13}C NMR (100 MHz, $\text{CDCl}_3 + \text{DMSO}-d_6$): δ 145.3, 130.3, 99.7, 54.5, 47.8, 31.1, 19.5, 13.4.

1,5-Diphenylbenzobis(imidazole) ($\mathbf{8.5_{anti}}$): Benzobis(imidazole) **8.1** (500 mg, 3.16 mmol) was dissolved in dry DMF (15 mL) in a screw-cap vial. Under nitrogen atmosphere, PhI (1.42 mL, 12.6 mmol), CuI (60 mg, 0.32 mmol), 1,10-phenanthroline (114 mg, 0.63 mmol) and K_2CO_3 (1.75 g, 12.6 mmol) were added. The vial was then sealed with a Teflon-lined cap and the mixture was stirred at 130 °C for 17 h. Upon completion, the mixture was poured into H_2O (30 mL). Collection of the precipitated solids *via* vacuum filtration afforded 932 mg (95% yield) as a 1:1 mixture of two regioisomers $\mathbf{8.5_{syn}}$ and $\mathbf{8.5_{anti}}$. Recrystallization of the mixture from hot DMSO provided 392 mg (40% yield based on **8.1**) of $\mathbf{8.5_{syn}}$. Spectral data for $\mathbf{8.5_{syn}}$ were consistent with those previously reported (see Chapter 7). Data for $\mathbf{8.5_{anti}}$: ^1H NMR (300 MHz, CDCl_3): δ 8.20 (s, 2H), 8.00 (s, 2H), 7.63-7.62 (m, 8H), 7.52-7.45 (m, 2H); ^{13}C NMR (75 MHz, CDCl_3): δ 143.7, 142.2, 136.6, 131.5, 130.1, 128.0, 123.9, 100.4; HRMS m/z calcd for $\text{C}_{20}\text{H}_{15}\text{N}_4$ [$\text{M} + \text{H}^+$] 311.1297, found 311.1299.

1,5-Dimethyl-3,7-diphenylbenzobis(imidazolium) bis(methyl sulfate) ($\mathbf{8.6_{anti}}$): After dissolving diphenylbenzobis(imidazole) $\mathbf{8.5_{anti}}$ (50 mg, 0.15 mmol) in CH_3CN (1.0 mL) in a screw-cap vial, Me_2SO_4 (29 μL , 0.31 mmol) was added in a single portion. The vial was sealed with a Teflon-lined cap and placed in an oil bath at 80 °C for 4 h. The reaction mixture was then cooled and concentrated to afford 84 mg (> 99% yield) of the desired

product as a beige wax. ^1H NMR (400 MHz, $\text{DMSO-}d_6$): δ 10.35 (s, 2H), 8.64 (s, 2H), 7.92 (d, $J = 7.6$ Hz, 4H), 7.85-7.78 (m, 6H), 4.24 (s, 6H), 3.34 (s, 6H); ^{13}C NMR (75 MHz, $\text{DMSO-}d_6$): δ 147.4, 146.3, 132.9, 131.2, 130.9, 130.5, 130.1, 125.7, 99.1, 52.9, 34.0; HRMS m/z calcd for.

Benzimidazolium chloride 8.8: In a nitrogen-filled drybox, a screw-cap vial was charged with 5,6-dichloro-1-methylbenzimidazole **8.7** (375 mg, 1.87 mmol) and PhCH_3 (10 mL). To the solution was added $\text{Pd}(\text{OAc})_2$ (4 mg, 0.02 mmol), 1,3-bis(2,6-diisopropylphenyl)imidazolium chloride (16 mg, 0.04 mmol), NaO^tBu (368 mg, 3.83 mmol), and PhNH_2 (869 mg, 9.33 mmol). The vial was then sealed with a Teflon-lined cap and placed in an oil bath at 120 °C for 12 h. After cooling the reaction mixture to ambient temperature, it was poured into a solution of $\text{HC}(\text{OEt})_3$ (50 mL) and conc. HCl (1.0 mL). The resulting mixture was then stirred in an oil bath at 150 °C for 12 h, allowed to cool, and then poured into Et_2O (100 mL). The precipitated solids were collected *via* vacuum filtration, rinsed with Et_2O , and redissolved in a saturated solution of Na_2CO_3 in $^i\text{PrOH}$. After standing for 1 h, the mixture was filtered through Celite and the filtrate was concentrated to provide 523 mg (86% yield) of the desired product as a light brown powder. ^1H NMR (400 MHz, $\text{DMSO-}d_6$): δ 10.58 (s, 1H), 8.57 (s, 1H), 8.13 (s, 1H), 8.09 (s, 1H), 8.05-8.02 (m, 4H), 7.83-7.72 (m, 6H); ^{13}C NMR (75 MHz, $\text{DMSO-}d_6$): δ 149.2, 143.2, 143.0, 134.9, 133.5, 133.4, 130.5, 130.4, 128.1, 127.7, 125.6, 125.4, 102.6, 94.6, 31.5; HRMS m/z calcd for $\text{C}_{21}\text{H}_{17}\text{N}_4$ [M^+] 325.1453, found 325.1454.

1,3-Dimethyl-5,7-diphenylbenzobis(imidazolium) bis(methyl sulfate) (8.9): After dissolving benzimidazolium chloride **8.8** (50 mg, 0.15 mmol) in CH₃CN (1.0 mL), Me₂SO₄ (39 mg, 0.31 mmol) was added in a single portion. After stirring the solution at 80 °C for 2 h, it was concentrated to afford 84 mg (>99% yield) of the desired product as a tan solid. ¹H NMR (400 MHz, CDCl₃): δ 10.81 (s, 1H), 10.04, (s, 1H), 8.60 (s, 2H), 8.04 (d, *J* = 7.2 Hz, 4H), 7.85-7.78 (m, 6H), 4.18 (s, 6H), 3.35 (s, 6H); ¹³C NMR (75 MHz, DMSO-*d*₆): δ 147.4, 146.3, 132.9, 131.2, 130.9, 130.5, 130.1, 125.7, 99.1, 52.9, 34.0; HRMS *m/z* calcd for C₂₂H₁₉N₄ [M-H⁺] 339.1610, found 339.1607.

1,5-Bis(4-carboethoxyphenyl)amino-3,4-dinitrobenzene (8.11): A screw-cap vial was charged with 1,5-dichloro-3,4-dinitrobenzene (**8.10**) (413 mg, 1.74 mmol), benzocaine (1.44 g, 8.71 mmol), *i*PrOH (15 mL), and a stir bar. The vial was sealed with a Teflon-lined cap, placed in an oil bath at 120 °C and stirred for 48 h. After pouring the mixture into 5% HCl (50 mL), the precipitated solids were collected *via* vacuum filtration, rinsed with H₂O and dried under vacuum to provide 1.66 g (98% yield) of the desired product as a yellow powder. ¹H NMR (400 MHz, CDCl₃): δ 9.92 (br s, 2H), 9.32 (s, 1H), 8.05 (d, *J* = 8.4 Hz, 4H), 7.25 (d, *J* = 8.4 Hz, 4H), 6.83 (s, 1H), 4.38 (quart, *J* = 7.2 Hz, 4H), 1.41 (t, *J* = 7.2 Hz, 6H); ¹³C NMR (100 MHz, CDCl₃): δ 165.4, 145.6, 141.2, 131.3, 129.2, 128.2, 126.1, 123.0, 96.7, 61.2, 14.3; HRMS *m/z* calcd for C₂₄H₂₃N₄O₈ [M+H⁺] 495.1516, found 495.1517.

1,5-Bis(4-methoxyphenyl)amino-3,4-dinitrobenzene (8.12): After dissolving 1,5-dichloro-3,4-dinitrobenzene (**8.10**) (1.00 g, 4.22 mmol) in EtOH (75 mL), *p*-anisidine

(2.08 g, 16.9 mmol) was added in a single portion. The mixture was then placed in an oil bath at 80 °C and stirred for 48 h. The mixture was then poured into H₂O (200 mL) which caused solids to precipitate. The solids were collected *via* vacuum filtration, rinsed with H₂O and dried under vacuum to provide 1.42 g (96% yield) of the desired product as a red-orange powder. ¹H NMR (300 MHz, CDCl₃): δ 9.57 (br s, 2H), 9.31 (s, 1H), 7.05 (d, *J* = 8.9 Hz, 4H), 6.84 (d, *J* = 8.9 Hz, 4H), 6.18 (s, 1H), 3.80 (s, 3H); ¹³C NMR (75 MHz, CDCl₃): δ 158.2, 1147.7, 129.8, 129.4, 126.7, 125.0, 114.8, 94.9, 55.5; HRMS *m/z* calcd for C₂₀H₁₉N₄O₆ [M+H⁺] 411.1305, found 411.1301.

1,7-Bis(4-carboethoxyphenyl)benzobis(imidazole) (8.13): Dinitroarene **8.11** (400 mg, 0.81 mmol) was dissolved in HC(OEt₃) (10 mL) in a screw-cap vial. To the solution was added HCO₂H (88%, 1 mL), HCO₂Na (1.65 g, 24.3 mmol) and Pd/C (172 mg, 5 wt%, 0.08 mmol Pd). The vial was then sealed with a Teflon-lined cap and the mixture was heated in an oil bath at 110 °C for 48 h. Upon cooling the mixture to ambient temperature, it was filtered through Celite. The filtrate was treated with 5% HCl, stirred for ca 30 min, and then brought to pH 9 using saturated aqueous Na₂CO₃. Precipitated solids were subsequently collected *via* vacuum filtration, rinsed with H₂O, and dried under vacuum to provide 352 mg (96% yield) of the desired product as a tan powder. ¹H NMR (400 MHz, CDCl₃): δ 8.38 (s, 1H), 8.26 (d, *J* = 8.4 Hz, 4H), 8.21 (s, 2H), 7.63 (s, 1H), 7.61 (d, *J* = 8.4 Hz, 4H), 4.43 (quart, *J* = 7.2 Hz, 4H), 1.43 (t, *J* = 7.2 Hz, 6H); ¹³C NMR (75 MHz, CDCl₃): δ 165.5, 143.1, 141.8, 140.1, 131.8, 131.7, 129.9, 123.3, 111.6, 90.4, 61.4, 14.3; HRMS *m/z* calcd for C₂₆H₂₃N₄O₄ [M+H⁺] 455.1719, found 455.1716.

1,7-Bis(4-methoxyphenyl)benzobis(imidazole) (8.14): Dinitroarene **8.12** (1.00 g, 2.44 mmol) was suspended in HCO₂H (88%, 100 mL). To the suspension was added HCO₂Na (1.99 mg, 29.2 mmol) and Pd/C (103 mg, 5 wt%, 0.05 mmol Pd). The mixture was heated in an oil bath at 110 °C for 48 h. Upon completion, the cooled reaction mixture was filtered through Celite and the filtrate volume was reduced to ca 25 mL under vacuum. The solution was then added slowly into a vigorously stirred saturated solution of aqueous Na₂CO₃ (150 mL). Precipitated solids were collected *via* vacuum filtration, rinsed with H₂O, and dried under vacuum to provide 705 mg (78% yield) of the desired product as a tan powder. ¹H NMR (300 MHz, CDCl₃): δ 8.31 (s, 1H), 8.08 (s, 2H), 7.41 (d, *J* = 8.8 Hz, 4H), 7.35 (s, 1H), 7.06 (d, *J* = 8.8 Hz, 4H), 3.88 (s, 6H); ¹³C NMR (75 MHz, CDCl₃): δ 159.2, 143.6, 141.2, 132.8, 129.3, 125.9, 115.2, 110.5, 89.8, 55.6; HRMS *m/z* calcd for C₂₂H₁₉N₄O₂ [M+H⁺] 371.1508, found 371.1511.

1,7-Bis(4-carboethoxyphenyl)-3,5-dimethylbenzobis(imidazolium) diiodide (8.15): Benzobis(imidazole) **8.13** (300 mg, 0.66 mmol) was dissolved in CH₃CN (10 mL) and MeI (1.0 mL) in a screw-cap vial. The vial was sealed with a Teflon lined cap and the mixture was heated at 80 °C for 8 h. Upon completion, the mixture was concentrated under vacuum to provide 485 mg (>99% yield) of the desired product as a dark brown powder. ¹H NMR (400 MHz, DMSO-*d*₆): δ 10.48 (s, 2H), 9.12 (s, 1H), 8.27 (d, *J* = 8.2 Hz, 4H), 8.24 (s, 1H), 8.03 (d, *J* = 8.2 Hz, 4H), 4.38 (quart, *J* = 7.2 Hz, 4H), 4.30 (s, 6H), 1.35 (t, *J* = 7.0 Hz, 6H); ¹³C NMR (75 MHz, DMSO-*d*₆): δ 164.7, 147.4, 136.6, 131.6, 131.3, 131.2, 129.9, 125.7, 107.3, 99.9, 98.5, 61.4, 34.4, 14.2; HRMS *m/z* calcd for C₂₈H₂₇N₄O₄ [M-H⁺] 483.2032, found 483.2033.

1,7-Bis(4-methoxyphenyl)-3,5-dimethylbenzobis(imidazolium) diiodide (8.16):

Benzobis(imidazole) **8.14** (500 mg, 1.35 mmol) was dissolved in CH₃CN (10 mL) and MeI (1.0 mL) in a screw-cap vial. The vial was sealed with a Teflon lined cap and the mixture was heated at 80 °C for 8 h. Upon completion, the mixture was concentrated under vacuum to provide 877 mg (99% yield) of the desired product as a dark brown powder. ¹H NMR (400 MHz, DMSO-*d*₆): δ 10.30 (s, 2H), 9.06 (s, 1H), 7.87 (s, 1H), 7.76 (d, *J* = 8.8 Hz, 4H), 7.25 (d, *J* = 8.8 Hz, 4H), 4.27 (s, 6H), 3.86 (s, 6H); ¹³C NMR (100 MHz, DMSO-*d*₆): δ 160.7, 147.1, 130.9, 130.6, 127.0, 125.4, 115.5, 99.4, 97.8, 55.8, 34.2; HRMS *m/z* calcd for C₂₄H₂₃N₄O₂ [M-H⁺] 399.1821, found 399.1817.

1,5-Bis(4-butylphenyl)amino-3,4-dinitrobenzene (8.17): Following a similar procedure used to prepare **8.12**, 1,5-dichloro-3,4-dinitrobenzene (**8.10**) (1.00 g, 4.22 mmol) and 4-butylaniline (2.52 g, 16.88 mmol) afforded 1.83 g (94% yield) of the desired product as a burnt orange powder. ¹H NMR (400 MHz, CDCl₃): δ 9.68 (br s, 2H), 9.30 (s, 1H), 7.14 (d, *J* = 8.2 Hz, 4H), 7.05 (d, *J* = 8.2 Hz, 4H), 6.48 (s, 1H), 2.58 (t, *J* = 7.6 Hz, 4H), 1.61-1.53 (m, 4H), 1.40-1.31 (m, 4H), 0.95 (t, *J* = 7.2 Hz, 6H); ¹³C NMR (100 MHz, CDCl₃): δ 147.0, 141.5, 134.6, 129.4, 129.3, 125.1, 124.6, 95.1, 35.1, 33.6, 22.2, 13.9; HRMS *m/z* calcd for C₂₆H₃₁N₄O₄ [M+H⁺] 463.2345, found 463.2343.

General procedure for the reduction of dinitroarenes 8.11 and 8.17. The dinitroarene (1.0 mmol, 1.0 equiv) was dissolved in EtOH (20 mL) in a 100 mL flask. Pd/C (5 wt%, 0.10 mmol Pd, 0.10 equiv) was added. The flask was fitted with a H₂O-jacketed

condenser and $\text{H}_2\text{NNH}_2 \cdot \text{H}_2\text{O}$ (80%, 16 mmol, 16 equiv) was added dropwise followed by 1.2 N HCl (7 mL, 8.0 mmol, 8.0 equiv). The solution was stirred in an oil bath at 80 °C for 4 h. The cooled reaction mixture was filtered through Celite and concentrated under vacuum to provide the corresponding tetraamines as their di-hydrochloride salts. These products were used directly in subsequent steps without further purification. Note: these materials were found to decompose upon prolonged standing under ambient atmosphere and thus were stored in a nitrogen-filled desiccator prior to use.

General procedure for the synthesis of C1-aryl benzobis(imidazole)s 8.20 – 8.25.

Under an atmosphere of dry nitrogen, the corresponding tetraaminobenzene (1.0 mmol, 1.0 equiv) was suspended in THF (10 mL). The aryl chloride (2.0 mmol, 2.0 equiv) was added, followed by Na_2CO_3 (10.0 mmol, 10.0 equiv). After stirring the solution for 12 h at ambient temperature, it was slowly poured into AcOH (30 mL). The resulting suspension was heated open-air in an oil bath at 110 °C for 24 h, during which time AcOH was added in portions to maintain the solution volume at what?. Upon completion, the solution volume was reduced to ca 10 mL under reduced pressure, and the resulting solution was slowly poured into a vigorously stirred solution of 10% NaOH containing an equal mass of crushed ice. The resulting solids were collected *via* vacuum filtration, rinsed with 10% NaOH, then H_2O , and dried under vacuum.

1,7-Bis(4-butylphenyl)-2,6-diphenylbenzobis(imidazole) (8.20): Yield: 580 mg (96%).

^1H NMR (300 MHz, CDCl_3): δ 8.36 (s, 1H), 7.58 (dd, J = 6.3, 1.8 Hz, 4H), 7.37-7.26 (m, 10H), 7.20 (d, J = 8.7 Hz, 4H), 6.97 (s, 1H), 2.68 (t, J = 2.68 Hz, 4H), 1.70-1.60 (m, 4H),

1.45-1.32 (m, 4H), 0.96 (t, $J = 7.3$ Hz, 6H); ^{13}C NMR (75 MHz, CDCl_3): δ 153.1, 143.4, 135.8, 134.8, 130.1, 129.8, 129.4, 129.3, 128.2, 127.3, 109.0, 90.2, 35.3, 33.3, 22.3, 13.9; HRMS m/z calcd for $\text{C}_{40}\text{H}_{39}\text{N}_4$ $[\text{M}+\text{H}^+]$ 575.3175, found 575.3176.

1,7-Bis(4-butylphenyl)-2,6-bis(4-cyanophenyl)benzobis(imidazole) (8.21): Yield: 308 mg (93%). ^1H NMR (300 MHz, CDCl_3): δ 8.37 (s, 1H), 7.69 (d, $J = 8.7$ Hz, 4H), 7.58 (d, $J = 8.7$ Hz, 4H), 7.32 (d, $J = 8.4$ Hz, 4H), 7.19 (d, $J = 8.4$ Hz, 4H), 6.96 (s, 1H), 2.71 (t, $J = 7.7$ Hz, 4H), 1.72-1.61 (m, 4H), 1.46-1.34 (m, 4H), 0.97 (t, $J = 7.2$ Hz, 6H); ^{13}C NMR (75 MHz, CDCl_3): δ 151.2, 144.3, 140.8, 136.5, 134.3, 134.0, 132.0, 130.2, 129.7, 127.1, 118.4, 112.8, 109.9, 90.5, 35.3, 33.3, 22.4, 13.9; HRMS m/z calcd for $\text{C}_{42}\text{H}_{37}\text{N}_6$ $[\text{M}+\text{H}^+]$ 625.3080, found 625.3078.

1,7-Bis(4-butylphenyl)-2,6-bis(4-methoxyphenyl)benzobis(imidazole) (8.22): Yield: 287 mg (91%). ^1H NMR (300 MHz, CDCl_3): δ 8.28 (s, 1H), 7.50 (d, $J = 8.1$ Hz, 4H), 7.27 (d, $J = 7.3$ Hz, 4H), 7.19 (d, $J = 7.3$ Hz, 4H), 6.90 (s, 1H), 6.80 (d, $J = 8.1$ Hz, 4H), 3.80 (s, 6H), 2.68 (t, $J = 7.7$ Hz, 4H), 1.70-1.60 (m, 4H), 1.45-1.33 (m, 4H), 0.96 (t, $J = 7.2$ Hz, 6H); ^{13}C NMR (75 MHz, CDCl_3): δ 160.3, 152.9, 143.3, 140.5, 135.6, 135.0, 130.8, 129.8, 127.3, 122.7, 113.6, 108.4, 89.9, 55.2, 35.3, 33.3, 22.3, 13.9; HRMS m/z calcd for $\text{C}_{42}\text{H}_{43}\text{N}_4\text{O}_2$ $[\text{M}+\text{H}^+]$ 635.3386, found 635.3390.

1,7-Bis(4-butylphenyl)-2,6-bis(2-thienyl)benzobis(imidazole) (8.23): Yield: 200 mg (78%). ^1H NMR (300 MHz, CDCl_3): δ 8.25 (s, 1H), 7.37-7.26 (m, 10H), 6.89 (dd appearing as t, $J = 4.5$ Hz, 2H), 6.77 (d, $J = 3.6$ Hz, 2H), 6.59 (s, 1H), 2.73 (t, $J = 7.7$ Hz,

4H), 1.74-1.64 (m, 4H), 1.48-1.35 (m, 4H), 0.97 (t, $J = 7.2$ Hz, 6H); ^{13}C NMR (75 MHz, CDCl_3): δ 148.2, 144.6, 140.5, 136.4, 134.0, 132.9, 130.0, 128.25, 128.16, 127.9, 127.4, 108.4, 89.6, 35.4, 33.3, 22.4, 13.9; HRMS m/z calcd for $\text{C}_{36}\text{H}_{35}\text{N}_4\text{S}_2$ $[\text{M}+\text{H}^+]$ 587.2303, found 587.2307.

2,6-Bis(4-biphenyl)-1,7-bis(4-methoxyphenyl)benzobis(imidazole) (8.24): Yield: 492 mg (88%). ^1H NMR (400 MHz, CDCl_3): δ 8.36 (s, 1H), 7.67 (d, $J = 8.4$ Hz, 4H), 7.59 (d, $J = 7.2$ Hz, 4H), 7.54 (d, $J = 8.4$ Hz, 4H), 7.45-7.41 (m, 4H), 7.37-7.33 (m, 2H), 7.25 (d, $J = 6.8$ Hz, 4H), 7.01 (d, $J = 8.8$ Hz, 4H), 6.85 (s, 1H), 3.88 (s, 6H); ^{13}C NMR (75 MHz, CDCl_3): δ 159.4, 152.9, 141.8, 140.6, 140.1, 136.3, 130.0, 129.7, 129.0, 128.82, 128.8, 127.7, 127.0, 126.8, 115.2, 108.9, 90.0, 55.5; HRMS m/z calcd for $\text{C}_{46}\text{H}_{35}\text{N}_4\text{O}_2$ $[\text{M}+\text{H}^+]$ 675.2760, found 675.2763.

2,6-Bis(4-cyanophenyl)-1,7-bis(4-methoxyphenyl)benzobis(imidazole) (8.25): Yield: 469 mg (99%). ^1H NMR (400 MHz, $\text{CDCl}_3+\text{DMSO}-d_6$): δ 8.29 (s, 1H), 7.68 (d, $J = 8.2$ Hz, 4H), 7.55 (d, $J = 8.2$ Hz, 4H), 7.16 (d, $J = 8.4$ Hz, 4H), 6.97 (d, $J = 8.4$ Hz, 4H), 6.80 (s, 1H), 3.84 (s, 6H), ; ^{13}C NMR (75 MHz, $\text{CDCl}_3+\text{DMSO}-d_6$): δ 159.7, 151.1, 140.6, 136.8, 134.2, 131.9, 129.5, 128.9, 128.5, 118.2, 115.4, 112.6, 109.6, 90.3, 55.5; HRMS m/z calcd for $\text{C}_{36}\text{H}_{25}\text{N}_6\text{O}_2$ $[\text{M}+\text{H}^+]$ 573.2039, found 573.2038.

General procedure for the alkylation of benzobis(imidazole)s 8.20 – 8.25 to provide BBI salts 8.26 – 8.31. The benzobis(imidazole) (1.0 mmol, 1.0 equiv) was dissolved or suspended in CH_3CN (10 mL) and MeI (5.0 mmol, 5.0 equiv) in a screw-cap vial. The

vial was sealed with a Teflon-lined cap and the reaction mixture was stirred in an oil bath at 100 °C for 2 – 10 h. The reaction progress was monitored by No-D ^1H NMR spectroscopy^{ref} of aliquots taken periodically over time. Upon completion of the reaction, the reaction mixtures were cooled to ambient temperature and concentrated. Crude materials were then rinsed with cold EtOAc and then dried under vacuum to provide the desired products.

1,7-Bis(4-butylphenyl)-3,5-dimethyl-2,6-diphenylbenzobis(imidazolium) diiodide (8.26): Yield: 149 mg (>99%). ^1H NMR (300 MHz, CDCl_3): δ 8.44 (s, 1H), 7.88 (d, J = 7.5 Hz, 4H), 7.65-7.50 (m, 10H), 7.31 (s, 1H), 7.23 (d, J = 8.4 Hz, 4H), 4.27 (s, 6H), 1.60-1.50 (m, 4H), 1.35-1.23 (m, 4H), 0.89 (t, J = 7.2 Hz, 6H); ^{13}C NMR (75 MHz, CDCl_3): δ 153.7, 146.4, 133.1, 132.9, 132.0, 131.4, 130.2, 129.5, 129.3, 127.6, 120.6, 99.9, 98.0, 35.2, 34.9, 32.9, 22.1, 13.8; HRMS m/z calcd for $\text{C}_{42}\text{H}_{43}\text{N}_4$ [M-H^+] 603.3488, found 603.3492.

1,7-Bis(4-butylphenyl)-2,6-bis(4-cyanophenyl)benzobis(imidazolium) diiodide (8.27): Yield: 255 mg (>99%). ^1H NMR (400 MHz, $\text{DMSO}-d_6$): δ 9.33 (s, 1H), 8.12 (d, J = 7.8 Hz, 4H), 8.05 (d, J = 7.8 Hz, 4H), 7.49 (d, J = 8.2 Hz, 4H), 7.38 (s, 1H), 7.36 (d, J = 8.2 Hz, 4H), 4.19 (s, 3H), 2.59 (t, J = 7.4 Hz, 4H), 1.52-1.48 (m, 4H), 1.25-1.20 (m, 4H), 0.84 (t, J = 7.2 Hz, 6H); ^{13}C NMR (75 MHz, $\text{CDCl}_3+\text{DMSO}-d_6$): δ 151.7, 146.5, 132.6, 132.3, 132.1, 131.8, 129.9, 128.7, 127.0, 124.8, 116.7, 116.3, 99.8, 97.3, 34.7, 34.3, 32.4, 21.7, 13.3; HRMS m/z calcd for $\text{C}_{44}\text{H}_{41}\text{N}_6$ [M-H^+] 653.3393, found 653.3398.

1,7-Bis(4-butylphenyl)-2,6-bis(4-cyanophenyl)benzobis(imidazolium)

bis(tetrafluoroborate) (8.27•BF₄): This compound was prepared analogously to **8.2•BF₄** from BBI **8.27** (59 mg, 0.06 mmol) to provide 49 mg (98% yield) of the desired product. ¹H NMR (300 MHz, DMSO-*d*₆): δ 9.30 (s, 1H), 8.15 (d, *J* = 8.4 Hz, 4H), 7.99 (d, *J* = 8.4 Hz, 4H), 7.46 (d, *J* = 8.1 Hz, 4H), 7.43 (s, 1H), 7.38 (d, *J* = 8.7 Hz, 4H), 4.20 (s, 6H), 2.62 (t, *J* = 7.8 Hz, 4H), 1.57-1.47 (m, 4H), 1.31-1.19 (m, 4H), 0.86 (t, *J* = 7.2 Hz, 6H); ¹³C NMR (75 MHz, DMSO-*d*₆): δ 152.4, 145.8, 132.8, 132.3, 131.9, 131.3, 130.2, 129.5, 127.4, 125.4, 117.6, 115.5, 99.4, 96.8, 34.3, 3.8, 32.5, 21.6, 13.7.

1,7-Bis(4-butylphenyl)-2,6-bis(4-methoxyphenyl)-3,5-

dimethylbenzobis(imidazolium) diiodide (8.28): Yield: 425 mg (95%). ¹H NMR (400 MHz, DMSO-*d*₆): δ 9.22 (s, 1H), 7.73 (d, *J* = 8.6 Hz, 4H), 7.48 (d, *J* = 8.2 Hz, 4H), 7.37 (d, *J* = 8.2 Hz, 4H), 7.15 (s, 1H), 7.13 (d, *J* = 8.6 Hz, 4H), 4.19 (s, 6H), 3.82 (s, 6H), 2.61 (t, *J* = 7.6 Hz, 4H), 1.55-1.48 (m, 4H), 1.26-1.21 (m, 4H), 0.85 (t, *J* = 7.2 Hz, 6H); ¹³C NMR (400 MHz, DMSO-*d*₆): δ 162.5, 153.8, 145.4, 133.4, 131.7, 131.1, 130.14, 130.09, 127.5, 114.5, 112.5, 55.7, 34.3, 34.0, 32.5, 21.6, 13.7; HRMS *m/z* calcd for C₄₄H₄₇N₄O₂ [M-H⁺] 663.3699, found 663.3701.

1,7-Bis(4-butylphenyl)-2,6-bis(2-thienyl)-3,5-dimethylbenzobis(imidazolium)

diiodide (8.29): Yield: 276 mg (93%). ¹H NMR (400 MHz, CDCl₃): δ 8.48 (s, 1H), 7.80 (d, *J* = 3.6 Hz, 2H), 7.78 (d, *J* = 4.8 Hz, 2H), 7.39 (d, *J* = 8.2 Hz, 4H), 7.31 (d, *J* = 8.2 Hz, 4H), 7.25 (d, *J* = 4.8 Hz, 2H), 7.11 (s, 1H), 4.32 (s, 6H), 2.67 (t, *J* = 7.8 Hz, 4H), 1.64-1.56 (m, 4H), 1.38-1.29 (m, 4H), 0.92 (t, *J* = 7.4 Hz, 6H); ¹³C NMR (100 MHz, CDCl₃):

δ 148.7, 147.1, 137.6, 135.5, 132.8, 132.2, 130.6, 129.5, 128.7, 127.8, 119.0, 98.8, 97.0, 35.3, 34.4, 33.0, 22.2, 13.8; HRMS m/z calcd for $C_{38}H_{39}N_4S_2$ $[M-H^+]$ 615.2616, found 615.2612.

2,6-Bis(4-biphenyl)-1,7-bis(4-methoxyphenyl)-3,5-dimethylbenzobis(imidazolium)

diiodide (8.30): Yield: 186 mg (94%). 1H NMR (400 MHz, $DMSO-d_6$): δ 9.28 (s, 1H), 7.95 (d, $J = 8.4$ Hz, 4H), 7.90 (d, $J = 8.4$ Hz, 4H), 7.58-7.43 (m, 10H), 7.37 (s, 1H), 7.10 (d, $J = 9.2$ Hz, 4H), 4.24 (s, 6H), 3.76 (s, 6H); ^{13}C NMR (75 MHz, $DMSO-d_6$): δ 160.6, 153.8, 144.1, 138.0, 132.3, 132.0, 131.2, 129.2, 128.8, 127.0, 126.9, 124.7, 119.8, 115.5, 99.1, 96.4, 55.6, 34.1; HRMS m/z calcd for $C_{48}H_{39}N_4O_2$ $[M-H^+]$ 703.3073, found 703.3077.

2,6-Bis(4-cyanophenyl)-1,7-bis(4-methoxyphenyl)-3,5-

dimethylbenzobis(imidazolium) diiodide (8.31): Yield: 102 mg (99%). 1H NMR (400 MHz, $DMSO-d_6$): δ 9.30 (s, 1H), 8.14 (d, $J = 8.6$ Hz, 4H), 8.04 (d, $J = 8.6$ Hz, 4H), 7.51 (d, $J = 9.0$ Hz, 4H), 7.49 (s, 1H), 7.07 (d, $J = 9.0$ Hz, 4H), 4.18 (s, 6H), 3.76 (s, 6H); ^{13}C NMR (100 MHz, $DMSO-d_6$): δ 160.7, 152.5, 132.8, 132.4, 131.3, 129.1, 125.5, 124.2, 117.6, 115.5, 115.4, 96.9, 88.0, 55.6, 34.0; HRMS m/z calcd for $C_{38}H_{29}N_6O_2$ $[M-H^+]$ 601.2352, found 601.2355.

1-(4-carboethoxyphenyl)-7-(4-methoxyphenyl)-3,5-dimethylbenzobis(imidazolium)

diiodide (8.32): This compound was prepared analogously to BBI **8.15** from benzobis(imidazole) **8.35** (100 mg, 0.24 mmol) to provide 169 mg (>99% yield) of the

desired product as a pale yellow powder. ^1H NMR (300 MHz, $\text{DMSO-}d_6$): δ 10.48 (s, 1H), 10.33 (s, 1H), 9.1 (s, 1H), 8.27 (d, $J = 8.7$ Hz, 2H), 8.07 (s, 1H), 8.04 (d, $J = 9.0$ Hz, 2H), 7.80 (d, $J = 9.0$ Hz, 2H), 7.25 (d, $J = 9.0$ Hz, 2H), 4.38 (quart, $J = 6.9$ Hz, 2H), 4.30 (s, 3H), 4.29 (s, 3H), 3.86 (s, 3H), 1.35 (t, $J = 7.2$ Hz, 3H); ^{13}C NMR (100 MHz, $\text{DMSO-}d_6$): δ 164.7, 160.6, 147.2, 136.7, 131.6, 131.3, 131.1, 131.0, 130.6, 129.8, 127.0, 125.8, 125.5, 115.5, 99.7, 98.2, 61.4, 55.8, 34.4, 34.3, 14.1; HRMS m/z calcd for $\text{C}_{26}\text{H}_{25}\text{N}_4\text{O}_3$ $[\text{M-H}^+]$ 441.1927, found 441.1930.

1-(4-carboethoxyphenyl)amino-5-chloro-2,4-dinitrobenzene (8.33): A screw-cap vial was charged with 1,5-dichloro-3,4-dinitrobenzene (**8.10**) (595 mg, 2.51 mmol), benzocaine (829 g, 5.02 mmol), EtOH (10 mL), and a stir bar. The vial was then sealed with a Teflon-lined cap and the mixture was placed in an oil bath at 50 °C and stirred for 12 h. Upon completion, the mixture was poured into 5% HCl (50 mL). Precipitated solids were collected *via* vacuum filtration, rinsed with H_2O and dried under vacuum to provide 875 mg (95% yield) of the desired product as a yellow powder. ^1H NMR (400 MHz, CDCl_3): δ 9.90 (br s, 1H), 9.06 (s, 1H), 8.18 (d, $J = 8.8$ Hz, 2H), 7.38 (d, $J = 8.8$ Hz, 2H), 7.32 (s, 1H), 4.41 (quart, $J = 7.2$ Hz, 2H), 1.42 (t, $J = 7.2$ Hz, 3H); ^{13}C NMR (100 MHz, CDCl_3): δ 165.4, 144.2, 140.4, 136.7, 135.8, 131.7, 130.3, 129.4, 126.5, 124.0, 118.1, 61.4, 14.3; HRMS m/z calcd for $\text{C}_{15}\text{H}_{13}\text{N}_3\text{O}_6\text{Cl}$ $[\text{M}+\text{H}^+]$ 366.0493, found 366.0489.

1-(4-carboethoxyphenyl)amino-2,4-dinitro-5-(4-methoxyphenyl)aminobenzene

(8.34): After dissolving aryl chloride **8.33** (380 mg, 1.04 mmol) in EtOH (10 mL), *p*-

anisidine (256 mg, 2.08 mmol) was added in a single portion. The mixture was then stirred at 80 °C for 24 h. After cooling to ambient temperature, the mixture was poured into 5% HCl (50 mL). Precipitated solids were collected *via* vacuum filtration, rinsed with H₂O and dried under vacuum to provide 462 mg (98% yield) of the desired product as an orange powder. ¹H NMR (300 MHz, CDCl₃): δ 9.85 (br s, 1H), 9.65 (br s, 1H), 9.33 (s, 1H), 7.98 (d, *J* = 8.7 Hz, 2H), 7.17 (d, *J* = 8.7 Hz, 2H), 7.12 (d, *J* = 8.7 Hz, 2H), 6.92 (d, *J* = 9.0 Hz, 2H), 6.53 (s, 1H), 4.38 (quart, *J* = 7.2 Hz, 2H), 3.81 (s, 3H), 1.41 (t, *J* = 7.2 Hz, 3H); ¹³C NMR (100 MHz, CDCl₃): δ 165.6, 158.7, 148.1, 145.1, 141.7, 131.1, 129.5, 129.3, 127.6, 127.0, 125.64, 125.55, 122.6, 115.1, 96.1, 61.1, 55.5, 14.3; HRMS *m/z* calcd for C₂₂H₂₁N₄O₇ [M+H⁺] 453.1410, found 453.1406.

1-(4-carboethoxyphenyl)-7-(4-methoxyphenyl)benzobis(imidazole) (8.35): This compound was prepared analogously to **8.13** from dinitroarene **8.34** (354 mg, 0.78 mmol) to provide 272 mg (84% yield) of the desired product as an off-white solid. ¹H NMR (300 MHz, CDCl₃): δ 8.33 (s, 1H), 8.24 (d, *J* = 8.7 Hz, 2H), 8.19 (s, 1H), 8.10 (s, 1H), 7.61 (d, *J* = 9.0 Hz, 2H), 7.49 (s, 1H), 7.41 (d, *J* = 9.0 Hz, 2H), 7.08 (d, *J* = 9.0 Hz, 2H), 4.42 (quart, *J* = 7.2 Hz, 2H), 3.89 (s, 3H), 1.42 (t, *J* = 7.2 Hz, 3H); ¹³C NMR (75 MHz, CDCl₃): δ 165.5, 159.4, 143.9, 142.7, 141.6, 141.5, 140.3, 133.1, 131.6, 131.5, 129.6, 129.1, 125.9, 123.2, 115.3, 111.1, 90.1, 61.4, 55.6, 14.3; HRMS *m/z* calcd for C₂₄H₂₁N₄O₃ [M+H⁺] 413.1614, found 413.1611.

References

- 1) For recent reviews, see: a) Holliday, B. J.; Swager, T. M. *Chem. Commun.* **2005**, 23. b) Pittman, C. U. *J. Inorg. Organomet. Poly. Mater.* **2005**, 15, 33. d) Moorlag, C.; Sih, B. C.; Stott, T. L.; Wolf, M. O. *J. Mater. Chem.* **2005**, 15, 2433. d) Bunz, U. H. F. *J. Organomet. Chem.* **2003**, 683, 269. e) Nguyen, P.; Gómez-Elipé, P.; Manners, I. *Chem. Rev.* **1999**, 99, 1515. f) Roncali, J. *J. Mater. Chem.* **1999**, 9, 1875. g) Pickup, P. G. *J. Mater. Chem.* **1999**, 9, 1641.
- 2) For excellent reviews, see: a) Herrmann, W. A.; Köcher, K. *Angew. Chem. Int. Ed.* **1997**, 36, 2162. b) Arduengo, III, A. J. *Acc. Chem. Res.* **1999**, 32, 913. c) Bourissou, D.; Guerret, O.; Gabbai, F. P.; Bertrand, G. *Chem. Rev.* **2000**, 100, 39.
- 3) a) Viciu, M. S.; Nolan, S. P. *Top. Organomet. Chem.* **2005**, 14, 241. b) Scott, N. M.; Nolan, S. P. *Eur. J. Inorg. Chem.* **2005**, 1815. c) Cavallo, L.; Correa, A.; Costabile, C.; Jacobsen, H. *J. Organomet. Chem.* **2005**, 690, 5407. d) Basato, M.; Michelin, R. A.; Mozzon, M.; Sgarbossa, P.; Tassan, A. *J. Organomet. Chem.* **2005**, 690, 5414. e) Braband, H.; Kückmann, T. I.; Abram, U. *J. Organomet. Chem.* **2005**, 690, 5421. f) Crabtree, R. H. *J. Organomet. Chem.* **2005**, 690, 5451. g) Lappert, M. F. *J. Organomet. Chem.* **2005**, 690, 5467. h) Frenking, G.; Solá, M.; Vyboishchikov, S. F. *J. Organomet. Chem.* **2005**, 690, 6178. i) Crudden, C. M.; Allen, D. P. *Coord. Chem. Rev.* **2004**, 248, 2247. j) Kavel, K. J.; McGuinness, D. S. *Coord. Chem. Rev.* **2004**, 248, 671. k) Peris, E.; Crabtree, R. H. *Coord. Chem. Rev.* **2004**, 248, 2239. l) César, V.; Bellemin-Laponnaz, S.; Gade, L. H.

- Chem. Soc. Rev.* **2004**, 33, 619. m) Perry, M. C.; Burgess, K. *Tetrahedron: Asymmetry* **2003**, 14, 951. n) Herrmann, W. A. *Angew. Chem. Int. Ed.* **2002**, 41, 1290. o) Arnold, P. *Heteroat. Chem.* **2002**, 13, 534. p) Cowley, A. H. *J. Organomet. Chem.* **2001**, 617-618, 105. q) Raubenheimer, H. G.; Cronje, S. *J. Organomet. Chem.* **2001**, 617-618, 170. r) Weskamp, T.; Böhm, V. P. W.; Herrmann, W. A. *J. Organomet. Chem.* **2000**, 600, 12. s) Herrmann, W. A.; Köcher, C. *Angew. Chem. Int. Ed. Eng.* **1997**, 36, 2162.
- 4) a) Chiu, P. L.; Chen, C. Y.; Zeng, J. Y.; Lu, C. Y.; Lee, H. M. *J. Organomet. Chem.* **2005**, 690, 1682. b) Marshall, C.; Ward, M. F.; Harrison, W. T. A. *Tetrahedron Lett.* **2004**, 45, 5703.
- 5) Grundemann, S.; Kovacevic, A.; Albrecht, M.; Faller, J. W.; Crabtree, R. H. *J. Am. Chem. Soc.* **2002**, 124, 10473.
- 6) Chichak, K.; Jacquemard, U.; Branda, N. R. *Eur. J. Inorg. Chem.* **2002**, 357.
- 7) Wagner, E. C.; Millett, W. H. *Org. Synth.* **1939**, 19, 12.
- 8) This method, and variations thereof, are well known for making bidentate and bis(NHC) organometallic complexes, see: Herrmann, W. A.; Schwarz, J.; Gardiner, M. G. *Organometallics* **1999**, 18, 4082.
- 9) Frøseth, M.; Netland, K. A.; Tornroos, K. W.; Dhindsa, A.; Tilset, M. *J. Chem. Soc., Dalton Trans.* **2005**, 1664.
- 10) M_n s are reported relative to polystyrene standards in DMF.
- 11) Louie, J.; Gibby, J. E.; Farnworth, M. V.; Tekavec, T. N. *J. Am. Chem. Soc.* **2002**, 124, 15188.

- 12) Boen, N. K.; Hillmyer, M. A. *Chem. Soc. Rev.* **2005**, 34, 267.
- 13) This is consistent with the reported ^{31}P chemical shift for $(\text{PCy}_3)_2\text{PdCl}_2$ ($\delta = 21.2$ ppm); see: Rüegger, H. *Mag. Reson. Chem.* **2004**, 42, 814.
- 14) Odian, G. *Principles of Polymerization*, 3rd ed.; Wiley-Interscience: New York, 1991.
- 15) Goethals, E. J. *Telechelic Polymers: Synthesis and Applications*; CRC Press: Boca Raton, FL, 1989.
- 16) a) Gstöttmayr, C. W. K.; Böhm, V. P. W.; Herdtweck, E.; Grosche, M.; Herrmann, W. A. *Angew. Chem. Int. Ed.* **2002**, 41, 1363. b) Titcomb, L. R.; Caddick, S.; Cloke, F. G. N.; Wilsona, D. J.; McKerrecherb, D. *Chem. Commun.* **2001**, 1388.
- 17) Claramunt, R. M.; Elguero, J.; Meco, T. *J. Heterocycl. Chem.* **1983**, 20, 1244.
- 18) Pause, L.; Robert, M.; Heinicke, J.; Köhl, O. *J. Chem. Soc. Perkin Trans. 2* **2001**, 1383.
- 19) For additional syntheses of benzimidazolium and benzimidazolylidene compounds, see: a) Huynh, H. V.; Holtgrewe, C.; Pape, T.; Koh, L. L.; Hahn, F. E. *Organometallics* **2006**, 25, 245. b) Hahn, F. E.; Langenhahn, V.; Lügger, T.; Pape, T.; Le Van, D. *Angew. Chem. Int. Ed.* **2005**, 44, 3759. c) Rivas, F. M.; Riaz, U.; Giessert, A.; Smulik, J. A.; Diver S. T. *Org. Lett.* **2001**, 3, 2673. d) Hahn, F. E.; Wittenbecher, L.; Le Van, D.; Fröhlich, R. *Angew. Chem. Int. Ed.* **2000**, 39, 541. e) Korotkikh, N. I.; Rayenko, G. F.; Kiselyov, A. V.; Knishevitsky, A. V.; Shvaika, O. P.; Cowley, A. H.; Jones, J. N.; Macdonald, C. L. B. "Synthesis of

- Stable Heteroaromatic Carbenes of the Benzimidazole and 1,2,4-Triazole Series and their Precursors,” *Selected Methods for Synthesis and Modification of Heterocycles*, Vol. 1, V. G. Kartsev, Ed., Moscow, 2002.
- 20) Hahn, F. E.; Wittenbecher, L.; Boese, R.; Bläser, D. *Chem. Eur. J.* **1999**, *5*, 1931.
 - 21) a) Hadei, N.; Kantchev, E. A. B.; O’Brien, C. J.; Organ, M. G. *Org. Lett.* **2005**, *7*, 1991. b) O’Brien, C. J.; Kantchev, E. A. B.; Chass, G. A.; Hadei, N.; Hopkinson, A. C.; Organ, M. G.; Setiadi, D. H.; Tang, T.-H.; Fang, D.-C. *Tetrahedron* **2005**, *61*, 9723.
 - 22) Arduengo, A. J., III; Tapu, D.; Marshall, W. J. *J. Am. Chem. Soc.* **2005**, *127*, 16400.
 - 23) Saravanakumar, S.; Oprea, A. I.; Kindermann, M. K.; Jones, P. G.; Heinicke, J. *Chem. Eur. J.* **2006**, *12*, 3143.
 - 24) For purine-based annulated NHCs, see: a) Schütz, J.; Herrmann, W. A. *J. Organomet. Chem.* **2004**, *689*, 2995. b) Kascatan-Nebioglu, A.; Panzner, M. J.; Garrison, J. C.; Tessier, C. A.; Youngs, W. J. *Organometallics* **2004**, *23*, 1928.
 - 25) Saravanakumar, S.; Kindermann, M. K.; Heinicke, J.; Köckerling, M. *Chem. Commun.* **2006**, 640.
 - 26) For recent reviews, see: a) Christmann, U.; Vilar, R. *Angew. Chem. Int. Ed.* **2005**, *44*, 366. b) Hillier, A. C.; Grasa, G. A.; Viciu, M. S.; Lee, H. M.; Yang, C.; Nolan, S. P. *J. Organomet. Chem.* **2002**, *653*, 69. c) Trnka, T. M.; Grubbs, R. H. *Acc. Chem. Res.* **2001**, *34*, 18.

- 27) a) B. Gehrhus, P. B. Hitchcock, M. F. Lappert, *Z. Anorg. Allg. Chem.* **2005**, 631, 1383. b) Hu, X.; Meyer, K. *J. Organomet. Chem.* **2005**, 690, 5474. c) Clyne, D. S.; Jin, J.; Genest, E.; Gallucci, J. C.; RajanBabu, T. V. *Org. Lett.* **2000**, 2, 1125. d) Herrmann, W. A.; Köcher, C.; Gooßen, L. J.; Artus, G. R. *J. Chem. Eur. J.* **1996**, 2, 1627. e) Herrmann, W. A.; Reisinger, C.-P.; Spiegler, M. *J. Organomet. Chem.* **1998**, 557, 93. f) Fehlhammer, W. P.; Bliss, T.; Kernbach, U.; Brüdgam, I. *J. Organomet. Chem.* **1995**, 490, 149.
- 28) Herrmann, W. A.; Elison, M.; Fischer, J.; Köcher, C.; Artus, G. R. *J. Chem. Eur. J.* **1996**, 2, 772.
- 29) Simons, R. S.; Custer, P.; Tessier, C. A.; Youngs, W. J. *Organometallics* **2003**, 22, 1979.
- 30) Guerret, O.; Solé, S.; Gornitzka, H.; Teichert, M.; Trinquier, G.; Bertrand, G. *J. Am. Chem. Soc.* **1997**, 119, 6668.
- 31) a) Yount, W. C.; Loveless, D. M.; Craig, S. L. *J. Am. Chem. Soc.* **2005**, 127, 14488. b) Yount, W. C.; Juwarker, H.; Craig, S. L. *J. Am. Chem. Soc.* **2003**, 125, 15302.
- 32) Beck, J. B.; Rowan, S. J. *J. Am. Chem. Soc.* **2003**, 125, 13922. For a related review on responsive materials using dynamic covalent chemistry, see: Rowan, S. J.; Cantrill, S. J.; Cousins, G. R. L.; Sanders, J. K. M.; Stoddart, J. F. *Angew. Chem. Int. Ed.* **2002**, 41, 898.

- 33) a) Veldhuizen, J. J. V.; Campbell, J. E.; Giudici, R. E.; Hoveyda, A. H. *J. Am. Chem. Soc.* **2005**, *127*, 6877. b) Larsen, A. O.; Leu, W.; Oberhuber, C. N.; Campbell, J. E.; Hoveyda, A. H. *J. Am. Chem. Soc.* **2004**, *126*, 11130.
- 34) Waltmann, A. W.; Grubbs, R. H. *Organometallics* **2004**, *23*, 3105.
- 35) For selected examples, see: a) Inamoto, K.; Kuroda, J.-I.; Hiroya, K.; Noda, Y.; Watanabe, M.; Sakamoto, T. *Organometallics* **2006**, *25*, 3095. b) Legault, C. Y.; Kendall, C.; Charette, A. B. *Chem. Commun.* **2005**, 3826. c) Clavier, H.; Coutable, L.; Toupet, L.; Guillemin, J.-C.; Mauduit, M. *J. Organomet. Chem.* **2005**, *690*, 5237. d) Jensen, T. R.; Schaller, C. P.; Hillmyer, M. A.; Tolman, W. B. *J. Organomet. Chem.* **2005**, *690*, 5881. e) Li, W.-F.; Sun, H.-M.; Wang, Z.-G.; Chen, M.-Z.; Shen, Q.; Zhang, Y. *J. Organomet. Chem.* **2005**, *690*, 6227. f) Liddle, S. T.; Arnold, P. L. *Organometallics* **2005**, *24*, 2597. g) Li, W.; Sun, H.; Chen, M.; Wang, Z.; Hu, D.; Shen, Q.; Zhang, Y. *Organometallics* **2005**, *24*, 5925. h) Clavier, H.; Coutable, L.; Guillemin, J.-C.; Mauduit, M. *Tetrahedron: Asymmetry* **2005**, *16*, 921. i) Arnold, P. L.; Scarisbrick, A. C.; Blake, A. J.; Wilson, C. *Chem. Commun.* **2001**, 2340.
- 36) Hahn, F. E.; Holtgrewe, C.; Pape, T.; Martin, M.; Sola, E.; Oro, L. A. *Organometallics* **2005**, *24*, 2203.
- 37) Hahn, F. E.; Jahnke, M. C.; Gomez-Benitez, V.; Morales-Morales, D.; Pape, T. *Organometallics* **2005**, *24*, 6458.
- 38) Çetinkaya, B.; Demir, S.; Özdemir, I.; Toupet, L.; Sémeril, D.; Bruneau, C.; Dixneuf, P. G. *Chem. Eur. J.* **2003**, *9*, 2323.

- 39) In this context, the term “desymmetrized” refers to a system in which each imidazole moiety features two different N-substituents.
- 40) Tulloch, A. A. D.; Danopolous, A. A.; Kleinhenze, S.; Light, M. E.; Hursthouse, M. B.; Eastham, G. *Organometallics* **2001**, *20*, 2027.
- 41) Wang, H. M. J.; Lin, I. J. B. *Organometallics* **1998**, *17*, 972.
- 42) Herrmann, W. A.; Gerstberger, G.; Spiegler, M. *Organometallics* **1997**, *16*, 2009.
- 43) a) Odian, G. *Principles of Polymerization*; Wiley: Hoboken, New Jersey, 2004, pp. 39 - 63. b) Carothers, W. H. *Trans. Faraday Soc.* **1936**, *32*, 39.
- 44) a) Shi, Z.; Thummel, R. P. *J. Org. Chem.* **1995**, *60*, 5935. b) Winberg, H. E.; Downing, J. R.; Coffman, D. D. *J. Am. Chem. Soc.* **1965**, *87*, 2054.
- 45) Çetinkaya, B.; Çetinkaya, E.; Chamizo, J. A.; Hitchcock, P. B.; Jasim, H. A.; Küçükbay, H.; Lappert, M. F. *J. Chem. Soc., Perkin Trans. I* **1998**, 2047.
- 46) Kamplain, J. W.; Bielawski, C. W. *Chem. Commun.* **2006**, 1727.
- 47) For an excellent review on Ag-NHC complexes, see: Garrison, J. C.; Youngs, W. *J. Chem. Rev.* **2005**, *105*, 3978. For other examples demonstrating carbene transfer from related Ag complexes, see: a) de Frémont, P.; Scott, N. M.; Stevens, E. D.; Nolan, S. P. *Organometallics* **2005**, *24*, 2411. b) Arnold, P.; Scarisbrick, A. C. *Organometallics* **2004**, *23*, 2519. c) Catalano, V. J.; Malwitz, M. A.; Etogo, A. O. *Inorg. Chem.* **2004**, *43*, 5714. d) Chianese, A. R.; Li, X.; Janzen, M. C.; Faller, J. W.; Crabtree, R. H. *Organometallics* **2003**, *22*, 1663. e) Tulloch, A. A. D.; Danapoulos, A. A.; Tizzard, G. J.; Coles, S. J.; Hursthouse, M. B.; Hay-Motherwell, R. S.; Motherwell, W. B. *Chem. Commun.* **2001**, 1270.

- 48) For similar S_NAr reactions using 1-fluoronitrobenzene, see: a) Shi, M.; Qian, H. *Tetrahedron* **2005**, *61*, 4949. b) Murahashi, S.-I.; Ono, S.; Imada, Y. *Angew. Chem. Int. Ed.* **2002**, *41*, 2366.
- 49) For an alternate synthesis of **2.15**, see: Allinger, N. L.; Youngdale, G. A. *J. Am. Chem. Soc.* **1962**, *84*, 1020.
- 50) For an alternative synthesis of **2.16**, see: Tashiro, M.; Itoh, T.; Fukata, G. *Synthesis* **1982**, 217.
- 51) a) Zou, G.; Huang, W.; Xiao, Y.; Tang, J. *New. J. Chem.* **2006**, *30*, 803. b) Huynh, H. V.; Neo, T. C.; Tan, G. K. *Organometallics* **2006**, *12*, 1298. c) Page, P. C. B.; Buckley, B. R.; Christie, S. D. R.; Edgar, M.; Poulton, A. M.; Elsegood, M. R. J.; McKee, V. *J. Organomet. Chem.* **2005**, *690*, 6210. d) Huynh, H. V.; Ho, J. H. H.; Neo, T. C.; Koh, L. L. *J. Organomet. Chem.* **2005**, *690*, 3854. e) Hahn, F. E.; von Fehren, T.; Lügger, T. *Inorg. Chim. Acta* **2005**, *358*, 4137. f) Hahn, F. E.; Holtgrewe, C.; Pape, T. *Z. Naturforsch.* **2004**, *59b*, 1051. g) Hahn, F. E.; von Fehren, T.; Wittenbecher, L.; Fröhlich, R. *Z. Naturforsch.* **2004**, *59b*, 541. h) Baker, M. V.; Skelton, B. W.; White, A. H.; Williams, C. C. *J. Chem. Soc., Dalton Trans.* **2001**, 111. i) Hahn, F. E.; Foth, M. *J. Organomet. Chem.* **1999**, 585, 241.
- 52) The ¹H NMR spectrum of crystals of **2.19•Pd** (confirmed by X-ray to be a cis complex) matched those of the crude powder.

- 53) Reactions conducted in PhCH₃, PhH, and CH₂Cl₂ were unsuccessful and resulted in incomplete consumption of starting materials ascribed to the poor solubility of the azolium, metal, and/or NaOAc salts.
- 54) a) Chamizo, J. A.; Morgado, J. *Transition Met. Chem.* **2000**, 25, 161. b) Herrmann, W. A.; Schwarz, J.; Gardiner, M. G.; Spiegler, M. *J. Organomet. Chem.* **1999**, 18, 4584. c) Lappert, M. F.; Pye, P. L. *J. Chem. Soc., Dalton Trans.* **1977**, 2172.
- 55) The non-chelated Pt intermediate analogous to **2.18·Pd** was observed by NMR spectroscopy (diagnostic signals: phenol ¹H at approximately δ = 10.0 ppm and absence of azolium ¹H at δ = 10.8 ppm).
- 56) Consistent with **2.19·Pd** and **2.19·Ni**, the oxygen-substituted carbon of the phenol ring also appears in this range and is also consistent with one of the two signals observed in **2.19·Pt**.
- 57) Demidov, V. N.; Kukushkin, Y. N.; Vedeneeva, L. N.; Belyaev, A. N. *Zh. Obshch. Khim.* **1988**, 58, 738.
- 58) a) Bacciu, B.; Cavell, K. J.; Fallis, I. A.; Ooi, L. *Angew. Chem. Int. Ed.* **2005**, 44, 5282. b) Frøseth, M.; Netland, K. A.; Rømming, C.; Tilset, M. *J. Organomet. Chem.* **2005**, 690, 6125. c) Liu, Q.-X.; Xu, F.-B.; Li, Q.-S.; Song, H.-B.; Zhang, Z.-Z. *J. Mol. Struct.* **2004**, 697, 131. d) Liu, Q.-X.; Xu, F.-B.; Li, Q.-S.; Song, H.-B.; Zhang, Z.-Z. *Organometallics* **2004**, 23, 610. e) Quezada, C. A.; Garrison, J. C.; Tessier, C. A.; Youngs, W. J. *J. Organomet. Chem.* **2003**, 671, 183. f) Meuhlhofer, M.; Strassner, T.; Herdtweck, E.; Herrmann, W. A. *J. Organomet.*

- Chem.* **2002**, 660, 121. g) Hasan, M.; Kozhevnikov, I. V.; Siddiqui, R. H.; Femoni, C.; Steiner, A.; Winterton, N. *Inorg. Chem.* **2001**, 40, 795.
- 59) a) Poyatos, M.; Maisse-François, A.; Bellemin-Lapponnaz, S.; Gade, L. H. *Organometallics* **2006**, 25, 2634. b) Liu, Q.-X., Song, H.-B.; Xu, F.-B.; Li, Q.-S.; Zeng, X.-S.; Leng, X.-B.; Zhang, Z.-Z. *Polyhedron* **2003**, 22, 1515.
- 60) Pd(OAc)₂ was found to be equally as effective as PdCl₂.
- 61) A 4:1 ratio of total acetate ions relative to bis(azolium) salt **2.23** was used.
- 62) The reactions were monitored as follows: Stirring was stopped and solids allowed to settle. An aliquot was taken and analyzed by No-D ¹H NMR spectroscopy for the consumption of azolium starting material. For a reference describing No-D NMR technique, see: Hoyer, T. R.; Eklov, B. M.; Ryba, T. D.; Voloshin, M.; Yao, L. J. *Org. Lett.* **2004**, 6, 953.
- 63) a) Nietzki, R.; Hagenbach, E. *Ber. Dtsch. Chem. Ges.* **1887**, 20, 328. (b) Nietzki, R. *Ber. Dtsch. Chem. Ges.* **1887**, 20, 2114.
- 64) Azophenines generally refer to N,N',N'',N'''-tetrakis(phenyl) 1,4-diamino-2,5-benzoquinonediimine and their respective derivatives, see: a) Fischer, O.; Hepp, E. *Ber. Dtsch. Chem. Ges.* **1888**, 21, 676. b) Kimich, C. *Ber. Dtsch. Chem. Ges.* **1875**, 8, 1026.
- 65) a) Shimakoshi, H.; Hirose, S.; Ohba, M.; Shiga, T.; Okawa, H.; Hisaeda, Y. *Bull. Chem. Soc. Jpn.* **2005**, 78, 1040. b) Frantz, S.; Rall, J.; Hartenback, I.; Scheid, T.; Zalis, S.; Kaim, W. *Chem. Eur. J.* **2004**, 10, 149. c) Groselj, U.; Bevk, D.; Jakse, R.; Meden, A.; Pirc, S.; Recnik, S.; Stanovnik, B.; Svete, J. *Tetrahedron:*

- Asymmetry* **2004**, *15*, 2367. d) Beckmann, U.; Bill, E.; Weyhermueller, T.; Wieghardt, K. *Inorg. Chem.* **2003**, *42*, 1045. e) Gordon-Wylie, S. W.; Blanton, W. B.; Claus, B. L.; Horwitz, C. P.; Collins, T. J.; Boskovic, C.; Christou, G. *Inorg. Synth.* **2002**, *33*, 1. f) Chichak, K.; Jacquemard, U.; Branda, N. R. *Eur. J. Inorg. Chem.* **2002**, *2*, 357. g) Siri, O.; Braunstein, P. *Chem. Comm.* **2000**, *22*, 2223. h) Masui, H.; Freda, A. L.; Zerner, M. C.; Lever, A. B. P. *Inorg. Chem.* **2000**, *39*, 141. i) Aukauloo, A.; Ottenwaelder, X.; Ruiz, R.; Poussereau, S.; Pei, Y.; Journaux, Y.; Fleurat, P.; Volatron, F.; Cervera, B.; Munoz, M. C. *Eur. J. Inorg. Chem.* **1999**, *7*, 1067. j) Gordon-Wylie, S. W.; Claus, B. L.; Horwitz, C. P.; Leychkis, Y.; Workman, J.; Marzec, A. J.; Clark, G. R.; Rickard, C. E. F.; Conklin, B. J.; Sellers, S.; Yee, G. T. Collins, T. J. *Chem. Eur. J.* **1998**, *4*, 2173. k) Rall, J.; Stange, A. F.; Hubler, K.; Kaim, W. *Angew. Chem. Int. Ed.* **1998**, *37*, 2681. l) Espenson, J. H.; Kirker, G. W. *Inorg. Chim. Acta* **1980**, *40*, 105. m) Merrell, P. H.; Maheu, L. J. *Inorg. Chim. Acta* **1978**, *28*, 47. n) Hasty, E. F.; Colburn, T. J.; Hendrickson, D. N. *Inorg. Chem.* **1973**, *12*, 2414.
- 66) a) Elhabiri, M.; Siri, O.; Sornosa-tent, A.; Albrecht-Gary, A.-M.; Braunstein, P. *Chem. Eur. J.* **2004**, *10*, 134. b) Siri, O.; Braunstein, P.; Rohmer, M.-M.; Benard, M.; Welter, R. *J. Am. Chem. Soc.* **2003**, *125*, 13793.
- 67) Archer, R. D.; Illingsworth, M. L.; Rau, D. N.; Hardiman, C. J. *Macromolecules* **1985**, *18*, 1371.
- 68) Kleij, A. W.; Kuil, M.; Tooke, D. M.; Lutz, M.; Spek, A. L.; Reek, J. N. H. *Chem. Eur. J.* **2005**, *11*, 4743.

- 69) Staab, H. E.; Elbl-Weiser, K.; Krieger, C. *Eur. J. Org. Chem.* **2000**, 2, 327.
- 70) Ruggli, P.; Fischer, R. *Helv. Chim. Acta* **1945**, 28, 1270.
- 71) a) Rumpel, H.; Limbach, H.-H. *J. Am. Chem. Soc.* **1989**, 111, 5429. (b) Paetzold, F.; Niclas, H. J.; Foerster, H. J. *J. Prakt. Chem.* **1986**, 328, 5. (c) Paetzold, F.; Niclas, H. J.; Foerster, H. J. *J. Prakt. Chem.* **1986**, 328, 921. (d) Ruggli, P.; Buchmeier, F. *Helv. Chim. Acta* **1945**, 28, 850.
- 72) Adams, R.; Schowalter, K. A. *J. Am. Chem. Soc.* **1952**, 74, 2597.
- 73) Wenderski, T.; Light, K. M.; Ogrin, D.; Bott, S. G.; Harlan, C. J. *Tetrahedron Lett.* **2004**, 45, 6851.
- 74) a) Prim, D.; Campagne, J.-M.; Joseph, D.; Andrioletti, B. *Tetrahedron* **2002**, 58, 2041. b) Wolfe, J. P.; Wagaw, S.; Marcox, J.-F.; Buchwald, S. L. *Acc. Chem. Res.* **1998**, 31, 805. c) Hartwig, J. F. *Angew. Chem., Int. Ed.* **1998**, 37, 2046. d) Louie, J.; Hartwig, J. F. *Tetrahedron Lett.* **1995**, 36, 3609.
- 75) In a related example, Pd-catalyzed aryl amination was used to synthesize 1,2,4,5-tetra(morpholino)benzene in 76% yield via coupling of 1,2,4,5-tetrabromobenzene with morpholine, see: Witulski, B.; Senft, S.; Thum, A. *Synlett* **1998**, 504.
- 76) PdCl₂ was found to be equally effective as Pd(OAc)₂.
- 77) Aside from IPr and H₂IPr, a variety of other ligands for Pd including bulky phosphines (PCy₃, rac-BINAP, PtBu₃) and imidazolylienes (1,3-bis(2,6-di-*tert*-butyl)imidazolylidene, 1,3-bis(2,6-dimesityl)imidazolylidene) were screened, but did not afford appreciable yields of product.

- 78) Residual inorganic salts were removed by filtering chloroform solutions of the tetraaminobenzenes followed by evaporation.
- 79) Use of an oxygen atmosphere effects azophenine formation more rapidly than use of ambient (aerated) solvents.
- 80) A solution to the crystal structure of 1,2,4,5-tetrakis(mesitylamino)benzene (**3.8**) was also determined; key bond distances (Å) and angles (°): N1-C1, 1.413(2); N2-C3, 1.424(2); C1-C2, 1.391(2); C2-C3, 1.398(2); C1-C3A, 1.404(2); N1-C1-C3A, 119.9(1); N2-C3-C1A, 118.5(1); C3A-C1-N1-C4, 173.9(2); C1A-C3-N2-C13, 172.9(2). Using the procedure described in the text, the corresponding azophenine (**3.9**) was synthesized and a solution to its corresponding crystal structure was determined; key bond distances and angles: N1-C1, 1.293(2); N2-C3, 1.357(2); C1-C2, 1.440(2); C2-C3, 1.356(2); C1-C3A, 1.494(2); N1-C1-C3A, 115.6(1); N2-C3-C1A, 114.2(1); C3A-C1-N1-C4, 176.9(1); C1A-C3-N2-C13, 171.3(1).
- 81) Oxidative susceptibilities of the 1,2,4,5-tetraminobenzenes can be greatly reduced through protonation with HCl prior to isolation.
- 82) For discussions comparing relative stabilities of electron deficient arylamines, see:
a) Li, Z.; Cheng, J.-P. *J. Org. Chem.* **2002**, 68, 7350. b) Kemnitz, C. R.; Karney, W. L.; Borden, W. T. *J. Am. Chem. Soc.* **1998**, 120, 3499. c) Miura, Y.; Kitagishi, Y.; Ueno, S. *Bull. Chem. Soc. Jap.* **1994**, 67, 3282.
- 83) Lehmler, H.-J.; Robertson, L. W.; Kania-Korwel, I. *Chemosphere*, **2004**, 56, 735.

- 84) The aryl amination reaction was determined to be quantitative by ^1H NMR spectroscopy; however, the isolation of **3.13** was challenged by its high solubility in common solvents.
- 85) A similar approach utilizing aryl amination of 1,2-dibromobenzene followed by cyclization has been reported: Rivas, R. M.; Riaz, U.; Giessart, A.; Smulik, J. A.; Diver, S. T. *Org. Lett.* **2001**, 3, 1673. For syntheses of related benzimidazolium and benzimidazolylidene compounds, see ref 19.
- 86) Haas, Y.; Zilberg, S. *J. Am. Chem. Soc.* **2004**, 126, 8991.
- 87) a) Yamashita, M.; Goto, K.; Kawashima, T. *J. Am. Chem. Soc.* **2005**, 127, 7294. b) Böhrer, C.; Stein, D.; Donati, N.; Grützmacher, H. *New J. Chem.* **2002**, 26, 1291. c) Niehus, M.; Erker, G.; Kehr, G.; Schwab, P.; Fröhlich; Blacque, O.; Berke, H. *Organometallics* **2002**, 21, 2905. d) Jafarpour, L.; Stevens, E. D.; Nolan, S. P. *J. Organomet. Chem.* **2000**, 606, 49.
- 88) a) Donia, R. A.; Shotton, J. A.; Bentz, L. O.; Smith, G. E. P. *J. Org. Chem.* **1949**, 14, 952. b) Bildstein, B.; Malaun, M.; Kopacka, H.; Wurst, K.; Mitterbock, M.; Ongania, K.-H.; Opromolla, G.; Zanello, P. *Organometallics* **1999**, 18, 4325.
- 89) Schwarz, D. E.; Cameron, T. M.; Hay, P. J.; Scott, B. L.; Tumas, W.; Thorn, D. L. *Chem. Commun.* **2005**, 5919. For a related example, see: Montgrain, F.; Ramos, S. M.; Wuest, J. D. *J. Org. Chem.* **1988**, 53, 1489.
- 90) In an alternate approach, attempts at direct conversion to bis(azolium) salts with mixtures of electrophiles (e.g., equimolar amounts of $\text{HC}(\text{OEt})_3$ and paraformaldehyde) under equilibrating conditions was met with limited success.

- 91) General procedure for preparing compounds **4.1b–e**: A 20 mL vial charged with 1,3-bis(2,6-diisopropylphenyl)imidazolium chloride (0.02 mmol), NaOt-Bu (0.02 mmol), Pd(OAc)₂ (0.01 mmol), and toluene (5 mL). After stirring the resulting mixture for 10 min, 1,2,4,5-tetrabromobenzene (1.00 mmol), amine (4.10 mmol), NaOtBu (4.20 mmol) and toluene (5 mL) were added. The resulting mixture was sealed and stirred at 110 °C for 8 h. After cooling to ambient temperature, the resulting mixture was diluted with hexanes and precipitated solids were collected by filtration. Residual inorganic salts were removed by filtering CHCl₃ solutions of the products. The synthesis of **4.7a** was complicated by its relatively poor solubility in acidified solutions of PhCH₃. Characterization data for new compounds: Azophenine **4.1b**: ¹H NMR (CDCl₃): δ 8.55 (s, 2H), 7.05 – 6.91 (m, 16H), 6.16 (s, 2H) 3.83 (s, 12H); ¹³C NMR (CDCl₃) δ 150.4, 148.2, 134.4, 130.5, 121.0, 120.6, 119.1, 114.4, 111.3, 110.3, 93.1, 55.7, 55.5; HRMS: [M]⁺ calcd for C₃₄H₃₂N₄O₄, 560.2424; Found: 560.2428; Compound **4.1d**: ¹H NMR (CDCl₃): δ 6.69 (br, 2H), 5.77 (s, 2H), 2.10 (br, 12H), 1.97 (br, 24H), 1.68 (br, 24H); ¹³C NMR (CDCl₃): δ (ca 138), 92.2, 52.7, 42.6, 36.9, 29.8; HRMS: [M]⁺ calcd for C₄₆H₆₄N₄, 672.5131; Found: 672.5134; Azophenine **4.1e**: ¹H NMR (CDCl₃): δ 8.13 (s, 2H), 7.03 (s, 2H), 6.78 (br, 8H), 6.31 (s, 2H), 1.17 (s, 72H); ¹³C NMR (CDCl₃): δ 151.4, 117.6, 90.7, 34.8, 31.4; HRMS: [M+1]⁺ calcd for C₆₂H₈₈N₄, 889.7009; Found, 889.7089.
- 92) General procedure for preparing benzobis(imidazolium) salts *via* tandem cyclization - Wuest-Thorn oxidation: In a 50 mL round-bottom flask, the 2,5-

diamino-1,4-benzoquinonediimine (0.5 mmol) was first suspended in toluene (20 mL). Paraformaldehyde (1.2 mmol) and conc. HCl (1 drop) were then added and the reaction mixture was stirred in an oil bath thermostatted at 110 °C for 2 – 6 h during which time the initial intense color of the azophenine dissipated and the mixture became a light yellow-brown suspension. The temperature was then reduced to 50 °C and *i*-PrOH (2 mL) was added to facilitate partial dissolution of solids. Pd(OAc)₂ (5 μmol, 1 mol %) was then added and slow gas evolution followed. The mixture was heated and stirred for an additional 2 – 4 h and concentrated. Yields were determined by ¹H NMR analysis of the crude product mixtures. Note: this reaction sequence was found to work equally well in other solvents, including: CH₃CN, DMF, DMSO, and EtOH. The increased solubility of **4.1e** allowed the tandem cyclization/oxidation reactions to be carried out in PhCH₃ alone at 50 °C for each step. Spectral data of **4.7a–d** reported compounds were in accord with their previously reported values. Characterization data for benzobis(imidazolium) **4.7e**: ¹H NMR (CDCl₃): δ 9.98 (br, 2H), 7.97 (br, 8H), 7.82 (br, 2H), 7.62 (s, 4H), 1.32 (s, 72H); ¹³C NMR (CDCl₃): δ 154.0, 144.7, 132.1, 125.5, 120.7, 114.9, 99.6, 35.5, 31.4; HRMS: [M]⁺ calcd for C₆₄H₈₈N₄, 912.7009; Found, 912.6983.

- 93) a) Arduengo, III, A. J.; Harlow, R. L.; Kline, M. *J. Am. Chem. Soc.* **1991**, *113*, 361. b) Arduengo, III, A. J.; Davidson, F.; Dias, H. V. R.; Goerlich, J. R.; Khasnis, D.; Marshall, W. J.; Prakasha, T. K. *J. Am. Chem. Soc.* **1997**, *119*, 12742.

- 94) a) Enders, D.; Breuer, K.; Raabe, G.; Runsink, J.; Teles, J. H.; Melder, J.-P.; Ebel, K.; Brode, S. *Angew. Chem. Int. Ed.* **1995**, *34*, 1021. b) Alder, R. W.; Allen, P. R.; Murray, M.; Orpen, A. G. *Angew. Chem. Int. Ed.* **1996**, *35*, 1121. c) Arduengo, III, A. J.; Goerlich, J. R.; Marshall, W. J. *Lieb. Ann./Recueil.* **1997**, 365. d) Weiss, R.; Reichel, S.; Handke, M.; Hampel, F. *Angew. Chem. Int. Ed.* **1998**, *37*, 344. e) Burstein, C.; Lehmann, C. W.; Glorius, F. *Tetrahedron* **2005**, *61*, 6207. f) Präsang, C.; Donnadiou, B.; Bertrand, G. *J. Am. Chem. Soc.* **2005**, *127*, 10182.
- 95) For theoretical treatments of NHC-metal interactions, see: a) Boehme, C.; Frenking, G. *Organometallics* **1998**, *17*, 5801. b) McGuinness, D. S.; Saendig, N.; Yates, B. F.; Cavell, K. J. *J. Am. Chem. Soc.* **2001**, *123*, 4029. c) Deubel, D. V.; *Organometallics* **2002**, *21*, 4303. d) Abernethy, C. D.; Codd, G. M.; Spicer, M. D.; Taylor, M. K. *J. Am. Chem. Soc.* **2003**, *125*, 1128. e) Termaten, A. T.; Schakel, M.; Ehlers, A. W.; Lutz, M.; Spek, A. L.; Lammertsma, K. *Chem. Eur. J.* **2003**, *9*, 3577. f) Hu, X.; Castro-Rodriguez, I.; Olsen, K.; Meyer, K. *Organometallics* **2004**, *23*, 755.
- 96) Janus ligands are named after the Roman god *Janus Geminus*, represented in Roman art as two-faced, featuring one face looking forward fused to another looking backward. For examples, see: a) Cristol, S. J.; Lewis, D. C. *J. Am. Chem. Soc.* **1967**, *89*, 1476. b) Marsh, A.; Nolen, E. G.; Gardinier, K. M.; Lehn, J.-M.; *Tetrahedron Lett.* **1994**, *35*, 397.
- 97) a) Arduengo III, A. J.; Goerlick, J. R.; Marshall, W. J. *J. Am. Chem. Soc.* **1995**, *117*, 11027. b) Denk, M. K.; Thadani, A.; Hatano, K.; Lough, A. J. *Angew. Chem.*

- Int. Ed.* **1997**, *36*, 2067. c) Hahn, F. E.; Paas, M.; Van, D. L.; Lügger, T. *Angew. Chem. Int. Ed.* **2003**, *42*, 5243.
- 98) a) Çetinkaya, E.; Hitchcock, P. B.; Küçükbay, H.; Lappert, M. F.; Al-Juaid, S. J.; *Organomet. Chem.* **1994**, *481*, 89. b) Hahn, F. E.; von Fehren, T.; Lars, W.; Froehlich, R. *Z.fuer Naturforsch.* **2004**, *59*, 544.
- 99) Feitelson, B. N.; Mamalis, P.; Moualim, R. J.; Petrow, V.; Stephenson, O.; Sturgeon, B. *J. Chem. Soc.* **1952**, 2389.
- 100) a) Chiappe, C.; Pieraccini, D. *J. Phys. Org. Chem.* **2005**, *18*, 275. b) Koel, M. *Crit. Rev. Anal. Chem.* **2005**, *35*, 177. c) Buzzeo, M. C.; Evans, R. G.; Compton, R. G. *ChemPhysChem* **2004**, *5*, 1106. d) Wilkes, J. S. *Green Chem.* **2002**, *4*, 73. e) Wassersheid, P.; Keim, W. *Angew. Chem. Int. Ed.* **2000**, *39*, 3772. f) Welton, T.; *Chem. Rev.* **1999**, *99*, 2071. g) *Ionic Liquids in Synthesis*; Welton, T.; Wasserscheid, P., Eds.; VCH-Wiley: Weinheim, Germany, 2002.
- 101) For recent examples of ILs as environment-friendly alternatives to traditional organic solvents, see: a) Pereiro, A. B.; Tojo, E.; Rodríguez, A.; Canosa, J.; Tojo, J. *Green Chem.* **2006**, *8*, 307. b) Nishi, N.; Kawakami, T.; Shigematsu, F.; Yamamoto, M.; Kakiuchi, T. *Green Chem.* **2006**, *8*, 349. c) Kralisch, D.; Stark, A.; Körsten, S.; Kreisel, G.; Ondruschka, B. *Green Chem.* **2005**, *7*, 301. d) Peng, J.; Shi, F.; Gu, Y.; Deng, Y. *Green Chem.* **2003**, *5*, 224. e) Uzagare, M. C.; Sanghvi, Y. S.; Salunkhe, M. M. *Green Chem.* **2003**, *5*, 370. f) Wasserscheid, P.; van Hal, R.; Bösmann, A. *Green Chem.* **2002**, *4*, 400. g) Hangarge, R. V.; Jarikote, D. V.; Shingare, M. S. *Green Chem.* **2002**, *4*, 266. h) Zhu, H.-P.; Yang,

- F.; Tang, J.; He, M.-Y. *Green Chem.* **2003**, 5, 38. i) Scott, J. L.; MacFarlane, D. R.; Raston, C. L.; Teoh, C. M. *Green Chem.* **2000**, 2, 123.
- 102) López-Martin, I.; Burello, E.; Davey, P. N.; Seddon, K. R.; Rothenberg, G. *ChemPhysChem* **2007**, 8, 690.
- 103) For selected examples involving the nucleophilicity of organic halide salts, see: a) Man, B. Y. W.; Hook, J. M.; Harper, J. B. *Tetrahedron Lett.* **2005**, 46, 7641. b) Kamal, A.; Chouhan, G. *Tetrahedron Lett.* **2005**, 46, 1489. c) Lancaster, N. L.; Welton, T. *J. Org. Chem.* **2004**, 69, 5986. d) Crowhurst, L.; Lancaster, N. L.; Alrandis, J. M. P.; Welton, T. *J. Am. Chem. Soc.* **2004**, 126, 11549. e) Boovanahalli, S. K.; Kim, D. W.; Chi, D. Y. *J. Org. Chem.* **2004**, 69, 3340. f) Lourenço, N. M. T.; Afonso, C. A. M. *Tetrahedron* **2003**, 59, 789. g) Kim, D. W.; Song, C. E.; Chi, D. Y. *J. Org. Chem.* **2003**, 68, 4281. h) Leadbeater, N. E.; Torenus, H. M.; Tye, H. *Tetrahedron* **2003**, 59, 2253. i) Nguyen, H.-P.; Matondo, H.; Baboulène, M. *Green Chem.* **2003**, 5, 303. j) Lancaster, N. L.; Salter, P. A.; Welton, T.; Young, G. B. *J. Org. Chem.* **2002**, 67, 8855. k) Lancaster, N. L.; Welton, T.; Young, G. B. *J. Chem. Soc., Perkin Trans. 2* **2001**, 2267. l) Ren, R. X.; Wu, J. X. *Org. Lett.* **2001**, 3, 3727. m) Ford, W. T.; Hauri, R. J.; Smith, S. G. *J. Am. Chem. Soc.* **1974**, 96, 4316. n) Gordon, J. E.; Varughese, P. *Chem. Commun.* **1971**, 1160.
- 104) a) Kaupp, G. *Top. Curr. Chem.* **2005**, 254, 95. b) DeSimone, J. M. *Science* **2002**, 297, 799. c) Tanaka, K.; Toda, F. *Chem. Rev.* **2000**, 100, 1025. d) Metzger, J. O.; *Angew. Chem. Int. Ed.* **1998**, 37, 2975.

- 105) [BPY][OTs] is reported to have a melting point of 114 °C, see: Sekera, V. C.; Marvel, C. S. *J. Am. Chem. Soc.* **1933**, *55*, 345.
- 106) a) Bates, E. D.; Mayton, R. D.; Ntai, I.; Davis, J. H., Jr. *J. Am. Chem. Soc.* **2002**, *124*, 926. b) Xu, H.; Meng, R.; Xu, C.; Zhang, J.; He, G.; Cui, Y. *Appl. Phys. Lett.* **2003**, *83*, 1020. c) Chondroudis, K.; Mitzi, D. B. *Appl. Phys. Lett.* **2000**, *76*, 58. d) Paul, A.; Mandal, P. K.; Samanta, A. *J. Phys. Chem. B* **2005**, *109*, 9148. e) Paul, A.; Mandal, P. K.; Samanta, A. *Chem. Phys. Lett.* **2005**, *402*, 375. f) M. J. Earle, K. R. Seddon, World Patent: WO 2006043110 (2006). g) Binnemans, K. *Chem. Rev.* **2005**, *105*, 4148. i) Kato, T. *Science* **2002**, *295*, 2414.
- 107) For an example of a macromolecular fluorescent IL, see: Huang, J.-F.; Luo, H.; Liang, C.; Sun, I.-W.; Baker, G. A.; Dai, S. *J. Am. Chem. Soc.* **2005**, *127*, 12784.
- 108) Sonoluminescence has also been observed from imidazolium salts, see: Oxley, J. D.; Prozorov, T.; Suslick, K. S. *J. Am. Chem. Soc.* **2003**, *125*, 11138.
- 109) Notably, the dicationic BBIs can accommodate two dissimilar counterions. For example, incorporating one BF₄ and one MeSO₄ anion (i.e., mixing equimolar amounts of **7.4•MeSO₄** and **7.4•BF₄**, or anion metathesis of **7.4•I** with 1.0 molar equiv each of Me₃O•BF₄ and Me₂SO₄) produced a BBI with a T_g of 19 °C.
- 110) a) O'Neill, M.; Kelly, S. M. *Adv. Mater.* **2003**, *15*, 1135. b) Levitsky, I. A.; Kishikawa, K.; Eichhorn, S. H.; Swager, T. M. *J. Am. Chem. Soc.* **2000**, *122*, 2474.
- 111) a) Lydon, J. *Curr. Opin. Colloid Interface Sci.* **2004**, *8*, 480. b) Tortora, L.; Park, H.-S.; Antion, K.; Finotello, D.; Lavrentovich, O. D. *Proc. of SPIE* **2007**, *6487*,

- 64870I-1. c) Tam-Chang, S.-K.; Helbley, J.; Carson, T. D.; Seo, W.; Iverson, I. K. *Chem. Commun.* **2006**, 503.
- 112) When PLM samples were prepared between glass slides, sheering resulted in birefringence. Upon standing, the material returned to an isotropic cubic phase.
- 113) The solution absorption and photoluminescence of compounds **7.8a** and **7.8b** were found to be consistent with their structural analogues **7.1** and **7.3**, respectively (see Table 7.1).
- 114) a) Berlman, I. B. *Handbook of Fluorescence Spectra of Aromatic Molecules* 2nd Ed. New York, Academic Press, 1971. b) Allen, M. T.; Whitten, D. G. *Chem. Rev.* **1989**, 89, 1691.
- 115) For select reviews, see: a) Thomas, S. W., III; Joly, G. D.; Swager, T. M. *Chem. Rev.* **2007**, 107, 1339. b) Finney, N. S *Curr. Opin. Chem. Biol.* **2006**, 10, 238. c) Glasbeek, M. Zhang, H. *Chem. Rev.* **2004**, 104, 1929. d) Lakowicz, J. R. *Principles of Fluorescence Spectroscopy*, 2nd ed.; Plenum Publisher: New York, 1999.
- 116) For a excellent reviews, see: a) Hu, Z, Margulis, C. J. *Acc. Chem. Res.* **2007**, in press. b) Demchenko, A. P. *Luminescence* **2002**, 17, 19.
- 117) Wang, S.; Chang, Y.-T. *J. Am. Chem. Soc.* **2006**, 128, 10380.
- 118) Chen, L.; McBranch, D. W.; Wang, H.-L.; Helgeson, R.; Wudl, F.; Whitten, D. G. *Proc. Nat. Acad. Sci. U.S.A.* **1999**, 96, 12287.

- 119) a) Harrison, B. S.; Ramey, M. B.; Reynolds, J. R.; Schanze, K. S. *J. Am. Chem. Soc.* **2000**, *122*, 8561. b) Balanda, P. B.; Ramey, M. B.; Reynolds, J. R. *Macromolecules* **1999**, *32*, 3970.
- 120) a) Krishna, T. R.; Parent, M.; Wets, M. H. V.; Moreaux, L.; Gmouh, S.; Charpak, S.; Caminade, A.-M.; Majoral, J.-P.; Blanchard-Desce, M. *Angew. Chem. Int. Ed.* **2006**, *45*, 4645. b) Woo, H. Y.; Liu, B.; Kohler, B.; Korystov, D.; Mikhailovsky, A.; Bazan, G. C. *J. Am. Chem. Soc.* **2005**, *127*, 14721. c) Woo, H. Y.; Korystov, D.; Mikhailovsky, A.; Nguyen, T.-Q.; Bazan, G. C. *J. Am. Chem. Soc.* **2005**, *127*, 13794. d) Abbotto, A.; Beverina, L.; Bozio, R.; Facchetti, A.; Ferrante, C.; Pagani, G. A.; Pedron, D.; Signorini, R. *Org. Lett.* **2002**, *4*, 1495.
- 121) Fluorescent anion sensors require separate consideration, see: a) Sessler, J. L.; Tvermoes, N. A.; Davis, J.; Anzenbacher, P., Jr.; Jursíková, K.; Sato, W.; Siedel, D.; Lynch, V.; Black, C. B.; Try, A.; Andrioletti, B.; Hemmi, G.; Mody, T. D.; Magda, D. J.; Král, V. *Pure Appl. Chem.* **1999**, *71*, 2009. b) Martinez-Máñez, R.; Sancenón, F. *Chem. Rev.* **2003**, *103*, 4419. c) Gunnlaugsson, T.; Glynn, M.; Tocci, G. M.; Kruger, P. E.; Pfeffer, F. M. *Coord. Chem. Rev.* **2006**, *250*, 3094. d) Badugu, R.; Lakowicz, J. R.; Geddes, C. D. *Curr. Anal. Chem.* **2005**, *1*, 157.
- 122) For another example of this type of coupling using benzimidazole as a substrate, see: Harkal, S.; Rataboul, F.; Zapf, A.; Fuhrmann, C.; Riermeier, T.; Monsees, A.; Beller, M. *Adv. Synth. Catal.* **2004**, *346*, 1742.
- 123) For a synthesis of **8.7**, see ref 99.

- 124) For related synthetic approaches to the synthesis of C1-aryl benzimidazoles, see:
a) McKee, R.; Bost, R. *J. Am. Chem. Soc.* **1947**, *69*, 471. b) Xin, Z.; Serby, M. D.; Zhao, H.; Kosogof, C.; Szczaepankiewicz, B. G.; Liu, M.; BoLiu; Hutchins, C. W.; Sarris, K. A.; Hoff, E. D.; Falls, H. D.; Lin, C. W.; Ogiela, C. A.; Collins, C. A.; Brune, M. E.; Bush, E. N.; Droz, B. A.; Fey, T. A.; Knourek-Segel, V. E.; Shapiro, R.; Jaconson, P. B.; Beno, D. W. A.; Turner, T. M.; Sham, H. L.; Liu, G. *J. Med. Chem.* **2006**, *49*, 4459. c) Gong, B.; Hong, F. Kohm, C.; Bonham, L.; Klein, P. *Bioorg. Med. Chem. Lett.* **2004**, *14*, 1455.
- 125) For comparison, 1-methyl-3-phenylbenzimidazolium iodide exhibited λ_{abs} at 270 nm and λ_{em} at 392 nm under identical conditions.
- 126) For selected reviews, see: a) Buncel, E.; Rajagopal, S. *Acc. Chem. Rev.* **1990**, *23*, 226. b) Reichardt, C. *Chem. Rev.* **1994**, *94*, 2319. c) Reichardt, C. *Green Chem.* **2005**, *7*, 339. d) Minkin, V. I. *Chem. Rev.* **2004**, *104*, 2751.
- 127) For a discussion of solvatochromism and solvatofluorochromism in quadrupolar fluorophores, see: Terenziani, F.; Painelli, A.; Katan, C.; Charlot, M.; Blanchard-Desce, M. *J. Am. Chem. Soc.* **2006**, *128*, 15742.
- 128) Reichardt, C. *Solvents and Solvent Effects in Organic Chemistry*, 3rd ed.; Wiley-VCH: Weinheim, 2003.
- 129) Mertz, E. L.; Tikhomirov, V. A.; Krishtalik, L. I. *J. Phys. Chem. A* **1997**, *101*, 3433.
- 130) Marcus, R. A. *J. Chem. Phys.* **1963**, *38*, 1858.
- 131) Joshi, H. S.; Jamshidi, R.; Tor, Y. *Angew. Chem. Int. Ed.* **1999**, *38*, 2722.

- 132) To clarify, we use the terms “solvatochromism” and “solvatofluorochromism” to imply solvent-induced changes in the λ_{abs} and λ_{em} , respectively.
- 133) Gutmann, V. *Coordination Chemistry in Non-Aqueous Solutions*; Springer-Verlag: New York, 1968.
- 134) Doroshenko, A. O. *Theor. Exp. Chem.* **2002**, 38, 135.
- 135) a) Galley, W. C.; Purkey, R. M. *Proc. Natl. Acad. Sci. USA* **1970**, 67, 1116. b) Rubinov, A. N.; Tomin, V. I. *Opt. Spekt.* **1970**, 29, 1082. c) Weber, G.; Shinitzky, M. *Proc. Natl. Acad. Sci. USA* **1970**, 65, 823. d) Weber, G. *Biochem. J.* **1960**, 75, 335.
- 136) In solution, a REE is attributed to excitation of ground state molecules that are most strongly interacting with solvent molecules, see: Lakowicz, J. R. *Principles of Fluorescence Spectroscopy*; Plenum Publisher: New York, 1983.
- 137) The pKa of imidazolium salts is estimated to be 18 – 22, see: Amyes, T. L.; Diver, S. T.; Richard, J. P.; Rivas, F. M.; Toth, K. *J. Am. Chem. Soc.* **2004**, 126, 4366.

Vita

Andrew J. Boydston was born in Tulsa, Oklahoma on December 30, 1978, the son of Greg and Aeok Boydston. After completing his work at Willamette High School in Eugene, Oregon, he entered the University of Oregon in Eugene, Oregon. Andrew received his Bachelor of Science and Masters of Science degrees from the University of Oregon in 2001 and 2002, respectively. In September 2002, he entered the Graduate School of The University of Texas at Austin

Permanent Address: 110 E. Baseline Rd Apt 46
San Dimas, CA 91773

This dissertation was typed by the author